Copyright

by

Xianxiu Wan

2017

SIRT1 ACTIVATION IMPROVES HEART FUNCTION THROUGH INHIBITION OF INFLAMMATION IN CHAGAS DISEASE

by

Xianxiu Wan, M.S.

DISSERTATION

Presented to the Faculty of the Graduate School of

The University of Texas Medical Branch

in Partial Fulfillment

of the Requirements

for the Degree of

Doctor of Philosophy

The University of Texas Medical Branch

Auguest 2017

Dedication

To my family, for their endless love, unconditional support and encouragement giving me this life full of happiness

谨献给我的家人，他们无尽的爱，无条件的支持与鼓励

让我的生活充满幸福。

ACKNOWLEDGEMENTS

I would like to acknowledge everyone who has helped and contributed to making this dissertation possible.

My deepest gratitude is to my mentor, Dr. Nisha Garg for all her excellent guidance, caring, support, patience and encouragement. I am fortunate to have a mentor who has always there to listen, answer any questions and give me sincere advice. Dr. Garg also helps me to develop critical and creative thinking and encouraged me to develop independent analytical skills. Without Dr. Garg's help, I could not complete my graduate study.

I am also thankful for my dissertation committee members: Dr. N. Muge Kuyumcu-Martinez, Dr.Victor Reyes, Dr. Jianjun Wen, Dr. Ming-Hui Zou and Dr. Yuhui Whitney Yin, for their support and very helpful insights, comments and suggestions to my project. I especially thank our department director, Dr. Lynn Song's help in my project and guidance in my scientific career.

I would like to express my gratitude to all members of Dr. Garg's laboratory for helping with me and being good friends. I particularly wish to thank Dr. Wen for providing technical support when I had difficuties. My gratitude is extended to Yuejin Liang in Dr. Sun's lab for giving me excellent suggests on some experimental designs and helping me in conducting flow cytometry.

I want to thank Ms. Aneth Zertuche for her excellent work in administering the Microbiology and Immunology program. I also appreciate Ms. Mardelle Susman for her excellent editorial assistance in my proposals, manuscripts and dissertation.

Further, I want to acknowledge committee members of the James W. McLaughlin Foundation and American heart Association for providing me scholarship/fellowship.

Finally, my warmest thanks are for my husband, Zuliang Jie, for providing me with strength and loving care. In addition, I want to give my thanks to all my family and my friends. They were always there for me and made my learning experience enjoyable.

SIRT1 ACTIVATION IMPROVES HEART FUNCTION THROUGH INHIBITION OF INFLAMMATION IN CHAGAS DISEASE

Publication No. _____

Xianxiu Wan M.S.

The University of Texas Medical Branch
at Galveston, 2017

Supervisor: Dr. Nisha Garg

ABSTRACT

Chronic chagasic cardiomyopathy (CCM) is presented by increased oxidative/inflammatory stress and decreased mitochondrial bioenergetics. SIRT1 senses the redox changes and integrates mitochondrial metabolism and inflammation; and SIRT1 deficiency may be a major determinant in CCM. To test this, C57BL/6 mice were infected with *Trypanosoma cruzi* (*Tc*), treated with SIRT1 agonists (SRT1720), and monitored during chronic phase (~150 days post-infection). In this study, we determined whether enhancing the activity of sirtuin 1 (SIRT1) would be beneficial in maintaining heart health in Chagas disease. We found that treatment with SIRT1 agonists, given in a therapeutic window of time after *Trypanosoma cruzi* infection, had no beneficial effects in reducing the cardiac remodeling and mitochondrial biogenic defects in chagasic mice. SIRT1 agonist, however, controlled the NFκB signaling of oxidative and inflammatory responses and helped preserve the left ventricular function in chagasic mice. We also found that SRT1720 decreased the proinflammatory differentiation of macrophages in spleen and heart tissue in chronic chagasic mice. SRT1720-treated chagasic mice also significantly reduced in proinflammatory cytokines' mRNA level and protein level compared to splenic macrophages of chagasic mice. We concluded that co-delivery of SIRT1 agonists with other small molecules that inhibit mitochondrial dysfunction, cardiac fibrosis, and parasite persistence will potentially form a complete therapeutic regimen against Chagas disease.

TABLE OF CONTENTS

LIST OF ILLUSTRATIONS

Title **Page**

Chapter 1

Chapter 2

Chapter 3

LIST OF ABREVIATIONS

Amplex red	10-acetyl-3,7-dihydroxyphenoxazine
AOPP	Advanced oxidation protein products
Arg1	Arginase 1
iNOS	Inducible nitric oxide synthase
CO	Cardiac output
EF	Ejection fraction
FS	Fractional shortening
HNE	4-hydroxy-2-nonenal
IL-1β	Interleukin-1 beta
IL-4	Interleukin-4
IL-6	Interleukin-6
IL-10	Interleukin-10
IL-13	Interleukin-13
IFN-γ	Interferon gamma
LV	Left ventricle
mtDNA	Mitochondrial DNA
NRF1	Nuclear respiratory factor 1
Nrf2	Nuclear factor erythroid 2-related factor 2
3NT	3-nitrotyrosine
nuDNA	Nuclear DNA
OXPHOS	Oxidative phosphorylation
PGC1α	Peroxisome proliferator-activated receptor gamma coactivator-1α
ROS	Reactive oxygen species

SIRT1	Sirtuin 1
SV	Stroke volume
TNF-α	Tumor necrosis factor alpha
Tc	*Trypanosoma cruzi*
T. cruzi	*Trypanosoma cruzi*

CHAPTER 1 GENERAL INTRODUCTION

1.1 Chagas disease

Parasite, vector and transmission

Trypanosoma cruzi (*T. cruzi*) causes Chagas disease that is one of the most frequent causes of heart failure and sudden death in Latin America (1). It was described by the Brazilian scientist Carlos Chagas more than a century ago. According to World Health Organization estimates, about 16–18 million people are infected with *T. cruzi*, and about 120 million people are at risk of infection. Chagas disease is generally confined to Latin American countries, and is endemic in Mexico, Central and South America, where vector-borne transmission occurs in rural areas. Both domestic and wild mammals can serve as reservoirs for the parasite. Transmission of *T. cruzi* occurs by insect vectors of the subfamily Triatominae, in the family Reduviidae, known as “kissing bugs”. Currently, the US does not screen blood donations since there is no approved screening test available (2). Blood transfusion and organ transplantation are also important transmission routes of *T. cruzi*. Due to the immigration of infected persons to large urban cities and non-endemic countries, the epidemiological profile of the Chagas disease has changed to a globalized problem. It is estimated that ~300,000 people living in the United States are chronically infected with *T. cruzi* (3). Studies have reported the presence of the insect vector as well as *T. cruzi* infection of domestic and wild animals in the United States (4-7). In addition, Chagas disease also has been increasingly detected in Canada, Australia, European and some Western Pacific countries. Taken together, all these conditions indicating the potential

for Chagas disease as an emerging disease of public health importance in the USA and in the world (2, 8) (Fig 1.1).

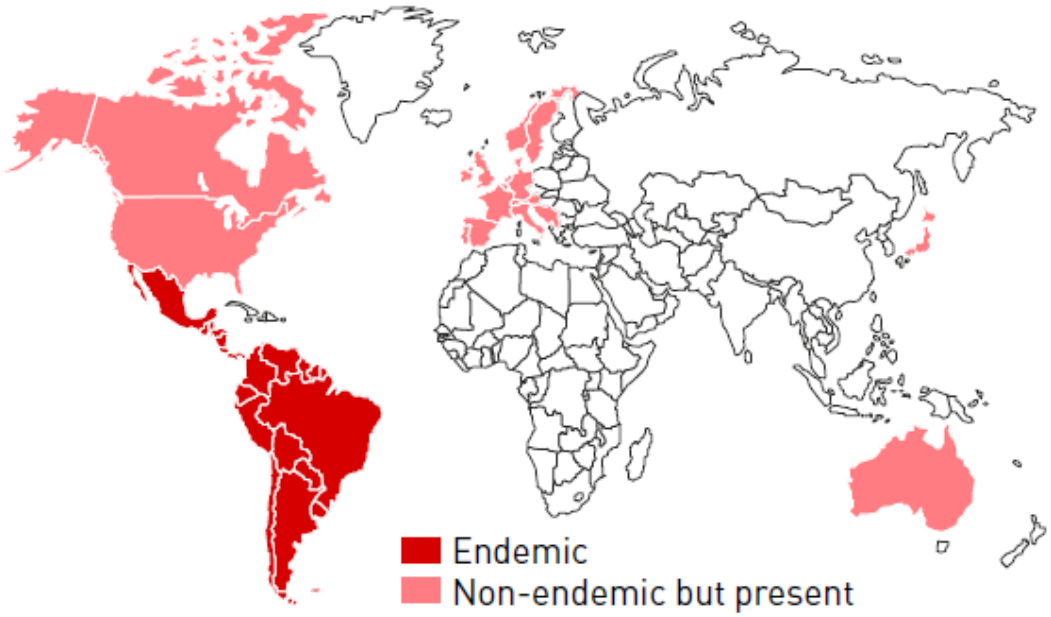

Fig1.1 Global distribution of Chagas disease.

Life cycle and infection

T. cruzi has a complex life cycle that involves four morphologically and biochemically distinct forms (Fig 2). The insect vector becomes infected by ingesting circulating parasites (trypomastigotes) while taking a blood meal from an infected mammalian host. In the mid gut of the vector, the trypomastigotes attach to perimicrovillar membranes through surface glycophosphatidylinositols and transform into epimastigotes and replicate. After 3–4 weeks, at the hindgut, epimastigotes differentiate into metacyclic trypomastigotes. *T. cruzi* is transmitted by deposits of feces, as infected triatomine bug takes a blood meal from sleeping human hosts, on

the membranes, the conjunctivas, the skin or other vulnerable surfaces. Oral ingestion of food or drink contaminated with infected faces can also lead to *T.cruzi* infection. Once in the host, the metacyclic trypomastigotes invade the nucleated cells and transform into the multiplying intracellular forms of amastigotes and multiply in the host cells, which then differentiate into trypomastigotes over a period of 4 to 5 days (9). Then trypomastigotes are released into the blood stream as the host cell ruptures and they then disseminate to invade new cells. Also, the trypomastigote may be ingested in blood meals taken by vectors. The trypomastigote then transform into epimastigotes in the midgut of the vector and complete the cycle.

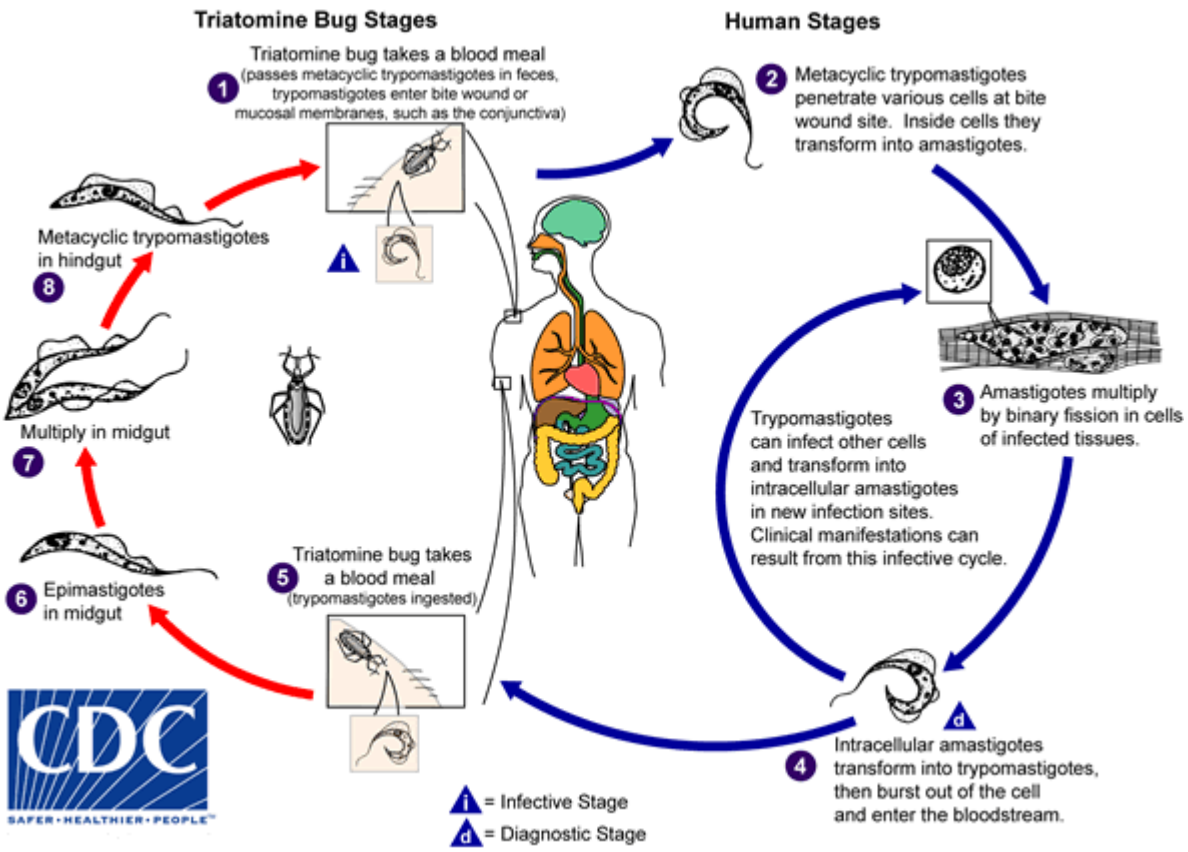

Fig 1.2 Life cycle of Chagas disease.

Clinical Chagas disease and pathology

There are three phases of Chagas disease: the acute phase, the indeterminate phase and the chronic phase. The acute phase happens shortly (1 to 2 weeks) after an initial infection. It is symptom free or exhibits only mild and nonspecific symptoms. The hallmark of the acute phase is microscopically detectable trypomastigotes in wet preparations of blood and cerebrospinal fluid. A newly infected individual may develop fever, chills, fatigue, vomiting, diarrhea, rash, headache and meningeal irritation. The signs on physical examination include enlarged liver or spleen, swollen glands and swelling at the site of entry- a chagoma (of the skin). The classic marker of acute Chagas disease is called Romaña's sign, which includes swelling of the conjunctiva or eyelids where the bug feces were deposited. The mortality rate of acutely infected patients (often children) are less than 1%, and they usually die due to congestive heart failure associated with severe inflammation of myocarditis and/or meningoencephalitis (10). The acute phase also can be very severe in people with depressed immune system. In most patients, the cell-mediated immune response controls parasitemia, and associated symptoms usually resolve spontaneously within 2 to 4 months (11). Approximately 70% of infected people do not present with evident tissue damage and organ dysfunction but in the presence of *T.cruzi* specific antibodies, and characterize the indeterminate phase. The remaining 30% of infected persons have progression to chronic Chagas' cardiomyopathy over a period of years or decades (12, 13). Patients develop either cardiac complications (cardiac form: cardiomyopathy) or digestive

disorders (digestive form: mainly megaesophagus and megacolon) or both (cardiodigestive form), and less than 5% of patients develop the neurological form of the disease (9, 14). The most serious and frequent manifestation of chronic Chagas disease is the dilated chagasic cardiomyopathy. The earliest signs are typically conduction system abnormalities, such as right bundle branch block or left anterior hemiblock (13). Left ventricular dysfunction are common in advanced Chagas' cardiomyopathy (15). Patients may develop atrial and ventricular arrhythmias, thromboembolism, dilated cardiomyopathy and congestive heart failure (16). Histological examination of the heart shows myocytolysis, myonecrosis and contraction band necrosis. Bands of fibrous tissue and extracellular collagen were also found as a result of massive and constant infiltration of inflammatory cells in the myocardium (17). Mother to baby transmission of infection from the placenta can cause abortion, prematurity and organic lesions in the foetus (18). Infected newborns may have no symptoms or exhibit low birth weight, hepatosplenomegaly, respiratory distress, cardiac failure and meningoencephalitis (19).

Treatment of Chagas' disease

Treatment of Chagas disease focuses on killing the parasite in acute infection and controlling signs and symptoms in chronic stages. Only two drugs are most effective early in the course of infection: benznidazole and nifurtimox. They are not yet approved by the Food and Drug Administration but can be obtained from the Centers for Disease Control and Prevention (CDC) and can be used under protocol. In patients

with acute Chagas' disease and early congenital Chagas' disease, both benznidazole and nifurtimox reduce the duration of parasitemia, attenuate the severity of symptoms and shorten the clinical course of illness. Cure rates reach 100% for congenitally infected newborns and over 60% for acute cases (9, 20, 21). However, both benznidazole and nifurtimox are not recommended to pregnant women or people with kidney or liver failure, and nifurtimox should not be taken by patients suffer from neurological or psychiatric disorders (22). Both benznidazole and nifurtimox have serious side effects that increase in frequency and intensity with the age of the patients (21, 23). The most common side effect of Nifurtimox in adult patients including gastric, psychiatric, and neurological complications (24, 25). Adverse effects of benznidazole includes dermatitis, peripheral neuropathy, angioedema, and bone marrow suppression (26). The treatment for chronic Chagas disease do not differ much from the treatment of other cardiomyopathies. The drug treatment for heart failure, arrhythmias and thromboembolism can be used. Yet the treatment outcome of chronic Chagas' patients with severe heart failure is very poor, so there is an urgent need to develop safe and effective new drugs for both disease stages.

1.2 Chronic Chagas heart disease: Potential pathological factors

It is suggested that compromised mitochondrial biogenesis, *T. cruzi*–induced inflammatory pathology and a feedback cycle of oxidative stress may contribute to chronic Chagas disease (27).

1.2a mitochondrial biogenesis and function defects in chronic Chagas disease

Heart function is supported by a high rate of ATP production through mitochondrial oxidative phosphorylation. Cardiomyocytes have a high copy number of mitochondrial DNA (mtDNA) that encodes essential components of respiratory complexes to support high-energy demands of the heart (28). Mitochondrial biogenesis is the processes and events resulting in growth and maintenance of mitochondria. Due to their bacterial origin, mitochondria have their own genome and possess the capacity of auto replication. Mitochondrial proteins are encoded by both the nuclear and the mitochondrial genomes. Mammalian mtDNA (mitochondrial DNA) is a circular double-stranded molecule of that encodes 13 proteins, all of which are subunits of electron transport chain necessary for respiration and oxidative phosphorylation. Mitochondrial DNA replication is mediated by a nuclear-encoded enzyme complex consisting of POLG (DNA polymerase gamma), SSBP (single strand binding protein) and PEO1 (DNA helicase). POLG1 is the only DNA polymerase present in the mammalian mitochondria essential for mtDNA replication.

Generation of new mitochondria requires the coordination between nuclear-encoded protein and mitochondrial-encoded proteins. PGC-1 (peroxisome proliferator–activated receptor gamma coactivator) is a master regulator of mitochondrial biogenesis. It is a member of the PGC family of transcription coactivators. It is preferentially expressed in tissues with high oxidative capacity and abundant mitochondria, such as the heart, kidneys, and skeletal muscle. PGC-1α is

located in the cell nucleus (29). PGC-1α plays an important role in the expression of nuDNA- and mtDNA-encoded genes that drive mitochondrial biogenesis and increase the capacity for oxidative phosphorylation (30). In response to a stimulus, PGC-1α activates estrogen-related nuclear orphan receptors ERR-α and ERR-γ which promote expression of genes involved in glucose and fatty acid uptake, energy production and ATP transportation (31). PGC-1 can also bind and co-activate transcription factors such as the nuclear respiratory factors 1 and 2 (NRF-1 and NRF-2) and upregulates the expression of nuclear genes encoding mitochondrial proteins, as well as the expression of mitochondrial transcription factor A (TFAM). Mitochondrial replication is initiated from the D-Loop region, where TFAM binds to the enhancer of the promoter and induces structural changes, which can expose the promoter region to the mitochondrial-specific RNA polymerase. This process generates mature RNA primers that are utilized by POLG to initiate mtDNA replication (32). Then the expression of the 13 mitochondrial DNA (mtDNA) encoded products is activated and assembled into enzyme complexes within the electron transport chain that mediate oxidative phosphorylation. This process leads to mitochondrial proliferation and increased mitochondrial content (29) (Fig 1.3).

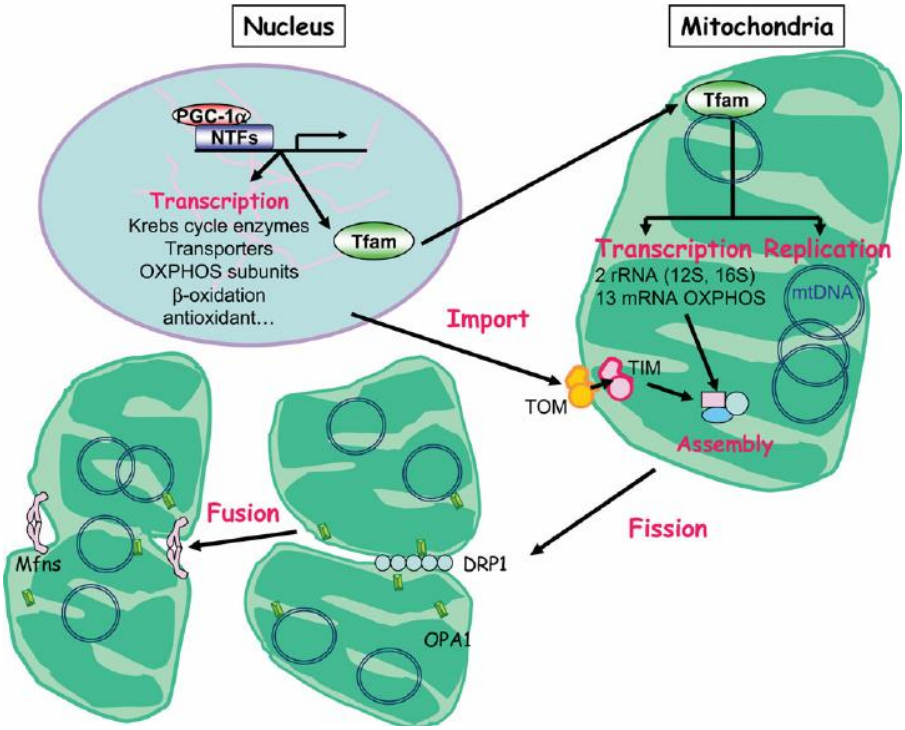

Fig 1.3 Transcriptional control of mitochondrial biogenesis.

The impairment of mitochondrial membrane phospholipids, DNA, or proteins can have multiple impact on mitochondria function, including enhanced permeability of the mitochondrial membranes, loss of the mitochondrial components, dissipation of the mitochondrial membrane potential and the decreased respiratory chain complexes activity (33) (34, 35). The eventual outcome is the impairment of the mitochondrial oxidative phosphorylation capacity, which has an adverse effect on energy production and cardiac performance. In infected human cardiomyocytes and chagasic hearts, mitochondrial biogenesis was impaired severely as evidenced by decreased mtDNA content. It is suggested that mtDNA replication impaired resulted in the significant loss of mtDNA and mtDNA-encoded proteins of oxidative phosphorylation pathway (36).

In a murine model of *T. cruzi* infection, *T. cruzi* alters plasma membrane and contributed to the mitochondrial permeability transition pore (MPTP) opening, leading to complex II and III activities constitutively decreased throughout the disease phase, and the complex V enzyme activity only defects during the chronic disease phase (37). Cardiac mtDNA content and mitochondria-encoded transcripts were also declined and the cardiac mitochondria OXPHOS-mediated ATP synthesis capacity were substantially reduced (36). Quantitative light and electron microscopic analysis showed that mitochondrial degenerative changes occur in early *T. cruzi* infection and are exacerbated with progression of disease in the myocardial biopsy samples from human chagasic patients and *T. cruzi* infected experimental models (38-41).

1.2b Oxidative stress in chronic Chagas disease

Oxidative stress results from elevated level of reactive oxygen species (ROS) and/or reactive nitrogen species (RNS). Reactive oxygen species (ROS) are chemically reactive species containing oxygen. Examples include superoxide (O2•−), hydroxyl radical (•OH), and hydrogen peroxide (H2O2). ROS are formed in the heart, vascular tissue, splenocytes and blood leukocytes through the action of specific oxidases and oxygenases (eg, NOX2), peroxidases (eg, myeloperoxidase, MPO) and as by-products of the electron transport chain of mitochondria (42). Reactive nitrogen species (RNS) are a family of molecules derived from nitric oxide (•NO) and superoxide (O2•−). In addition to ROS, activated macrophages can produce large amounts of nitric oxide (NO) by the inducible form of the NO synthase enzyme

(iNOS). ROS produced by the NOX2 catalyzed one-electron reduction of O2 and serves as the first line of host defense against microbes. In Chagas disease, two major ROS producers are NADPH oxidase (gp91phox or NOX2) and mitochondria (17). During *T. cruzi* infection, NOX2 was detected at the plasma membrane of peritoneal macrophages, resulting in activation and increased levels of ROS by NOX-dependent oxidative burst (43). Splenocytes of infected mice and *in vitro*-cultured macrophages also responded to *T. cruzi* infection by NOX2 activation and ROS production (44). In *T. cruzi* infected mice and in macrophages infected *in vitro* with *T. cruzi*, increased iNOS expression and •NO production is noted (45, 46). Also increased levels of myeloperoxidase and nitrite were found in the plasma of *T. cruzi*-infected mice (47). In humans, the •NO level was also elevated in patients with indeterminate Chagas disease in comparison to healthy controls (48). Phagosomal superoxide O2•− and nitric oxide (NO) promote peroxynitrite (ONOO−) mediated killing of *T. cruzi* in macrophages (49). Electron microscopic analysis of heart biopsies from chagasic patients and *T. cruzi* infected experimental animals has revealed that with disease development, mitochondria undergo degenerative changes including swelling, exhibit irregular membranes and loss of cristae (38-41). The functional decline of cardiac mitochondria in chagasic murine hearts was shown by impaired activities of respiratory complexes (37) and ATP synthase (CV) complex (50). Mitochondrial defects of the respiratory chain can lead to increased electron leakage and production of ROS that are harmful to mitochondrial and cellular components (51). Exposure to *T. cruzi* altered mitochondrial membrane potential and electron transport chain that result in leakage

of electrons to O2 and increased O2•− formation in infected human and murine cardiomyocytes and mouse chagasic heart (52, 53). ROS are also critical regulators of parasite control, modulating splenic inflammatory cell proliferation and the cytokine responses, and also play an essential role in the formation of adaptive immunity for parasite killing (45).

The overall level of cellular ROS is related with the relative rate of generation of ROS and the rate of reduction by antioxidants. The function of antioxidant system is to protect cells against oxidative damage. The critical antioxidants in cardiomyocytes including Mn2+ superoxide dismutase (MnSOD), glutathione peroxidase (GPx), Catalase (CAT) and Glutathione (GSH). The MnSOD catalyzes the dismutation of the superoxide (O2−) to produce either ordinary molecular oxygen (O2) or hydrogen peroxide (H2O2). Subsequently, H2O2 is converted to H2O by catalase (CAT) and guaiacol peroxidase (GPX). GPx converts H2O2 in the presence of GSH and form H2O and oxidized glutathione (GSSG). When the antioxidant system is compromised, ROS accumulation increase since cells are unable to efficiently scavenge the free radicals (54-56) . A variety of studies suggested that oxidative stress can be reliably evaluated by oxidative-damage biomarkers, such as lipid peroxides (57), protein carbonyls (58, 59) and GSSG levels (60, 61) .

During the acute phase of *T. cruzi* infection, glutathione antioxidant defense including GPx, GSR, and GSH were enhanced and contributes to host's ability to

control oxidative stress. In the chronic phase, ROS levels and GSSG, and lipid (MDA) and protein (carbonyl) oxidation products increased and associated with decreased MnSOD activity (62). In *T. cruzi* seropositive humans, increased GSSG and MDA contents are associated with decreased MnSOD, GPX activity, and GSH contents (63, 64). Moreover, the treatment of *T. cruzi*-infected rodents with an antioxidant preserved mitochondrial and cardiac function. *T. cruzi*-infected mice and rats, treated with phenyl-a-tertbutyl nitrone, a spin-trapping antioxidant, exhibited a significant decline in the myocardial accumulation of oxidative adducts and increased ATP synthesis (53, 65). Using a transgenic mouse model with overexpression of MnSOD decreased myocardial inflammatory and oxidative stress and remodeling responses elicited in Chronic Chagas Disease (66). All of these observations suggested that antioxidant inefficient scavenging of ROS resulting in sustained oxidative stress are important in the progression of human chagasic cardiomyopathy.

1.2c innate immune cells activated in in acute and chronic Chagas disease

Host resistance to *T. cruzi* depends both on innate and acquired immunity which are triggered during early phase of infection. We are focusing on the role of innate immune response in Chagas disease. Monocytes and Dendritic cells (DCs) are important mediators of the innate immune system and promote the development of adaptive immune responses. When infected with *T cruzi*, macrophages and dendritic cells and secrete IL-12, TNF-α, and costimulatory molecules, and then prime IFN- γ -producing specific T cells (67). These steps occur shortly after initial infection and

can help to control, but not complete elimination of parasitism. Others have shown that *T. cruzi* in DCs reduced DC antigen presentation capacity (68). It has also been reported *T. cruzi* enhances the production of IL-10 and reduces the IL-12 levels in DCs from Chagasic patients compared with DCs from healthy donors (69). The interaction of *T. cruzi* with macrophages and dendritic cells are mediated by pathogen recognition receptors such as TLRs that play an important role in the recognition of components of pathogens by the innate immune system. Upon binding to its specific ligand (Toll/IL-1R domains) via pattern recognition, TLRs induce the recruitment of cytosolic adaptor molecules myeloid differentiation primary-response protein 88 (MyD88) and subsequently activate nuclear factor-κB (NFκB) signaling, leading to the production of inflammatory cytokines (70). *T. cruzi*-derived molecules, such as glycosylphosphatidylinositol (GPIs) and mucins stimulate the TLR2-dependent leukocyte recruitment via CCL2 and led to the synthesis of IL-12 and TNF-α (71-73). Mice deficient in TLR2 and its adaptor molecule MyD88 infected with *T. cruzi* resulted in decreased production of proinflammatory cytokines and enhanced parasitemia (74). Infection of mice naturally deficient in TLR4 lead to reduced GIPL-induced neutrophil recruitment, higher parasitemia and earlier mortality (75). *T cruzi* also induces Th1 response by expressing kinin releasing cysteine protease (cruzipain), through maturation of Bradykinin B2 receptors (B2R) of dendritic cells (72, 76). Parasite-derived GIPLs and DNA are recognized by TLR2, TLR4 and TLR9, activating the production of proinflammatory cytokines and microbicidal effectors (71, 77). Upon *T. cruzi* infection, TLR9 and TLR2 deficient mice exhibit decreased *in vivo* IL-12/IFN- γ

responses and enhanced susceptibility to infection (78).Thus, parasite antigens and the released cytokines cooperate to promote the development of protective Th1 response and the control of parasite growth. Efficient control of intracellular *T. cruzi* infections is dependent on cytokine-mediated macrophage activation of macrophage-mediated killing of the parasite. The role of macrophage polarization in chronic Chagas disease is not well defined. So it is important to understand how M1/M2 macrophages lead to dysfunctional immune responses in chronic Chagas disease.

Blockage of type 1 cytokines (IFN-γ, TNF-α) by using genetic knockout mice or antibodies depletion of specific immune molecules is associated with an increased susceptibility to *T. cruzi* infection (79-81). The immunoregulatory cytokines IL-10 and TGF-β correlates with a susceptibility to acute *T. cruzi* infection (82, 83). Neutralization of endogenous IL-10 resulted in an increase in *T. cruzi*-induced IFN-γ production as well as parasite killing (82, 83). Mice deficient in IL-10 infected with *T. cruzi* had severe negative effects due to enhanced levels of TNF-α and IFN-γ (84). Collectively, these results suggested that both inflammatory and anti-inflammatory responses play an important role during *T. cruzi* infection and that the ratio of IL-4 + IL-10/TNF-α + IFN-γ may be an important determinant of disease outcome.

1.3 SIRT1: a potential therapy in Chronic Chagas disease

Sirtuins, initially named as Silent information regulator 2 (Sir2) proteins, are defined as class III histone deacetylases. Sirtuins are nicotinamide adenine

dinucleotide (NAD+) -dependent protein deacetylase. In the deacetylase reaction, sirtuins hydrolyze one NAD+ molecule and resulting in the production of nicotinamide (NAM), the deacetylated substrate, and an O-acetyl-ADP ribose (85). In mammals, seven members of sirtiuns have been found and named as SIRT1-SIRT7. Sirtuins are ubiquitously expressed in all organs of the body including brain, heart, liver, testis, ovary, muscle, lung, kidney, blood and spleen at various levels. The seven mammalian Sirtuins share a conserved catalytic core deacetylase domain, but differ in sequence, subcellular location, enzyme activity, substrate specificity and physiological functions (86, 87). SIRT1, SIRT6 and SIRT7 are generally localized in nucleus and modulate transcription through transcription factors, co-factors or histones (88-92). SIRT2 is found in the cytoplasm and regulates oligodendrocyte differentiation and cell cycle (93, 94). SIRT3, SIRT4, and SIRT5 primarily reside in mitochondria and mediate metabolic enzymes activities and oxidative stress pathways (95, 96)

SIRT1 is the closest homologue of yeast Sir2 and has been studied most (97). At the cellular level, SIRT1 is expressed in both the nucleus and cytoplasm with dominant presence in the nucleus. SIRT1 may shuttle between the nucleus and cytoplasm depending on environmental conditions (98). SIRT1 has two nuclear localization signals and a coiled-coil domain in addition to the core deacetylase domain. Endogenous substrates of SIRT1 are abundant including p53, NBS1, p65, c-Jun and c-Myc (99-103). SIRT1 activity is mainly dependent on its core deacetylase domain, but other domain regions could regulate substrate binding as well. SIRT1 mediated

deaceylation activity regulates a number of proteins and their translation and involved in critical physiological processes including oxidative stress, metabolism, cell proliferation, and genomic stability. SIRT1 has been reported to associate with chronic inflammatory diseases, metabolic dysfunctions, neurodegenerative diseases and cardiovascular dysfunction (104-107).

1.3a the role of SIRT1 in mitochondrial biogenesis

One of the primary targets of SIRT 1 deacetylation is the PGC-1 α. SIRT1 and its substrate, PGC-1α, regulate energy metabolism and induce mitochondrial biogenesis. PGC-1 α co-activates the transcription factor NRF1 and NRF 2, which, in turn, activates the expression of TFAM. TFAM translocates to mitochondrial matrix to regulate mitochondrial DNA replication and the expression of the 13 mitochondrial DNA (mtDNA) encoded gene products. PGC 1 α undergoes various post-translational modifications including acetylation and phosphorylation. Acetylation of PGC-1 α alters it's localization within the nucleus. Studies have shown that deacetylation of PGC-1 α is dependent on SIRT1 activity (108-112). Additionally, mutation of the acetylation sites which mimics the deacetylated state, markedly enhances basal PGC-1a activity (112). Early work from Finkel's group found out that SIRT 1 may physically and functionally interacts with PGC-1 α through ADP-ribosyltransferase domain of SIRT 1 (111). They found that ADP-ribosyltransferase domain mutation prevents SIRT 1's interaction with PGC-1 α. It is also believed that SIRT 1 acts as a sensor of changes in nutrient and energy metabolism. Puigserver's group showed that SIRT 1 was

activated by fasting, and the interaction of SIRT 1 and PGC-1 α enhanced the expression of hepatic gluconeogenic genes (112). The group also found that SIRT1 deacetylation of PGC-1 α in skeletal muscle is required for expression of mitochondrial fatty acid oxidation genes (109).

Resveratrol (3,5,4′-trihydroxy-*trans*-stilbene), is a natural phytoallexin which protects the plants from fungi infection. The structure of resveratrol is depicted in Fig 1.4. It is found in grapes skin, red wine, berries, peanuts, roots of rhubarb and other plants and has multiple biological effects. Resveratrol was first described in 1940 from the roots of white hellebore, however, in 1992 it was found that resveratrol have the cardio-protective effects of red wine and was suggested to be contribute to low incidence of cardiovascular disease in French population (12). In 1997, a report in Science suggested that resveratrol can inhibit growth of cancer cells in culture (113). In 2003, a compound screen for small molecule activators of SIRT1 identified 15 SIRT1 activators and resveratrol was the most potent one. In a number of studies, resveratrol has been found to increase life span in yeast, nematode, flies and fish (114, 115). In rodents, resveratrol has been shown to prevent or slow the progression of diverse illnesses, including cardiovascular diseases, brain disorders, and cancer (116-118). Auwerx's group showed that resveratrol treatment of mice resulted in the improved running time and increased oxygen consumption in the skeletal muscles,

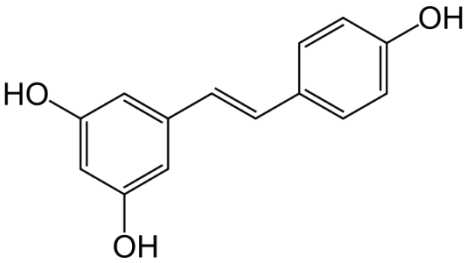

Fig 1.4 Structure of Resveratrol.

which is associated with the activation of genes for oxidative phosphorylation and mitochondrial biogenesis (110). The authors also revealed that resveratrol treatment prevented diet-induced-obesity and insulin resistance in mice and attributed these benefit to activation of SIRT1 and a consequential decreased PGC-1 α acetylation. Studies also showed that treatment with resveratrol produces a variety of benefits including increasing mitochondrial content, and the anti-oxidative capacity, reduced inflammation, improved metabolic and vascular function (110, 119-121). All of the resveratrol effects may be related to its ability to induce SIRT1 activity.

SRT1720 was first identified in a high-throughput *in vitro* fluorescence polarization assay which is used for screening SIRT1 agonists (122) . SRT1720 was found about 1,000-fold more potent than resveratrol in activating SIRT1 activity. SRT1720 binds to the SIRT1 enzyme-peptide substrate complex and contributed to deacetylation of SIRT1 target proteins in both cells and animals (122, 123). The structure of SRT1720 is depicted in Fig 1.5. It is one of the pharmaceutical compounds that are being studied for their efficacy in the treatment of metabolic and chronic diseases. It improves mitochondrial respiration in a SIRT1- and PGC-1α-dependent manner. *In vivo* studies, SRT1720 has been shown to improve insulin sensitivity, lower plasma glucose, improve mitochondrial capacity and oxidative metabolism in skeletal muscle, liver, and

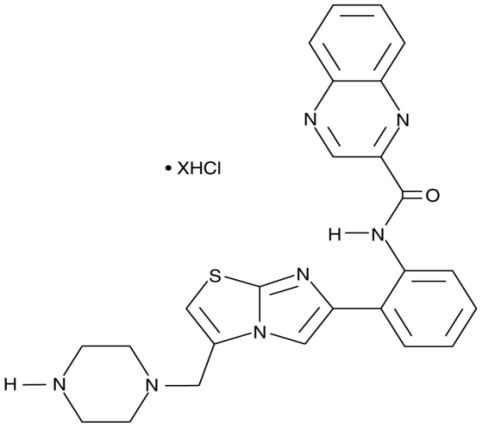

Fig 1.5 Structure of SRT1720.

brown adipose tissue of obese mice and rats (122-124). In addition, C2C12 cells treated with SRT1720 exhibited increased express of citrate synthase activity and ATP levels indicating the improvement of mitochondrial biogenesis (125). Poly(ADP-ribose) polymerase (PARP)-1 is an NAD + -dependent nuclear ADP-ribosyltransferase (112) which is activated upon binding to damaged or abnormal DNA (122), and catalyzes the formation of poly(ADP-ribose) (PAR) chains on itself and other proteins (113, 123, 126). The PARP family of proteins are involved in a number of cellular processes including: DNA damage, DNA response, cell death and regulation of transcriptional, cell cycle and telomere [19]. Because both SIRT1 and PARP-1 depends on NAD+ availability, cross talk between them has been suggested. It was reported that deletion of the PARP-1(a major NAD+-consuming enzyme) resulted in increased SIRT1activity. PARP-1 knockout mice exhibited an increased mitochondrial content and energy expenditure, and were protected against metabolic disease (126) confirming that SIRT1 activity is associated with mitochondrial biogenesis.

1.3b the role of SIRT1 in oxidative stress

Oxidative stress is characterized by increased intracellular levels of reactive oxygen species (ROS) and decreased antioxidant capacity (127). Oxidative stress is thought to play a key role in the pathophysiology of many diseases, including atherosclerosis, diabetic mellitus, and myocardial dysfunction (128). There is an extensive crosstalk between the SIRT1 expression and the level of oxidative stress.SIRT1 has gained much attention due to its role in oxidative stress resistance

through SIRT1/FOXOs, SIRT1/NF-κB, SIRT1/NOX, SIRT1/SOD, and pathways.

SIRT1 and FOXOs

FOXOs (Forkhead box) proteins are a family of transcription factors. FoxO family includes 4 members: FoxO1, FoxO3, FoxO4 and FoxO6 (129). In response to various stress events, FoxO proteins translocate from the cytosol into the nucleus and are involved in regulation of cell cycle, cell immunity and oxidative stress. The SIRT1/FoxO axis was shown to regulate cellular responses to both metabolic changes and oxidative stress. A number of studies have demonstrated that SIRT1 can deacetylate the FoxO factors, such as FoxO1, FoxO3a and FoxO4, and subsequently activate the expression of antioxidants catalase, MnSOD and Trx, and through an auto-feedback loop also enhance SIRT1 auto-transcription and expression (130-134). Under conditions of oxidative stress, SIRT1 has been shown to interact with FOXO3 and form a complex both *in vivo* and *in vitro*, and SIRT1 can deacetylate FOXO3 to enhance antioxidant response (135). SIRT1 increases FOXO1 and FOXO4 DNA-binding ability by deacetylating FoxO1 and prevented oxidative stress (131, 136). Overexpression of FoxO1 increases SIRT1 expression, and depletion of FoxO1 by siRNA reduces SIRT1 expression in vascular smooth muscle cells and HEK293 cells suggesting that FoxO1 is a positive transcriptional regulator of SIRT1(133).

SIRT1 and antioxidant

Antioxidants are a complex system of defenses that inhibit the accumulation of

oxidants. The antioxidant proteins including uncoupling protein 2 (UCP-2), Mn superoxide dismutase (MnSOD), glutathione peroxidase 4 (Gpx4), peroxiredoxin 5 (Prx5), thioredoxin 2 (Trx2) and glutation peroxidase 1 (GPx1)(137). Studies have demonstrated that MnSOD expression was significantly compromised in the aortas of diabetic WT mice, whereas endothelium-specific SIRT1 transgenic mice successfully restored the MnSOD expression, suggesting the the SIRT1/MnSOD pathway may contribute to the protection against hyperglycemia-induced endothelial dysfunction (138). Similarly, treatment of resveratrol increased MnSOD expression ameliorate endothelial oxidative stress. This effect was mimicked by SIRT1 overexpression and diminished by SIRT1 knockdown (139) suggested that SIRT1 promote MnSOD expression and increase the oxidative stress resistance. SIRT1 has also been reported to regulate some transcription factors which are involved in cellular redox balance. Nrf2 is a transcription factor that plays an important role in cellular antioxidant defense by binding to the antioxidant response element (ARE). It has been reported that Melatonin has anti-oxidative effect through activation of the SIRT1-dependent transcription factor Nrf2 in the developing rat brain and in BV2 cells, and SIRT1 inhibitor significantly decreased the protein expression of SIRT1 and Nrf2 in BV2 cells (140). SIRT1 has also been demonstrated to enhance the activation of the Nrf2/ARE antioxidant pathway, and thus inhibiting the apoptosis in mouse type II alveolar epithelial cells (141).

SIRT1 and NOXs/ROS

In aerobic organisms, ROS can be generated by various sources, such as mitochondrial electron transport chain, xanthine oxidase and myeloperoxidase. However, the nicotinamide adenine dinucleotide phosphate (NADPH) oxidase family (NOX enzymes) is the only enzyme family that produces ROS as its main product (142). The NADPH oxidase (NOX) family consists of seven members including: NOX 1–5 and two dual oxidases (DUOXs), DUOX 1 and DUOX 2 (143). NOX enzymes play an important role in host defense, posttranlational processing of proteins, regulation of pH and ion concentration in the phagosome and cell differentiation (143). However, NOX can also lead to a wide range of pathological processes and tissue damage for their participation in ROS production. SIRT1 has been demonstrated to inhibit NOX production. It was reported that SIRT1 inhibition contributed to upregulation of NOX oxidase subunits, p22phox, and NOX4, eventually leading to increased ROS levels and endothelial dysfunction (144, 145). Quercetin has been reported to induce SIRT1 expression and increased AMPK activity, and subsequently decreased NADPH production, thus providing protective effects against the hyperglycemia-induced oxidant damage in HUVECs (146).SIRT1 can also through inhibition of NF-κB signaling, reduce the expression of NADPH oxidase components, such as gp91 phox and p22phox and thus prevent the production of oxidative stress and reactive nitrogen radicals (147-151).

1.3c the role of SIRT1 in inflammatory stress

SIRT1 and NF-κB

The NF-κB transcription factor family consists of five proteins including p65 (RelA), RelB, c-Rel, p105/p50 (NF-κB1), and p100/52 (NF-κB2) that regulates transcription of DNA, cytokine production and cell survival. In the absence of stimuli, NF-κB remains in an inactive form in the cytoplasm through association with inhibitory IκB proteins. IκB kinase (IKK) mediates IκB phosphorylation and leads to the degradation of IκB, NF-κB is then translocated to nucleus and activated to induce transcription of target genes (152). SIRT1 plays a key role in regulating immune responses through NF-κB signaling and in that way also modulates the ROS production. SIRT1 deacetylates the RelA/p65 subunit of NF κB at Lys310 residue and inhibit NF-κB activity (101). The N-terminal domain of SIRT1 is a positive regulator of the SIRT1 deacetylation NF-κB p65 and inhibits NF-κB transcription (153). Resveratrol has been demonstrated to inhibit TNF-α-induced injury through SIRT1-induced repression of NF-κB and ROS generation in Human Umbilical Endothelial Cells (154). SIRT1 can also inhibit NF-κB by activating AMPK and PPARα, which inactive the NF-κB pathway and prevents ROS generation. At the same time, NF-κB transcription can also suppress SIRT1 activity by promoting ROS production (155). Taken together, all these findings suggest that SIRT1 controls NF-κB signaling and ROS, and NF-κB itself could regulate SIRT1 levels through ROS production.

SIRT1 and acute inflammation

Acute inflammation is a response to eliminate the source of the tissue injury and restore immune homeostasis and it occurs over seconds to days. Innate immune cells

initiate an acute inflammation in response to an intense environmental stimulus following an adaptive phase for termination. Innate immune cells including monocytes/macrophages, granulocytes, and dendritic cells all express Toll-like receptors (TLR) to sense different pathogen-associated molecular patterns (PAMPs) and rapidly initiate an inflammatory response, which is associated with activation of the NF-κB family of transcription mediators (156). The TLR signal lead to NF-κB /p65 to translocate to the nucleus and bind gene promoters of inflammatory mediators to represses the transcription of pro-inflammatory genes. Transcription regulation of the switching from the early acute inflammatory to the adaptive anti-inflammatory state requires SIRT1-dependent deacetylation of histone proteins including H1K26, H4K16, H3K9, and H3K14 and recruit of new methyltransferases (157). SIRT1 also regulates metabolism of the acute inflammatory process by mediating a metabolic switch during adaptation (158-160). In the initiation phase, TLR activation rapidly increases glucose level for supporting the expression of proinflammatory genes, and activates the expression of HIF-1α which switches mitochondrial glucose oxidation to glycolysis. SIRT1 activates PGC-1 and increases the flux of fatty acids and transfer of fatty acids into mitochondria, providing fat as an alternative source for mitochondrial respiration (157).

SIRT1 and chronic inflammation

Chronic inflammation is caused by persistent low-level of stimulation, even a life span. SIRT1 has been considered as a potential negative regulator of chronic

inflammation. Partial or complete loss of SIRT1 activity and/or protein levels in specific tissue were observed in many chronic inflammatory diseases. Examples include fat deposits in obesity (161), lung in chronic obstructive pulmonary disease (COPD) (162), brain in Alzheimer’s disease (163), and arterial inflammation in atherosclerosis (164), and skin in aging (165). Loss of SIRT1 activity in chronic inflammation may contribute to persistent hyperactivation of nuclear NFκB/p65 and elevation of pro-inflammatory cytokines which finally lead to metabolic syndromes (166). The mechanisms of SIRT1 levels decline during chronic inflammation are not very clear. Enhancing NAD+ levels (167) or activating SIRT1 by resveratrol suppressed chronic inflammation and regulate metabolism and homeostasis (168). It is suggested that cellular bioenergetics coordinated with SIRT1 provide a regulation axis (positive and negative) that controls both inflammation, cellular and whole organism metabolism (169).

1.4 The role of SIRT1 in phenotype and function of macrophages

Phenotype and function of macrophages

Macrophages are immune cells which quiescently survey the various tissue milieu for early signs of infection or damage (170). Macrophages were originally identified by Elie Metchnikoff (Nathan CF 2008), who won the Nobel Prize for Medicine in 1908 by proposing their phagocytic nature. Macrophages can be found in tissues or circulate in peripheral blood. Until recently, it was believed that macrophages were solely derived from circulating peripheral-blood mononuclear cells (PBMcs), which migrate into tissue under both steady-state and inflammatory conditions (171). These PBMcs

differentiate from common myeloid progenitor cells in the bone marrow. The monocytes originate from hematopoietic stem cell (HSC) monoblasts, and sequentially give rise to a series of differentiation stages: the common myeloid progenitor (CMP) (172), the granulocyte- macrophage progenitor (GMP) (172), the common macrophage and DC precursor (MDP) (173), and finally the monocyte progenitor (cMoP), which are released into the bloodstream. Monocytes migrate from the blood and then get recruited to injury sites. Recent studies have demonstrated that some tissue resident macrophages (e.g., brain, liver, heart and lung) may be develop in utero during fetal life (171). These embryonic macrophages have the ability to self-renew during development and throughout life in adult tissues. These tissue resident macrophages can maintain their local populations by rapid proliferation in response to injury.

Macrophages have different functions including phagocytosis of debris and pathogens, dead cell clearance, matrix turnover, modulate of fibrosis and wound healing. The plasticity of the inflammatory monocytes allows them to change their phenotype based on the environment cues or alter the immune responses after exposure to a specific stimulus. Macrophages have been classified as M1 (classically activated macrophages) or M2 (alternatively activated macrophages). Classical activation of macrophages occurs when the cell receives stimuli such as LPS, IFN-γ and granulocyte-macrophage colony stimulating factor (GM-CSF), which induces secretion of high levels of pro-inflammatory cytokines such as IL-1β, TNF-α, IL-12, IL-

18 and IL-23. The M1 macrophages play a central role in host defense against bacterial and viral infections (174, 175). It helps to drive antigen specific Th1 and Th17 cell inflammatory responses, produces pro-inflammatory cytokines, chemokines of CXCL9 and CXCL10, expresses high levels of major histocompatibility complex class II (MHC II), the CD68 marker, and co-stimulatory molecules CD80 and CD86. M1 macrophages have also been shown to harm neighboring cells in the microenvironment by producing toxic reactive oxygen intermediates (ROS) and up-regulate the expression of inducible nitric oxide synthase (NOS2 or iNOS) to produce NO from L-arginine (176-178). M2 macrophages play a central role in parasite control, wound-healing, fibrosis, tumor progression and immune regulation (178). M2 macrophage activation is induced by fungal cells, parasite infections, immune complexes, apoptotic cells, macrophage colony stimulating factor (M-CSF), IL-4, IL-13, IL-10 and TGF-β and chemokines CCL17, CCL22 and CCL24. This leads to the secretion of extracellular matrix (ECM) components, angiogenic and chemotactic factors and high amounts of IL-10. On the basis of the stimulus from the microenvironment and their distinct gene expression profiles, M2 macrophages can be further divided into subsets, specifically M2a, M2b, M2c and M2d (179, 180). M2a is a profibrotic phenotype and is elicited by IL-4, IL-13 or fungal and helminth infections (179, 181). M2b is induced by IL-1 receptor ligands, Toll-like receptor, immune complexes and LPS (179). M2c is elicited by IL-10, TGF-β and glucocorticoids (181). M2d, is stimulated by IL-6 and adenosine (182).

SIRT1 inhibits differentiation of monocytes to macrophages

Monocytes are a group of white blood cells which are produced in bone marrow and circulate in the blood, bone marrow, and spleen. Monocytes circulate in the bloodstream for about one to three days and then migrate to other tissues and differentiate into tissue resident macrophages or dendritic cells. Monocytes have been identified as the systemic reservoir of myeloid precursors for renewal of tissue macrophages and dendritic cells. The differentiation process is regulated by (a) signals leading to the migration of the monocyte into tissues, (b) signals which determine the characteristic subpopulation of macrophage and (c) cytokines released by other cells. Resveratrol has been reported to inhibit the expression of macrophages surface markers CD11b, CD14, and CD36 in RAMCs (synovial fluid of rheumatoid arthritis) and THP-1 monocytes, and the suppressive effect was antagonized by pretreatment with sirtinol (SIRT1 inhibitor). PMA-stimulated BMDMs from SIRT1 Tg mice displayed reduced adhesion to culture dishes and decreased CD11b and CD14 mRNA expressions as compared with wild-type mice. And this inhibition of monocyte differentiation by SIRT1 was through suppression of PU.1 phosphorylation (183).

SIRT1 regulates macrophage migration

Cell migration is a complicated process in the development and maintenance of multicellular organisms. It is regulated by the activation of various signaling molecules. SIRT1 deletion in myeloid cells results in the development of systemic insulin resistance through hyperactivation of the NF-κB pathway suggested that SIRT1 might

mediate macrophage migration by targeting NF-κB pathway (184). Other studies also indicated that NF-κB is an essential coordinator of macrophage migration both *in vitro* and *in vivo* in murine models of obesity-induced inflammation (185-187). Myeloid-specific SIRT1-deleted mice (mS1KO) fed a high-fat diet (HFD) displayed significant increased macrophage infiltration into pancreas, liver and adipose tissue compared with WT mice (188). Deletion of SIRT1 promote nuclear translocation and acetylation of NF-κB subunits as well as acetylation and expression of FAK in macrophages suggested that SIRT1 might regulate macrophage migration by targeting both NF-κB and FAK pathways. In inflammatory arthritis, mSIRT1 KO mice displayed increased macrophage infiltration in the synovial tissues as compared to WT mice (189). In a non-obese mouse model of type 1 diabetes, resveratrol has been found to block the macrophage migration from peripheral lymphoid organs to the pancreas (190). In addition, in a mouse model of colitis, resveratrol treatment decreased percentage of CD11b+ macrophages to the normal level in mesenteric lymph nodes and the lamina propria which are otherwise increased during colitis (191).

SIRT1 regulates macrophage polarization and tissue inflammation

In response to distinct signals, macrophages are functionally polarized into classically activated macrophages (M1 macrophages), and alternatively activated macrophages (M2 macrophages) (192) (179). SIRT1 regulates macrophage polarization by inhibition of M1 and stimulation of M2 macrophage activation. In high fat diet-induced mouse model of obesity, increasing obesity triggers a switch in the

macrophage phenotype from M2 macrophages towards M1 cells in adipose tissues, leading to insulin resistance (193). SIRT1-deficient bone marrow derived macrophages exhibited a significant increase in basal and IFN-r/LPS stimulated iNOS expression, suggesting that SIRT1 deletion promoted polarization of classically activated M1 macrophages (194). SIRT1-deficient bone marrow derived macrophages also displayed a significant inhibition of IL-4-stimulated expression of M2 macrophage markers of Arg-1 and MGL1 (194). Moreover, myeloid cell-specific deletion of SIRT1 increased infiltration of M1 macrophages and decreased M2 macrophages in adipose tissue (194). Macrophages are implicated in initiating and sustaining inflammation. When macrophages are exposed to inflammatory stimuli, they induce secretion of large amounts of cytokines such as TNF-α, IL-1, IL-6, IL-8, and IL-12. SIRT1 inhibition on the NF-κB pathway has a vital role in suppressing the pro-inflammatory phenotype of macrophages. *In vitro*, knockdown of SIRT1 in RAW264.7 cell line and in mouse intraperitoneal macrophages, activates the JNK and IKK inflammatory pathways, and enhanced expression of TNF-α, IL-1β, MMP9, MCP-1, KC and IL-6 when stimulated with LPS (118). SRT1720 treatment inhibited LPS-stimulated inflammatory pathways, as well as secretion of TNF-α in RAW264.7 cells and in primary intraperitoneal macrophages (118). Myeloid-specific SIRT1-deleted mice (mS1KO) fed a high-fat diet (HFD) displayed increased accumulation of macrophages TNF-α, IL-1β and IL-6 in mS1KO mice compared with WT mice (188).

SIRT1 in regulation of phagocytosis and killing

Macrophages are professional phagocytes and highly specialized in engulfing particles, including apoptotic cells and invading pathogenic organisms, which are crucial for nonspecific immune responses (195). Besides regulating the NF-kB pathway, SIRT1 also has an essential role in activator protein 1(AP-1) transcriptional activity through deacetylation in macrophages. SIRT1 could inhibit the transcriptional activity of AP-1 by directly interacting with the basic leucine zipper domains of both c-Fos and c-Jun, decreasing the expression of COX2, the enzyme for prostaglandin synthase. Consequently, over-expression of SIRT1 in macrophages prevent the prostaglandin E2 production, and improved PGE2-related phagocytosis activity and the bacterial killing function as well as tumoricidal activities in RAW264.7 cells and peritoneal macrophages (196-198). While antitumoral activity has been significantly impaired by knockdown of SIRT1 in peritoneal macrophages (198). SIRT1 has also been reported to be negatively regulated by miR-34a, which is recognized as a p53-dependent tumor suppressor, negative mediate apoptotic cell uptake by resident murine and human tissue macrophages. Another study demonstrated that SIRT1 knockdown in bone marrow-derived macrophages modestly reduced the ability of bacterial killing (199). However, pharmacologic activation or inhibition of SIRT1 does not change bacterial killing capacity of mouse- or human-derived intraperitoneal macrophages and alveolar macrophages (199). Further study needs to be done to understand how SIRT1 regulates efferocytosis and killing as well as what causes the different effects of SIRT1 on the phagocytosis and killing.

SIRT1 regulates autophagy in macrophages

Autophagy is an intracellular self-digestion process pathways that degrade lysosomes to recycle soluble macromolecules and damaged organelles and has been recently shown to regulate inflammatory responses. Macrophages involved in the inflammatory process and autophagy exerts a protective effect against cellular stresses such as atherosclerosis (200). SIRT1 could influence autophagy directly through its deacetylation of Atgs (as Atg5, Atg7 and Atg8 which are autophagy proteins required for the formation and elongation of the autophagosomal membrane) and is NAD+ dependent (201, 202). Nucleus-localized SIRT1 has also been demonstrated to enhance the expression of autophagy pathway components *via* the activation of FoxO transcription factors (203). Resveratrol treatment can induce both autophagosomes and autophagy marker proteins such as Atg5, Atg7 and LC3-II/LC3-I by a moderate stimulus of oxidized low-density lipoprotein, and enhance efferocytosis of apoptotic RAW264.7 cells (204). In human THP-1 cells, treatment with Sirtinol (a chemical inhibitor of SIRT1) induced inflammation through NF-kB activation and is associated with autophagy dysfunction, through p62/Sqstm1 accumulation and decreased expression of light chain (LC) 3 II. In addition, inhibition of SIRT1 resulted in the activation of the mammalian target of rapamycin (mTOR) pathway and decreased 5'-AMP activated kinase (AMPK) activation, leading to the impairment of autophagy (205). Studies also suggested that SIRT1-mediated autophagy is one of the mechanisms of metformin treatment ameliorate hepatosteatosis in type 2 diabetic ob/ob mice (206). Also, silencing of SIRT1 expression by siRNA inhibited gAcrp-

induced nuclear translocation of FoxO3A and LC3II protein expression, indicating that SIRT1 expression contributes to autophagy in RAW 264.7 macrophages (207). Further studies are needed to characterize the detailed mechanism of SIRT1 dysregulation of autophagy in macrophages.

SIRT1 attenuated nitric oxide (NO) production

NO (Nitric oxide, nitrogen oxide, nitrogen monoxide) is a diffusible radical gas produced by the activity of a group of enzymes known as nitric oxide synthase (NOS). Nitric oxide (NO) is a critical mediator of macrophage function. NOS activity in macrophages has a protective role against invading pathogens through generation of reactive nitrogen intermediates (RNIs). Compared with wild-type control mice, iNOS-deficient mice exhibited enhanced classically activated M1 macrophage polarization but no major effects on alternatively activated M2 macrophages; eNOS and nNOS mutant mice also displayed comparable M1 macrophage differentiation (208). iNOS inhibition by N6-(1-iminoethyl)-L-lysine dihydrochloride in tumor microenvironment facilitated M1 macrophage polarization, resulting in the decrease of tumor size (208). SIRT1 activation by celecoxib inhibit Nitric oxide (NO) and activates catalase as well as peroxidase enzymes and inhibits bacterial inflammation in in RAW 264.7 macrophages (208). Ectopic expression of constitutively active FoXO in RAW264.7 cells enhances LPS-induced gene expression of iNOS. A gene-specific shRNA depletion of FoXO transcription factors expression prevented this effect and SIRT1 deacetylation of FoXO can reverse it (136, 209). In the M1 polarization condition,

iNOS expression was significantly increased in BMMs from mSIRT1 KO mice (189).

In summary, there are still many questions to establish the role of SIRT1 in regulation of macrophage function. Further studies on the detailed mechanism and development of new techniques for probing the role of SIRT1 in macrophage are needed. The future goal is clinical application of SIRT1 in treating chronic inflammation and it holds substantial therapeutic promise.

CHAPTER 2: SIRT1-PGC1α-NFκB pathway of oxidative and inflammatory stress during *Trypanosoma cruzi* infection: benefits of SIRT1-targeted therapy in improving heart function in Chagas disease

2.1 Introduction

Trypanosoma cruzi (*T. cruzi* or *Tc*) is the etiological agent of Chagas disease that is endemic in Latin America (1). After an exposure to parasite, infected individuals develop mild-to-no overt clinical symptoms. However, several decades later, ~30% of the infected individuals progress to heart failure associated with cardiac fibrosis, ventricular dilation, and thrombosis (210, 211). Vectors infected with *T. cruzi* are also present in the southern US (212), and CDC estimates that >300,000 infected individuals are living in the US (3, 213). Currently only two drugs are available for the treatment of *T. cruzi* infection: nifurtimox and benznidazole. These drugs are curative in early infection phase, but exhibit high toxicity and limited-to-no efficacy against chronic infection (214). Thus, there is a need for new drugs for the treatment of chronic Chagas disease.

Mitochondria are the prime source of energy, providing ATP through oxidative phosphorylation (OXPHOS) pathway. A high copy number of mitochondrial DNA (mtDNA), reported to be ~6500 copies per diploid genome in myocardium (215), as well as the integrity of each mtDNA molecule is required to meet the high energy demand of the heart (216). The mtDNA encodes 13 proteins that are essential for the

normal assembly and function of the respiratory chain complexes. Peroxisome proliferator-activated receptor gamma coactivator-1α (PGC1α) is a member of the PGC family of transcription coactivators. PGC1α plays an important role in the expression of nuclear DNA and mtDNA encoded genes that drive mitochondrial biogenesis and increase the oxidative phosphorylation (OXPHOS) capacity (217). Recently, we showed the mitochondrial respiratory chain activity and oxidative phosphorylation capacity were compromised in the myocardium of chronically infected rodents (53). Further, mtDNA content and mtDNA encoded gene expression were decreased in *Tc*-infected cardiac myocytes and cardiac biopsies of chagasic patients (218). Whether PGC1α activation of mitochondrial biogenesis and oxidative metabolism is compromised in CCM is not known.

Besides mitochondrial metabolic defects, chronic oxidative and inflammatory stress are hallmarks of Chagas disease. Acute infection by *T. cruzi* results in intense inflammatory activation of macrophages and $CD8^+$T lymphocytes accompanied by increased expression of inflammatory mediators such as cytokines, chemokines, and nitric oxide synthase (NOS) in the heart (reviewed in (219, 220)). Further, reactive oxygen species (ROS) are produced by neutrophils and macrophages activated by *T. cruzi* infection (220). Besides infiltration of inflammatory infiltrate, cardiomyocytes are also reported to produce cytokines and mitochondrial ROS in response to *T. cruzi* infection (221, 222). The ROS induced adducts of DNA, protein and lipids were exacerbated in the myocardium of chronically infected rodents and human patients

(218, 223). NFκB transcriptional factor signals oxidative and inflammatory responses (224), though mechanistic role of NFκB in chronic oxidative and inflammatory stress during CCM is yet to be elucidated.

Sirtuin 1 (SIRT1) is a highly conserved member of the family of NAD^+-dependent Sir2 histone deacetylases, which deacetylates PGC1α at multiple lysine sites, consequently increasing PGC1α activity (225). SIRT1 has also been reported to sense the redox shifts and integrate mitochondrial metabolism and inflammation through post-transcriptional regulation of the transcription factors and histones (226). Several small molecule agonists of SIRT1 have been reported in literature. For example, resveratrol (3,5,4'-trihydroxy-trans-stilbene), a polyphenol found in red grape skins and red wine, is a natural agonist of SIRT1, and has been shown to increase mitochondrial number and the expression of genes for oxidative phosphorylation (227). SRT1720 is a selective small molecule activator of SIRT1 and it is 1,000-fold more potent than resveratrol (228). SRT1720 has been demonstrated to improve mitochondrial oxidative metabolism (229), and attenuate aging-related cardiac myocyte dysfunction (230).

In this study, we aimed to determine whether treatment with SIRT1 agonists will be beneficial in improving the heart function in Chagas disease. C57BL/6 mice were infected with *T. cruzi*, and treated with small molecule agonists of SIRT1. We demonstrate the therapeutic window of the efficacy of SIRT1 agonists in arresting the

cardiac dysfunction in chagasic mice. Our results demonstrate a link between SIRT1, PGC1α, and NFκB in regulating ROS and inflammatory responses during *T. cruzi* infection and CCM.

2.2 Material and methods

Ethics statement

All animal experiments were performed according to the National Institutes of Health Guide for Care and Use of Experimental Animals, and approved by the Institutional Animal Care and Use Committee (IACUC) at the University of Texas Medical Branch, Galveston (protocol number: 0805029).

Mice and parasites and cell culture

All chemicals were of molecular grade, and purchased from Sigma-Aldrich (St. Louis, MO) unless otherwise stated. *T. cruzi* trypomastigotes (SylvioX10 strain, ATCC 50823) were propagated by *in vitro* passage in C2C12 cells. C57BL/6 mice were purchased from Harlan Laboratories (Indianapolis, IN). Mice (6-weeks-old) were infected with *T. cruzi* (10,000 trypomastigotes/mouse, intraperitoneal), and harvested at days 150 post-infection (pi) corresponding to chronic disease phase. To enhance the SIRT1 activity, two approaches were applied. One, mice were treated with resveratrol (20 mg/ml in drinking water) for three weeks, during days 90-111 pi. Two, mice were given SRT1720 (1 mg/100 µl/mouse, intraperitoneally, Selleck Chemicals, Houston, TX) three times a week during days 45-66 pi. Tissue samples were stored at

-80°C. Protein levels were determined by using the Bradford Protein Assay (Bio-Rad, Hercules CA).

Human cardiomyocytes were cultured and maintained in Dulbecco's modified Eagle's medium/F-12 medium with 12.5% fetal bovine serum. Cardiomyocytes were seeded in T75 flasks (3×10^6 cells per flask, 70% confluence), and infected with *T. cruzi* trypomastigotes (cell: parasite ratio, 1:3). Cells were incubated in presence or absence of SIRT1 agonist (1 µM SRT1720) and NF-κB inhibitor (50 µM emodin) for 24 h.

Echocardiography assessment of LV function

Mice were continuously anesthetized by inhalant 1.5% isoflurane/100% O_2 to maintain a light sedation level. Mice were placed supine on an electrical heating pad at 37°C and heart rate and respiratory physiology were continuously monitored by electrocardiography. Mice chests were shaved, and warm ultrasound gel was applied to the area of interest. Transthoracic echocardiography was performed using the Vevo 2100 ultrasound system (Visual Sonics, Toronto, Canada) equipped with a high-frequency linear array transducer (MS400, 18-38 MHz) (231). Heart was imaged in B-mode and M-mode to examine the parameters of left ventricle (LV) in diastole (-d) and systole (-s). All measurements were obtained in triplicate and acquired in long-axis and short-axis views. Data were analyzed by using Vevo 2100 standard measurement software.

Histology

Histological preparation and staining of the tissues was performed at the Research Histopathology Core at the UTMB. Briefly, tissue sections were fixed in 10% buffered formalin, dehydrated in absolute ethanol, cleared in xylene, and embedded in paraffin. Five-micron tissue sections were subjected to Masson's Trichrome or Hematoxylin and Eosin (H&E) staining, and evaluated by light microscopy using an Olympus BX-15 microscope equipped with a digital camera and Simple PCI software (v.6.0, Compix, Sewickley, PA). In general, we analyzed each tissue section for >10 microscopic fields (20X magnification), and examined three different tissue sections/mouse (4 mice/group). The collagen area as a percentage of the total myocardial area was assessed as a measure of fibrosis. All pixels with blue stain in Masson's trichrome-stained sections were selected to build a binary image, subsequently calculating the total area occupied by connective tissue. Sections were categorized based on percent fibrotic area as: (0) <1%, (1) 1 – 5%, (2) 5 – 10%, (3) 10 – 15%, and (4) >15% (232).

Myocarditis (presence of inflammatory cells) was scored as 0 (absent), 1 (focal/mild, ≤1 foci), 2 (moderate, ≥2 inflammatory foci), 3 (extensive coalescing of inflammatory foci or disseminated inflammation), and 4 (diffused inflammation, tissue necrosis, interstitial edema, and loss of integrity). Inflammatory infiltrate was characterized as diffused or focal depending upon how closely the inflammatory cells were associated (232).

Gene expression analysis

Heart tissue sections (10 mg) were homogenized in 500 µl of TRIzol reagent (Invitrogen, Carlsbad, CA), and RNA was extracted by chloroform/isopropanol/ethanol method. Total RNA (2 µg) was reverse transcribed by using poly(dT)18 with an iScript™ kit (Bio-Rad). The cDNA was utilized as template with SYBR-Green super-mix (Bio-Rad), and real time quantitative PCR (qPCR) was performed on an iCycler Thermal Cycler. The gene-specific oligonucleotide pairs used for amplifying the mRNAs are listed in supplemental Table S1. The PCR Base Line Subtracted Curve Fit mode was applied for threshold cycle (Ct), and mRNA level was calculated by iCycler iQ Real-Time Detection Software (Bio-Rad). The Ct values for target mRNAs were normalized to geometric mean of GAPDH mRNA, and the relative expression level of each target gene was calculated as $2^{-\Delta Ct}$, where ΔC_t represents the C_t (sample) - C_t (control) (233, 234).

Tissue and cell homogenates and fractionation

Freshly harvested heart tissue sections (30 mg) were washed with ice-cold Tris-buffered saline and homogenized in RIPA buffer (tissue: buffer ratio, 1: 10, w/v) [17]. Homogenates were centrifuged for 10 min at 10,000 g, and supernatants were stored at −80°C. For the preparation of nuclear and cytosolic fractions, heart tissue sections (50 mg) were homogenized in ice-cold HMK buffer (10 mM HEPES pH 7.9, 1.5 mM $MgCl_2$, 10 mM KCl) containing 1 mM DTT and 1% Protease Inhibitor Cocktail (Sigma-

Aldrich). Tissue lysates were centrifuged at 4ºC, 10000 g for 20 min and supernatants stored as a cytosolic fraction. The pellets were re-suspended in HMK buffer containing 0.42 M NaCl, 0.2 mM EDTA, and 25% (v/v) glycerol, centrifuged at 4ºC, 20, 000 g for 5 minutes, and nuclear fractions were stored at −80°C.

Cardiomyocytes were infected with *T. cruzi* and incubated in presence or absence of SRT1720 (with 1 µM) for 24 h. Cells were lysed for 30 min on ice in lysis buffer containing 50 mM Tris pH 7.5, 150 mM NaCl, 1 mM EDTA, 1 mM EGTA, 1% NP-40, 2.5 mM KH_2PO_4, and 1 mM Na_3VO_4. Cell lysates were centrifuged at 3000 g at 4°C for 15 min and the resultant supernatants were stored at −80°C**.** For the preparation of nuclear and cytosolic fractions, cells (7×10^6/ml) were incubated on ice for 30 minutes in buffer A (10 mM HEPES, pH 7.9, 10 mM NaCl, 0.1 mM EDTA, 0.1 mM EGTA, 1 mM DTT, 1 mM PMSF) containing 0.625% NP-40 and 1% protease inhibitor cocktail. Cell lysates were centrifuged at 4°C at 10,000 g for 1 min and supernatants stored as a cytosolic fraction. Pellets were washed with buffer A containing 1.7 M sucrose, re-suspended in buffer B (20 mM HEPES pH 7.9, 0.4 M NaCl, 1 mM EDTA, 1 mM EGTA, 1 mM DTT, and 1 mM PMSF), and centrifuged at 4°C at 13 000 g for 5 minutes. The resultant supernatants were stored at −80°C as nuclear extracts.

Western blotting

Heart or cell homogenates and nuclear fractions (30 µg protein) were electrophoresed on a 4-15% Mini-Protein® TGXTM gel using a Mini-PROTEAN electrophoresis chamber (Bio-Rad), and proteins were transferred to a PVDF

membrane using a Criterion Trans-blot System (Bio-Rad). Membranes were blocked with 50 mM Tris, 150 mM NaCl (TBS) containing 5% non-fat dry milk (NFDM), washed three times for 10 min each with TBS - 0.1% Tween 20 (TBST), and incubated overnight at 4°C with antibodies against CYTB (Santa Cruz Biotech, Dallas, TX, sc11436), COI (Abcam, Cambridge, UK, ab147053), GAPDH (Cell signaling, Danvers, MA, 3683), 4-hydroxynonenal (4HNE, Alpha Diagnostic Inc, San Antonio, TX, HNE11-S), iNOS (Abcam, ab49999), Lamin A/C (Santa Cruz, sc20681), NF-κB-p65 subunit (Santa Cruz , F-6 clone, sc-8008); NF-κB-acetyl- p65 (Abcam, acetyl K310 clone, ab198703), nitrotyrosine (3NT, Merck Millipore, Billerica, MA, 06-284), NRF1 (Santa Cruz, sc33771), Nrf2 (Santa Cruz, sc722), PGC1α (Santa Cruz, sc13067), POLG (Santa Cruz, 390634), SIRT1 (Abcam, ab32441), TOP1 (Abcam, ab3825), IL-10 (A2, Santa Cruz, sc-365858) and anti-acetylated-lysine antibody (Cell Signaling, 9441). All antibodies from Santa Cruz were used at 1:200 dilution in TBST-5% NFDM. All other antibodies were used at 1:1000 dilution in TBST-5% NFDM. Membranes were washed as above, incubated with HRP-conjugated secondary antibody (1:10,000 dilution, Southern Biotech, Birmingham, AL), and images were acquired by using an ImageQuant LAS4000 system (GE Healthcare, Pittsburgh, MA). Immunoblots were subjected to Ponceau S staining to confirm equal loading of samples. Densitometry analysis of protein bands of interest was performed using a Fluorchem HD2 Imaging System (Alpha-Innotech, San Leandro, CA), and normalized against GAPDH (tissue homogenates) or Lamin A/C (nuclear fractions).

SIRT1 activity

SIRT1 deacetylase activity was measured by using a SIRT1 Fluorometric Assay Kit (Abcam, ab156065). Briefly, nuclear fractions (100 µg) isolated from heart tissues were added to acetylated Lys^{382} p53 peptide (50 µl) that is coupled with fluorophore and quencher at the amino terminal and carboxyl terminal, respectively. The reaction was initiated with addition of 100 µl NAD^+, and SIRT1 dependent deacetylation of the substrate peptide coupled with its digestion by the action of proteases, and fluorescence release recorded. The fluorescence intensity (Ex_{350nm}/Em_{440nm}) was measured at two min intervals for 60 minutes using a SpectraMax M5 microplate reader (Molecular Devices, Sunnyvale CA). Standard curve was prepared with recombinant SIRT1 (0-120 ng), and results were presented as relative fluorescence units per µg protein.

Mitochondrial DNA (mtDNA) and *T. cruzi* DNA (*Tc*DNA)

Tissue sections (5 mg) were subjected to Proteinase-K lysis, and total DNA was purified using a DNeasy Blood & Tissue Kit (Qiagen, Hilden, Germany). Total DNA (20 ng) was utilized as template with SYBR Green Super-mix (Bio-Rad) and primer pairs specific for mtDNA-encoded cytochrome b (CYTB) and cytochrome oxidase 2 (COII) regions, and real-time qPCR was performed on an iCycler thermal cycler. The mtDNA content was normalized to β-globin nuDNA. For the evaluation of parasite burden, *Tc*18SrDNA-specific primers were utilized for qPCR, and data were normalized to GAPDH.

Citrate synthase (CS) activity is a sensitive measure of mitochondrial mass, and was measured by using the MitoCheck Citrate Synthase Activity Assay Kit (Cayman, Ann Arbor, MI) following the protocol provided by the manufacturer.

Oxidant and antioxidant levels

To measure the total H_2O_2 levels, tissue homogenates (100 µg) were added in triplicate to flat-bottom (dark-walled) 96-well plates. The reaction was started with addition of 33-µM amplex red (10-acetyl-3, 7-dihydroxyphenoxazine) and 0.1U/ml horseradish peroxidase (final reaction volume: 150 µl). The oxidation of amplex red to fluorescent resorufin by H_2O_2 (Ex_{563nm}/Em_{587nm}) was recorded on a SpectraMax M2 microplate reader (Molecular Devices). Standard curve was prepared with 0-5 µM H_2O_2.

Advanced oxidation Protein Products (AOPP) are produced through the reaction of proteins with chlorinated oxidants (e.g. chloramines, hypochlorous acid), and provide a sensitive measure of total oxidative stress. AOPP contents were assayed by using the OxiSelect AOPP Assay Kit (Cell Biolabs, San Diego, CA). Briefly, tissue homogenates (10 µg) were mixed with 10 µl of 1.16 M KI and 20 µl of 100% acetic acid (final volume: 200 µl). Reaction was stopped after 5 min and absorbance was recorded at 340 nm. AOPP concentration was expressed as chloramine-T equivalents (standard curve: 0–100 µmol chloramine-T/ml) (235).

A commercially available kit (Abcam ab65329) was utilized to measure the total antioxidant capacity (TAC). The assay uses lag time by antioxidants against the myoglobin-induced oxidation of 2,2'-azino-di(3-ethylbenzthiazoline-6-sulfonic acid (ABTS) with H_2O_2. Briefly, 20 µl of tissue homogenates (diluted 1:20, v/v) were added in triplicate to 96-well plates, and mixed with 90 µl of 10 mM PBS (pH 7.2), 50 µl of myoglobin solution, and 20 µl of 3 mM ABTS. Reaction was initiated with H_2O_2 (20 µl) and change in color monitored at 570 nm (standard curve: 2-25 µM trolox).

Transient transfection and NFκB activity assay

The NFκB-TATA-luciferase reporter plasmid was graciously provided by Dr. Shao-Cong Sun (University of Texas MD Anderson Cancer Center). The pRL-TK vector containing *Renilla* luciferase (positive control) was purchased from Promega (Madison, WI). HEK-293 cells (CRL-1573, ATCC Manassas, VA) were cultured in Dulbecco's Modified Eagle Medium (DMEM) media in T75 flasks. Cells were seeded in 96-well tissue culture plates ($2.5X10^4$ cells/well), allowed to adhere for 1 h, and acclimatized overnight to antibiotic-free Opti-MEM medium. Cells were transfected with NFκB-TATA-luciferase (100 ng) and pRL-TK (10 ng) using Lipofectamine 2000 (Invitrogen) according to the instructions provided by the manufacturer. After 6 h of incubation, cells were washed, replenished with complete medium for 3-5 h, and then infected with *T. cruzi* (cell: parasite ratio, 1:3). Cells were incubated in presence or absence of 1 µM each of SRT1720 for 24 h. The relative NFκB transcriptional activity

was measured by using a Dual Luciferase Reporter Assay System (Promega, Madison, WI) and data were normalized to *Renilla* luciferase activity.

Data analysis

All experiments were conducted with triplicate observations per sample (n=6 mice per group per experiment, at least two experiments per group), and data are expressed as mean ± standard deviation (SD). All data were analyzed using GraphPad Prism 5 (GraphPad Software, La Jolla, CA). Data were analyzed by Student's t test (comparison of 2 groups) and one-way ANOVA with Tukey's test (comparison of multiple groups). Significance is presented by * (infected vs. normal) or # (infected/treated vs. infected/untreated) ($^{*,\#}p<0.05$, $^{**,\#\#}p<0.01$, $^{***,\#\#\#}p<0.001$).

2.3 Results

We first determined if enhancing the SIRT1 activity would preserve the cardiac function in Chagas disease. Mice were infected with *T. cruzi* and then treated with resveratrol or SRT1720 as described in Materials and Methods. *In vivo* transthoracic echocardiography was performed at ~150 days pi to evaluate the changes in LV function (Table 1, Fig 1). Chagasic mice, as compared to normal controls, exhibited a substantial increase in LV end systolic volume (ESV, >2-fold), and a decline in stroke volume (SV, 35%), cardiac output (CO, 59%), and ejection fraction (EF, 33%) (Fig 1.a-d, all, $p<0.001$). The LV internal diameter at systole ($LVID_s$) was increased by >2-fold, and consequently, fractional shortening (FS) was decreased by 53% in chagasic (vs.

normal) mice (Fig 1.e&f, p<0.001). The *Tc*-infected/SRT1720-treated mice, in comparison to normal controls, exhibited only 20%, 27% and 16% decline in SV, CO, EF, respectively, that were not statistically significant. In comparison to *Tc*-infected/untreated mice, infected/SRT1720-treated mice exhibited 55% decline in ESV and 29%, 33%, 37%, and 36% increase in SV, CO, EF, and FS, respectively (Fig 1A.a-e, Table 1, all, #p<0.05-0.001). *Tc*-infected/resveratrol-treated mice (vs. infected/untreated mice) exhibited a moderate (up to 20%) but significant improvement in *Tc*-induced loss in ESV, SV and CO; and a modest, but statistically insignificant, improvement in EF and FS (S1 Fig, panels a-f). These results suggested that SRT1720 treatment was effective in arresting the LV dysfunction in chagasic mice. Resveratrol provided a partial recovery of cardiac output in *Tc*-infected mice.

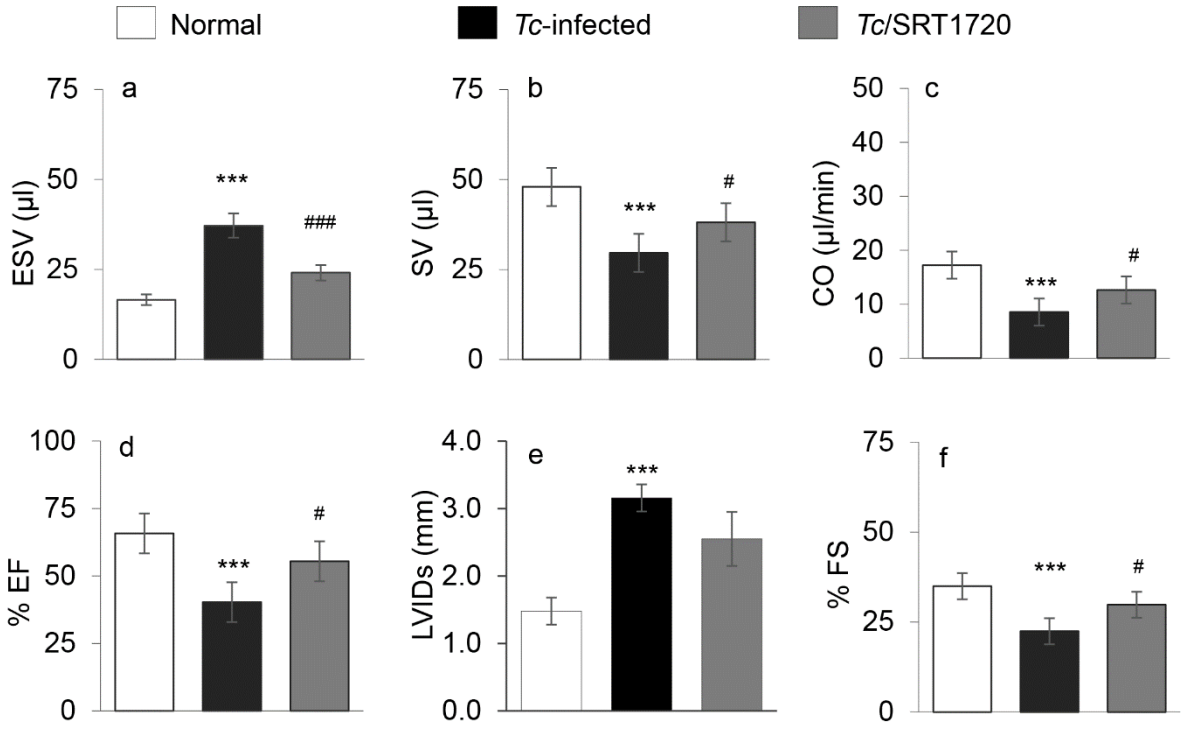

Figure 2.1. SRT1720 treatment improved the left ventricular function in chagasic mice. C57BL/6 mice were infected with *Trypanosoma cruzi* (10,000 *Tc*/mouse, ip), and treated with SRT1720 (SIRT1 agonist) during 45-66 days post-infection (pi), as described in Materials and Methods. Transthoracic echocardiography was performed by using a Vevo 2100 System to assess the left ventricular (LV) function at ~150 days pi. Shown are LV (a) end systolic volume (ESV), (b) stroke volume (SV), (c) cardiac output (CO), (d) ejection fraction (EF), (e) LV internal diameter at systole (LVIDs), and (f) fractional shortening (FS). Detailed data are presented in Table 1. For all figures, bar graphs show mean ± SD (n=6-10 mice per group per experiment, triplicate observations per mouse per treatment, two experiments per group). Significance (*normal control vs. *Tc*-infected, #*Tc*-infected vs. *Tc*-infected/SRT1720-treated) was calculated by one-way ANOVA with Tukey's test and shown as *,#p<0.05, **,##p<0.01, ***,###p<0.001.

Echocardiography imaging in M mode was performed to gain an anatomo-pathological view of the heart in chronically infected mice. These data showed that systolic and diastolic thickness of inter-ventricular septum (IVS), LV area, and LV mass were increased by 44%, 40%, 28%, and 28% respectively, while LV posterior wall (LVPW) was thinned by 41% in chagasic (vs. normal) mice (Fig 2.Aa-e, all, p<0.001, Table 1). Histological evaluation of the tissue sections subjected to Masson's Trichrome staining showed an increase in diffused collagen deposition in chagasic myocardium (score: 4.0 ± 0.4 vs. 0.3 ± 0.04, *Tc*-infected vs. normal controls, p<0.05, Fig 2B.a&b). An increase in cardiac fibrosis in chagasic myocardium was also evidenced by 1.6-fold, 1.8-fold and 3.2-fold increase in mRNA levels for COLI, COLIII, and αSMA, respectively (Fig 2C.a-c, all, p<0.01). In infected/SRT1720-treated mice, LV area (systole) was normalized (Fig 2A.e, #p<0.05), though SRT1720 treatment provided no benefits in normalizing the IVS and LVPW thickness and LV mass in chagasic mice (Fig 2A). The myocardial deposition of collagen (score: 2.5 ± 0.8) and collagen-related gene expressions were also not significantly changed in SRT1720-treated (vs. untreated) chagasic mice (Fig 2B&C). Chagasic mice treated with

resveratrol also exhibited modest control of LV mass, but no improvement in the IVS and LVPW thickness and LV area (S2 Fig, panels a-e, Table 1). Together, the results presented in Fig 2 and S2 Fig suggested that a) an increase in passive stiffness (enhanced ESV, IVS_s, IVS_d, $LVID_s$) alongside thinning of the LVPW contributed to depressed LV function in chagasic mice, and b) SRT1720 benefits in arresting the LV dysfunction were not delivered through control of cardiac collagenosis and hypertrophy in chagasic mice.

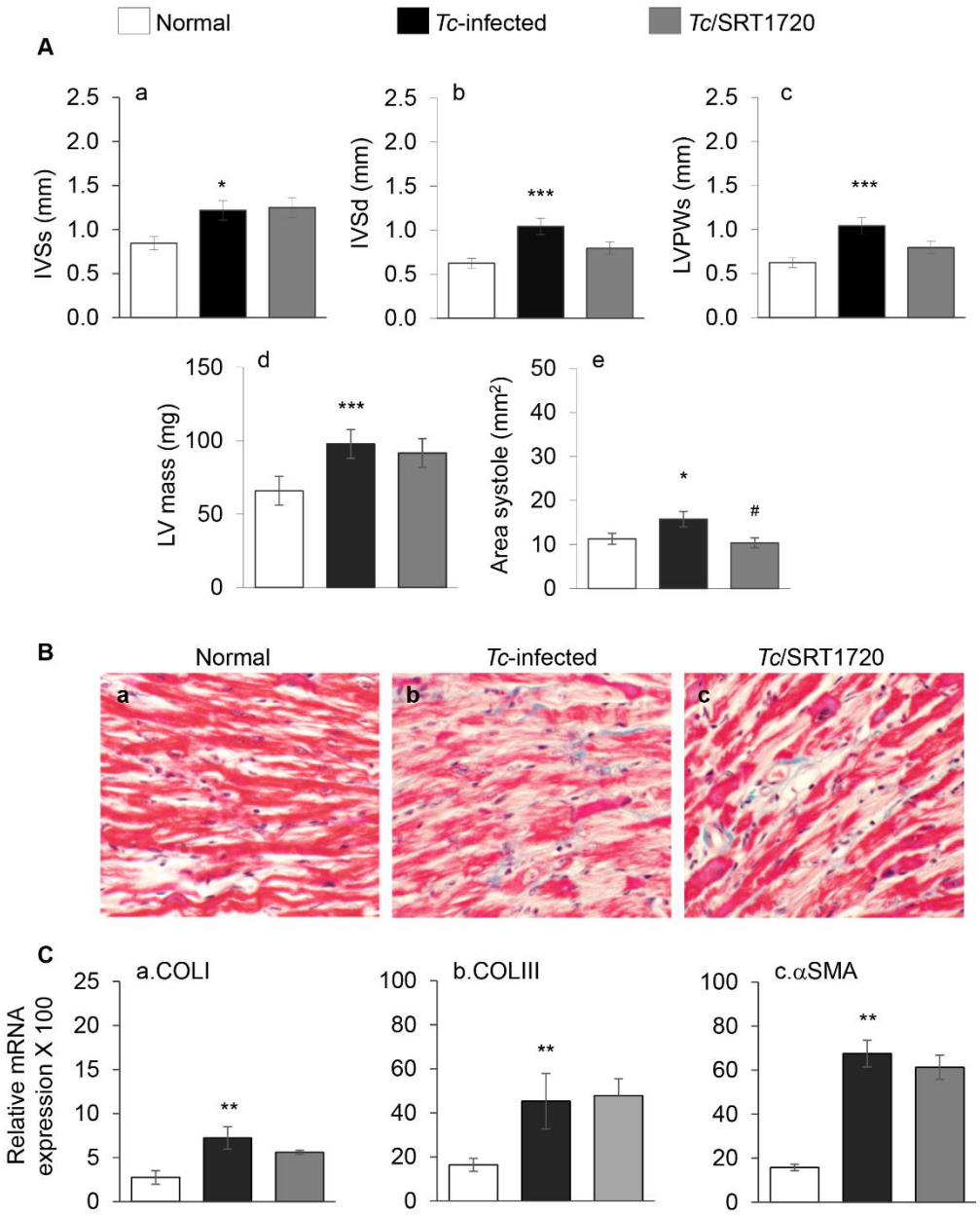

Figure 2.2. Effects of SRT1720 on cardiac remodeling in chagasic disease. Mice were infected with *T. cruzi,* treated with SRT1720, and examined at 150 days pi. **(A)** Cardiac structural changes were analyzed by echocardiography using a Vevo 2100 System. Shown are systolic (-s) and diastolic (-d) values for inter-ventricular septum (IVS) thickness (a&b), LV posterior wall (LVPW) thickness (c), LV mass (d), and LV area (e) in chronically infected mice. **(B)** Representative images show Masson's Trichrome staining of the heart tissue sections from (a) normal control, (b) *Tc*-infected, and (c) infected/ SRT1720-treated mice. **(C)** Quantitative real-time RT-PCR for collagen isoforms (COLI and COLIII, panel a&b) and alpha smooth muscle actin (αSMA, panel c). Data were normalized to GAPDH mRNA. Significance was calculated and presented as in Fig 1.

T. cruzi infection results in respiratory chain inefficiency in mice and humans

(236, 237). SIRT1 deacetylates PGC1α, and PGC1α coactivation of nuclear respiratory factor (NRF1) signals the expression of key metabolic genes required for respiration and mtDNA transcription and replication. Western blotting showed the total and nuclear levels of SIRT1, PGC1α and NRF1 proteins were either increased or not changed in the myocardium of infected/untreated and infected/SRT1720-treated mice as compared to that noted in normal controls (Fig 3A&B.a&b). However, total and nuclear concentration of acetylated PGC1α (inactive form) were increased by >9-fold (Fig 3A&B.a&b, $p<0.01$), and associated with a 53% decline in SIRT1 activity (Fig 3C, $p<0.05$) in the myocardium of chronically infected (vs. normal) mice. SRT1720 treatment of chagasic mice resulted in 84% and 58% decline in total and nuclear levels of the acetylated PGC1α level, respectively (Fig 3A&B, $^{\#}p<0.001$) and 60% increase in SIRT1 activity (Fig 3C, $^{\#}p<0.05$). The changes in mitochondrial biogenesis were examined by measuring the mitochondrial markers at the DNA, gene expression and protein levels. The mtDNA levels for CYTB and COII sequences, normalized to nuclear DNA sequence for β-globin, were decreased by 25% and 24%, respectively, in the myocardium of chronically infected mice (Fig 4A.a&b, $^{*}p<0.05$). No difference in the citrate synthase activity, a marker of mitochondrial mass, was noted in chagasic vs.

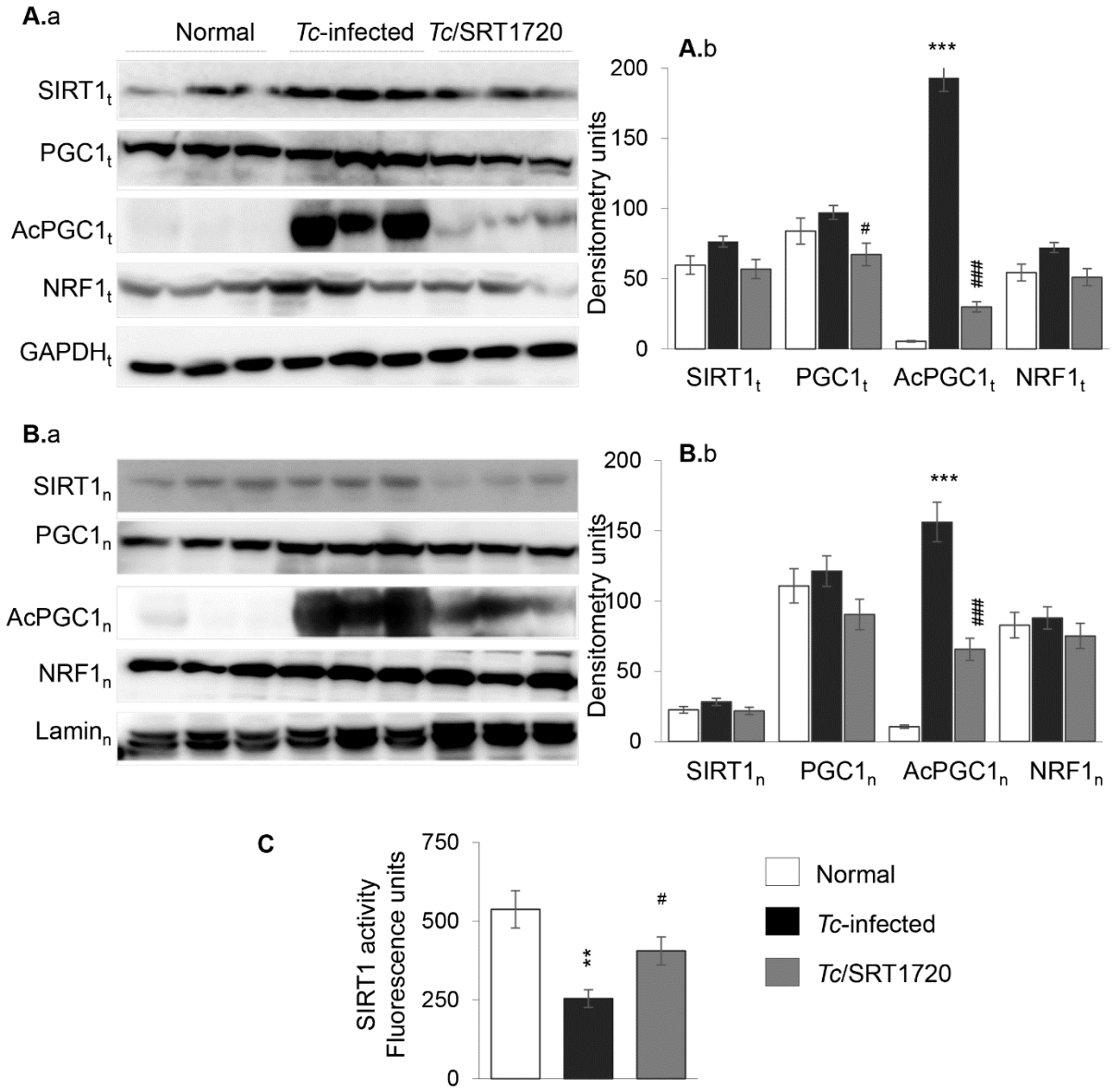

Figure 2.3. SIRT1 activity and nuclear localization of SIRT1, PGC1α, and NRF1 in chagasic mice (± SRT1720). Mice were infected with *T. cruzi*, treated with SRT1720, and harvested at ~150 days pi. Heart homogenates **(A)** and nuclear fractions **(B)** from normal and *Tc*-infected mice (±SRT1720 treatment) were submitted to Western blotting. Shown are representative immunoblots for myocardial (A.a) and nuclear (B.a) expression level of SIRT1, PGC1α (total and acetylated), and NRF1 in three mice per group. GAPDH and Lamin A/C were analyzed as controls. Densitometry analysis of bands from total homogenates (normalized to GAPDH) and nuclear fractions (normalized to Lamin A/C) was performed using the data from all mice in a group from two independent experiments and presented as mean value ± SD in A.b and B.b, respectively. **(C)** SIRT1 deacetylase activity in heart homogenates. Significance was calculated and presented as in Fig 1.

normal mice. The mRNA levels for mtDNA encoded ND1, COIII, and ATP6 subunits that are essential components of the CI, CIV, and CV respiratory complexes and required for maintaining the oxygen consumption and coupled OXPHOS, were decreased by 34%, 55% and 54%, respectively, in chagasic (vs. normal) murine myocardium (Fig 4B.a-c, *$p<0.05$). The protein levels of mtDNA-encoded CYTB and COI were also decreased by 60% and 33%, respectively, in chagasic myocardium (Fig 4C.a&b, *$p<0.01$). The decline in OXPHOS-related transcripts could be a result of changes in mtDNA replication/transcription efficiency. Our data showed the myocardial mRNA levels for mtDNA replication machinery, POLG1, SSBP1, and TOP1, were decreased by 51%, 47%, and 37%, respectively, in chagasic (vs. normal) mice (Fig 4B.d-f, *$p<0.05$). We also noted 35%-90% decline in POLG and TOP1 protein levels in chagasic mice (Fig 4C.a&b, *$p<0.01$). Treatment with resveratrol resulted in 30-40% increase in mtDNA level (S3 Fig, panels A.a&b, $^{\#}p<0.05$) and 40-55% increase in mRNA levels for mtDNA encoded ND1, COIII, and ATP6 genes (S3 Fig, panels B.a-c, $^{\#}p<0.05$), and no significant improvement in the mRNA levels for POLG1, SSBP1 and TOP1 (S3 Fig, panels B.d-f) in chagasic mice. Surprisingly, SRT1720-treated/chagasic mice exhibited no significant improvement in the PGC1α/NRF1-dependent mtDNA content (COII and CYTB levels, Fig 4A.a&b), mtDNA encoded gene expression (ND1, COIII, ATP6, Fig 4B.a-c), and mtDNA replication machinery (Fig 4B.d-f) that were compromised in the myocardium of chagasic mice. Likewise, protein levels of the mtDNA-encoded proteins (e.g. CYTB, COI) and the mtDNA replication/transcription

machinery (POLG1, TOP1) were not improved in SRT1720-treated chagasic mice (Fig 4C.a&b). Together, the results presented in Fig 3, Fig 4 and S3 Fig suggested that a) mtDNA content and mRNA and protein levels of the mtDNA-encoded genes were significantly decreased in the myocardium of chronically infected mice, and this outcome was associated with a decline in mtDNA replication machinery, and b) SRT1720 treatment was effective in activation of SIRT1/PGC1α in the chagasic myocardium. However, c) SRT1720-mediated increase in SIRT1 activity and deacetylated PGC1α did not improve the mitochondrial biogenesis in chagasic mice.

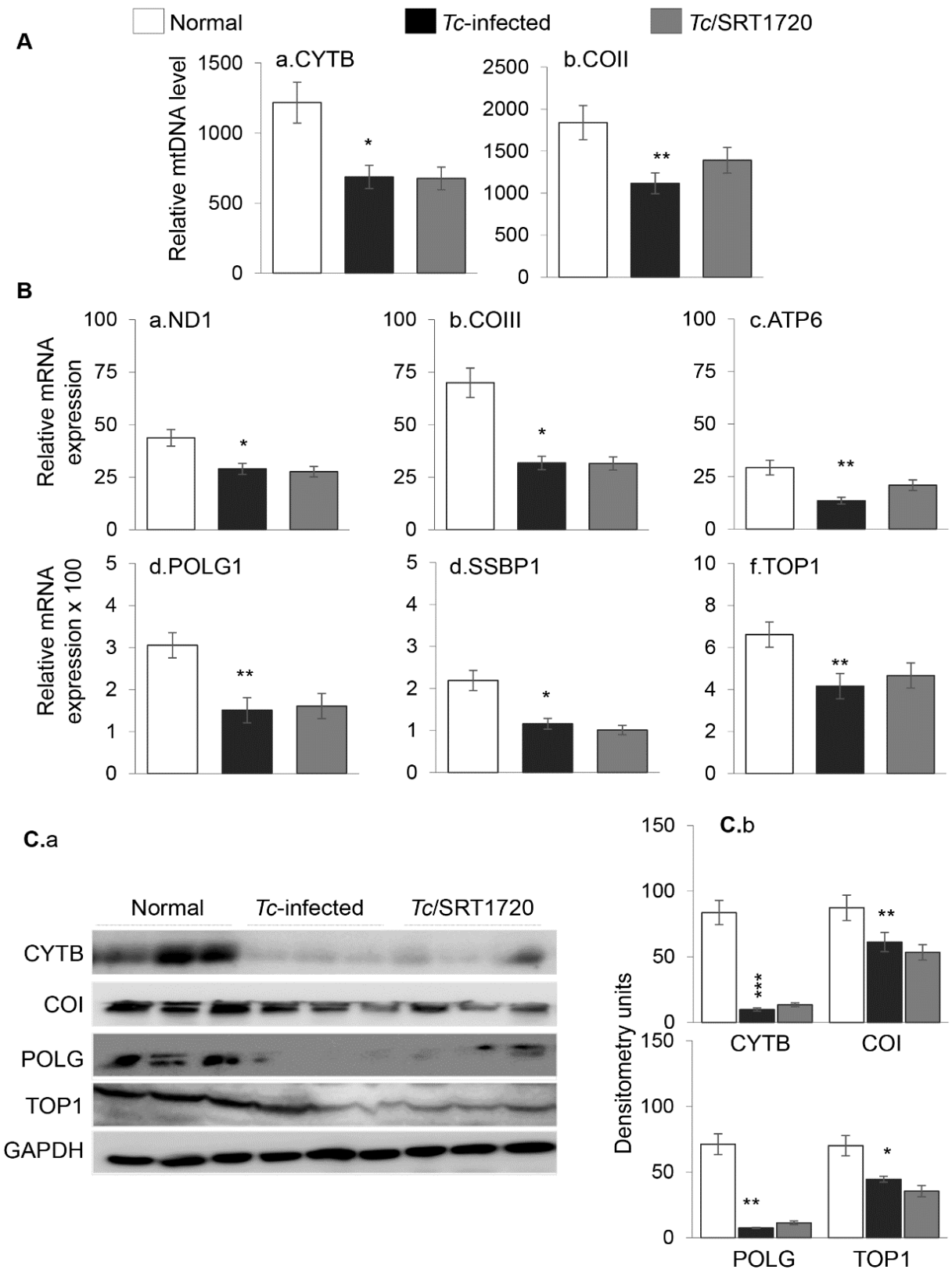
A
Normal
Tc-infected
Tc/SRT1720
Relative mtDNA level
a.CYTB
b.COII
B
Relative mRNA expression
a.ND1
b.COIII
c.ATP6
Relative mRNA expression x 100
d.POLG1
d.SSBP1
f.TOP1
C.a
Normal
Tc-infected
Tc/SRT1720
CYTB
COI
POLG
TOP1
GAPDH
C.b
Densitometry units
CYTB
COI
POLG
TOP1

Figure 2.4. Mitochondrial biogenesis is compromised in chagasic mice (± SRT1720). C57BL/6 mice were infected with *T. cruzi*, treated with SRT1720, and harvested during chronic disease phase (150 days pi) **(A)** Myocardial mtDNA content was determined by real-time quantitative PCR amplification of CYTB (panel a) and COII (panel b) regions of mtDNA, and normalized to β-globin nuDNA. **(B)** Real-time quantitative RT-PCR for mtDNA-encoded transcripts (ND1, COIII, ATP6, a-c panels) and mtDNA replication/transcriptional machinery (POLG1, SSBP1, TOP1, d-f panels). For each target gene, *C*t values were normalized to GAPDH expression. **(C)** Shown are representative immunoblots for CYTB, COI, POLG, TOP1 and GAPDH (panel a). Densitometry analysis of the signal, normalized to GAPDH, is shown in panel b. Significance was calculated and presented as in Fig 1.

We next determined if SIRT1 agonists controlled the chronic oxidative and inflammatory stresses that are hallmarks of Chagas disease (53). Fluorometric evaluation of ROS showed 2.3-fold increase in H_2O_2 levels in the myocardial homogenates of chronically infected (vs. normal) mice (Fig 5A, *p<0.001). Advanced oxidation protein products (AOPPs) are formed by HOCl-induced chlorination of amines and considered a biomarker of inflammatory and oxidative pathology. Our data showed a 57% increase in AOPP content in chagasic (vs. normal) myocardium (Fig 5B, *p<0.01). The expression of inducible NOS (iNOS, a major source of nitric oxide) and the levels of the oxidative/nitrosative stress markers 4-hydroxynonenal (4HNE) and 3-nitrotyrosine (3NT) were increased by 20-fold, 10-fold, and 8-fold, respectively, in chagasic (vs. normal) myocardium (Fig 5C.a&b, all, p<0.001). In contrast, protein level of Nrf2 (transcriptional regulator of antioxidant gene expression) and total antioxidant capacity were decreased by 60% and 41%, respectively, in chagasic (vs. normal) myocardium (Fig 5C&D, *p<0.001). Resveratrol treatment was not effective in controlling the chronic oxidative stress in chagasic mice (S4 Fig, panels a&b). However, SRT1720 treatment resulted in a 57% and 90% decline in *Tc*-induced H_2O_2 and AOPP

levels, respectively (Fig 5A&B, #p<0.01); 76%, 64% and 62% decline in *Tc*-induced iNOS, 4HNE and 3NT levels, respectively (Fig 5C.a&b, all #p<0.01); and 57% and 50% improvement in *Tc*-induced loss in Nrf2 expression and antioxidant capacity, respectively (Fig 5C&D, #p<0.05). These results suggested that SRT1720 activation of the SIRT1/PGC1α was beneficial in controlling the chronic oxidative stress in chagasic myocardium.

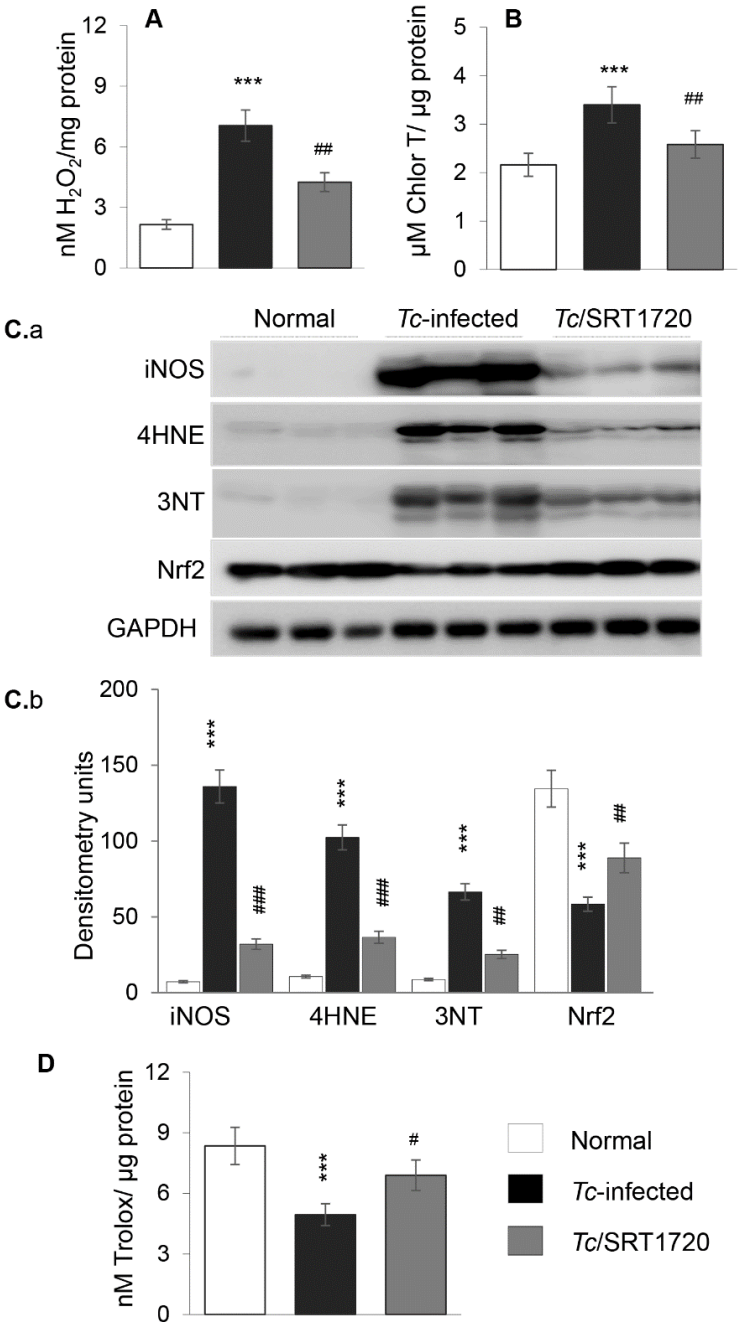

Figure 2.5. Oxidant/antioxidant status in chagasic mice (± SRT1720). Mice were *Tc*-infected, SRT1720-treated, and heart tissue harvested, as in Fig 4. Cardiac homogenates were used to measure **(A)** ROS (H_2O_2) and **(B)** advanced oxidation protein products (AOPP) levels. **(C)** Shown in panel a are representative immunoblots for inducible nitric oxide synthase (iNOS), 4-hydroxynonenal (4HNE), 3-nitrotyrosine (3NT), Nrf2, and GAPDH in cardiac homogenates of normal and *Tc*-infected (± SRT1720-treated) mice. Densitometry analysis of the western blot bands, normalized to GAPDH, is shown in panel b. **(D)** Total antioxidant capacity in cardiac homogenates. Significance was calculated and presented as in Fig 1.

Histological studies showed the myocardial level of inflammatory infiltrate constituted of diffused inflammatory foci (histological score: 2-3) was increased in heart tissue of chronically-infected/untreated (vs. normal) mice (Fig 6A.a&b). Chagasic mice exhibited a high degree of myocardial degeneration with enlarged myocytes. The cytokine gene expression was predominantly of proinflammatory nature evidenced by 9-fold, 3-fold and 2-fold increase in IFNγ, IL1β, and TNF-α mRNA (Fig 6B.a-c, all, *$p<0.01$) and 29% and 43% increase in IL10 and arginase 1 (Arg1) mRNA (Fig 6B.d&e, *$p<0.05$), respectively, in chagasic myocardium. The myocardial IL10 protein level was increased by 3-fold in chagasic mice (Fig 6C.a&b, *$p<0.05$). Resveratrol treatment resulted in a modest (but not statistically significant) control of pro-inflammatory cytokine expression in chagasic heart (S5 Fig, panels a-c). However, myocardial inflammation was significantly subsided in infected/SRT1720-treated mice, evidenced by the detection of minimal tissue inflammatory infiltrate (histological score: 0-1, Fig 6A.c). Further, SRT1720-treated chagasic mice exhibited 80%, 36% and 46% decline in the expression of IFNγ, IL1β and TNFα, respectively (Fig 6B a-c, all, $^{\#}p<0.05$), and no change in the myocardial expression of IL10 and Arg1 (Fig 6B&C). Chronic

persistence of parasite was noted in all infected mice, and was not changed by SRT1720 treatment (Fig 6D). These results suggested that SRT1720 was beneficial in attenuating the myocardial inflammatory infiltrate and proinflammatory cytokine response in chagasic mice.

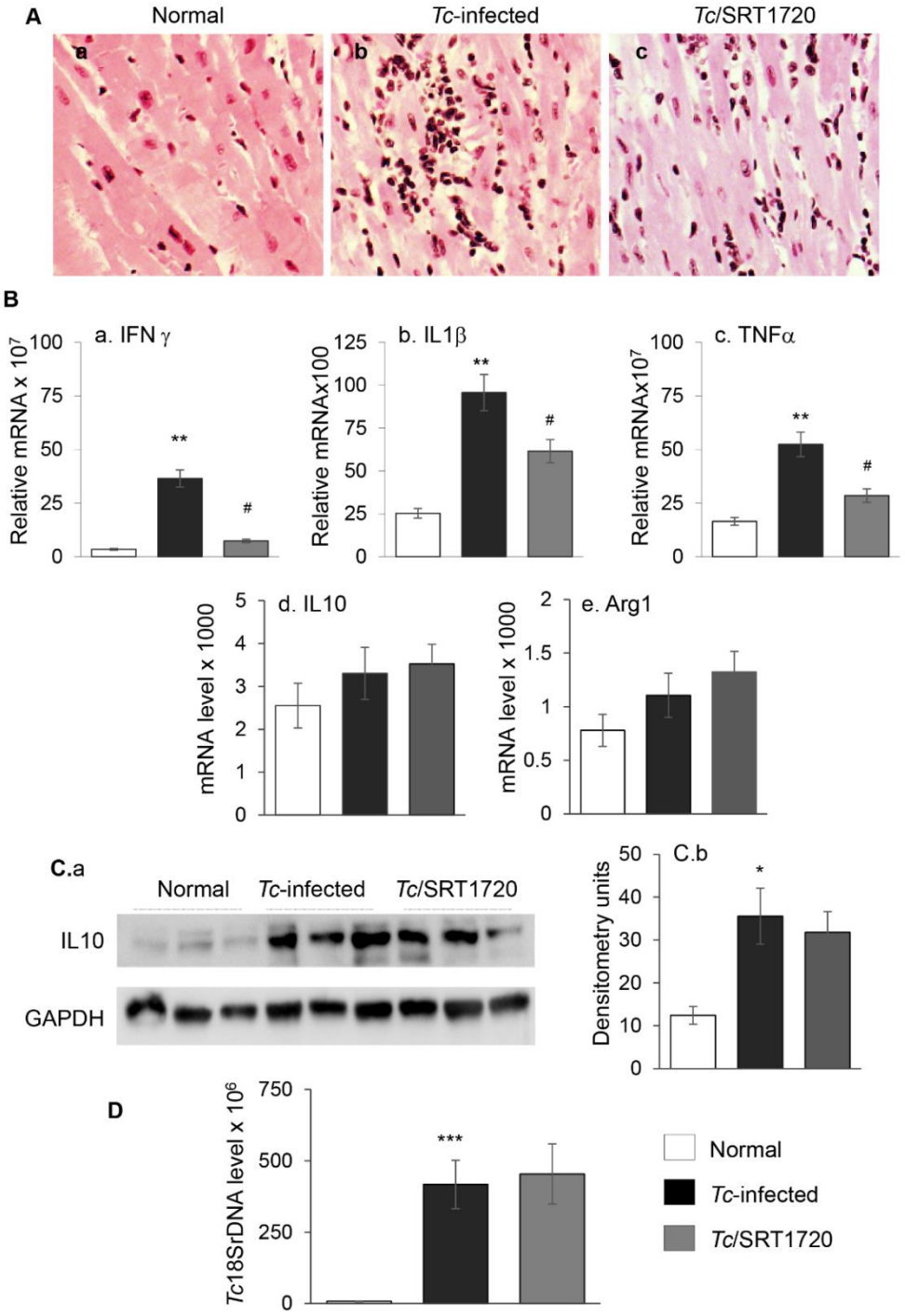

Figure 2.6. *T. cruzi* induced chronic inflammatory stress was controlled by SRT1720 treatment. Mice were *Tc*-infected, SRT1720-treated, and harvested at 150 days pi. **(A)** Hematoxylin and Eosin staining of LV tissue sections from (a) control, (b) *Tc*-infected, and (c) *Tc*-infected/SRT1720-treated mice are shown (pink: muscle/cytoplasm/keratin, dark brown: mononuclear infiltration). **(B)** Myocardial expression levels of (a) IFNγ, (b) IL1β, and (c) TNFα, (d) IL10 and (e) Arg1 were determined by real-time quantitative RT-PCR. For each target gene, *C*t values were normalized to GAPDH expression. **(C)** Shown in panel a are representative immunoblots for IL10 and GAPDH in cardiac homogenates of normal and *Tc*-infected (± SRT1720-treated) mice. Densitometry analysis of the western blot band for IL10, normalized to GAPDH, is shown in panel b. **(D)** Myocardial level of parasite burden was determined by quantitative PCR amplification of the *Tc*18SrDNA sequence. Significance was calculated and presented as in Fig 1.

NFκB family of transcription factors is of central importance in inflammation and immunity. Rel A (p65) is an important subunit of activated NFκB dimers (p50/p65, p65/p65, and p65/c-Rel). Western blotting showed the nuclear level of NFκB-p65 was increased by 76% in the myocardium of infected/untreated (Fig 7A.a&b, *p<0.05) mice, and normalized to control levels in infected/SRT1720-treated mice (#p<0.05), thus suggesting that SIRT1 might regulate NFκB activation in CCM. To verify this, we utilized an *in vitro* system. Cardiac myocytes were infected with *T. cruzi* and incubated for 24 h in presence or absence of SRT1720 or emodin (blocks IκB degradation and p65/Rel A release for nuclear translocation). As in chagasic heart, no changes in total levels of p65 were noted in any of the treatment groups, while the cytosolic level of p65 was decreased in *Tc*-infected cells (Fig 7B). Further, the nuclear translocation of p65 and acetylated-p65 were increased in *Tc*-infected cardiac myocytes (Fig 7B) and associated with 7-fold and 5-fold increase in the mRNA levels for IL1β and IL6, respectively (Fig 7C.a&b, *p<0.01). The *Tc*-induced cytokine gene expression was abolished by

59%-72% by emodin treatment (Fig 7C.a&b, #p<0.05), thus, verifying the role of NFκB in signaling inflammatory responses in infected cardiomyocytes. SRT1720 treatment normalized the nuclear p65 content to control levels, substantially diminished the nuclear acetylated-p65 level (Fig 7B), and decreased the cytokine gene expression by 41%-43% (Fig 7C, #p<0.05) in infected cardiomyocytes. SRT1720 treatment also decreased the *Tc*-induced oxidative stress (iNOS, 4HNE, 3NT) in cardiomyocytes (Fig 7D). We performed a dual reporter assay to evaluate the NFκB activity. HEK293 cells were transiently transfected with NFκB-TATA-luciferase reporter plasmid and pRL-TK plasmid (expresses renilla luciferase, control for transfection efficiency), infected with *T. cruzi* for 24 h, and NFκB-dependent luciferase activity was monitored. These data showed the NFκB-dependent luciferase activity (normalized to renilla luciferase) was increased by 2-fold in *Tc*-infected cells (Fig 7E, *p<0.01) and controlled by 66% when infected cells were treated with SRT1720 (Fig 7E, #p<0.05). Together, these results suggested that SIRT1 deacetylation of NFκB-p65 regulated inflammatory responses that otherwise were pronounced in *T. cruzi*-infected cardiomyocytes.

2.4 Discussion

In this study, we demonstrated that SIRT1 activity was decreased in chagasic heart, and treatment with SIRT1 agonist during a therapeutic window, i.e., after the immune control of acute parasitemia and before the onset of myocarditis, was beneficial in preserving cardiac function in CCM. The decline in SIRT1/PGC1α activity

was not the key mechanism in mitochondrial biogenic defects in Chagas disease, and therefore SIRT1-targeted therapy did not normalize the PGC1α/NRF1-dependent mitochondrial biogenesis and cardiac remodeling in chagasic disease. Instead, SIRT1 deacetylation of NFκB-p65 repressed the *Tc*-induced inflammatory stress and preserved the antioxidant/oxidant balance in the myocardium of SRT1720-treated chagasic mice. Our results, to the best of our knowledge, provide the first evidence for potential utility of SRT1720 mediated protection of LV function in CCM.

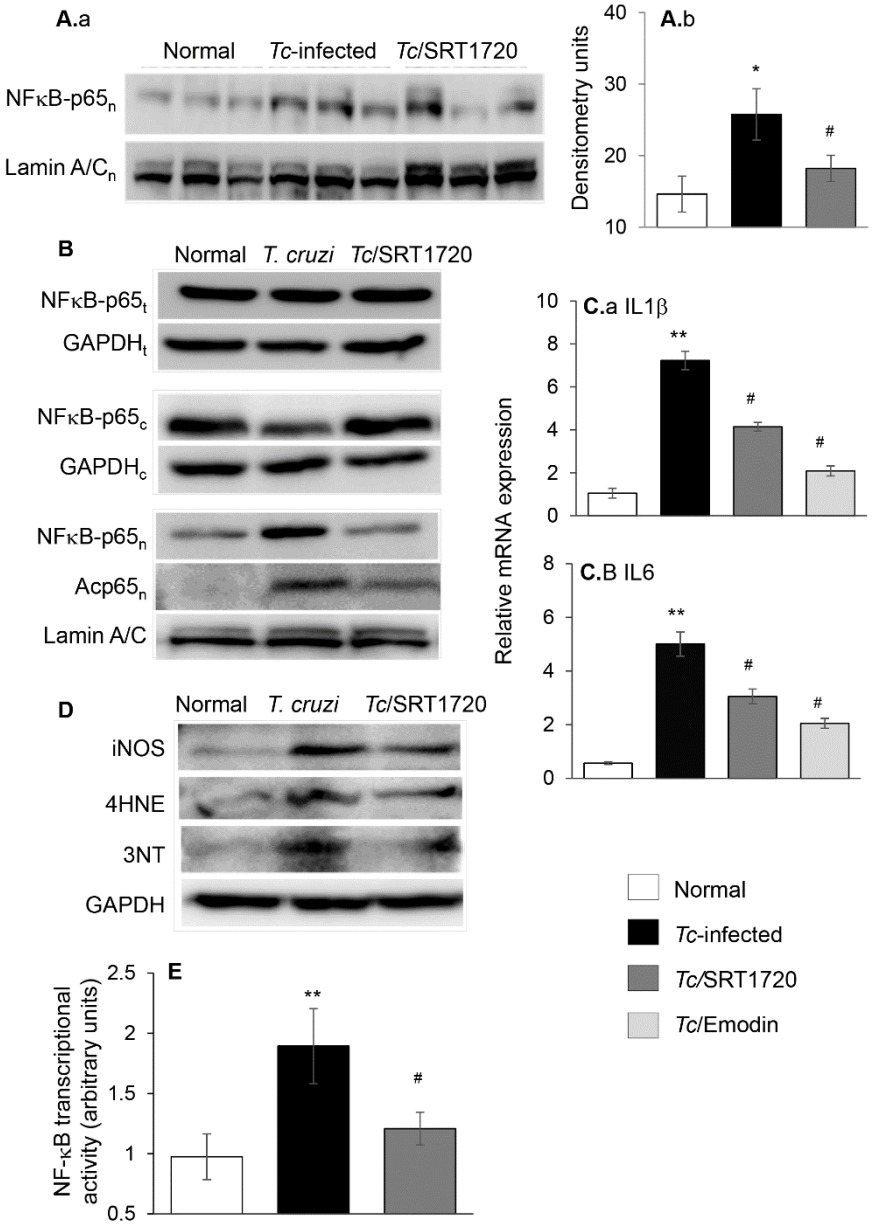

Figure 2.7. *T. cruzi* induced NF-κB transcriptional activity (± SRT1720). (A) Mice were *Tc*-infected, SRT1720-treated, and harvested at 150 days pi. Nuclear fractions from heart homogenates were prepared and submitted to Western blot analysis for NFκB p65 subunit and Lamin A/C (panel a). Densitometry analysis of NFκB p65 band, normalized to Lamin A/C, is shown in panel b. **(B)** Cardiac myocytes were infected with *T. cruzi* and incubated in presence or absence of 1 μM SRT1720 for 24 h. Shown are representative immunoblots for NFκB p65 subunit (total, cytosolic, and nuclear), and acetylated-p65 (nuclear) levels. Lamic A/C (nuclear fractions) and GAPDH (cytosolic and total homogenates) were analyzed for loading control. **(C)** Real time qRT-PCR measurement of mRNA levels for (a) IL1β and (b) IL6 in cardiomyocytes that were infected with *T. cruzi* and treated with SRT1720 (1 μM) or emodin (NFκB antagonist, 50 μM) for 24 h. Fold change was determined after normalizing the data with GAPDH mRNA. **(D)** Representative immunoblots for iNOS, 4-HNE and 3-NT (GAPDH control) levels in cell homogenates are shown. **(E)** NFκB transcriptional activity. HEK293

Others and we have shown the mitochondrial respiratory complexes and OXPHOS capacity are compromised in the cardiac biopsies of *Tc*-infected experimental animals and chagasic human patients (218, 223, 238). Our findings in this study suggested that a decline in mitochondrial biogenesis constituted at least one of the mechanisms involved in OXPHOS inefficiency in Chagas disease. This is because mtDNA content as well as the expression of the mtDNA encoded genes at mRNA and protein levels were significantly suppressed in chagasic myocardium (Fig 4); and mtDNA encoded 13 polypeptides are essential for normal assembly and function of the CI, CIII, CIV and CV complexes of the respiratory chain. The expression levels of SIRT1, PGC1α and NRF1 that are involved in regulating the mitochondrial biogenesis were not changed, yet SIRT1 activity and deacetylated-PGC1α (active form) were significantly decreased in chagasic heart (Fig 3). Though a decline in PGC1 isoforms (PGC1α and PGC1β) is noted in other metabolic diseases, such as obesity and diabetes (239-242); it is generally accepted that deacetylation, and not the changes in the expression level, of PGC1α is required for maintaining the

mitochondrial biogenesis.

We postulated that SIRT1 agonists, via enhancing the SIRT1/PGC1α activity, would offer a therapeutic option to improve the mitochondrial biogenesis, and subsequently, the heart function in CCM. We, first, used resveratrol as a therapeutic candidate for the treatment of chronic CCM. Resveratrol has been shown to induce mitochondrial biogenesis in many tissues (243, 244), control pressure overload induced hypertrophy and contractile dysfunction in mice (245, 246); and reverse the ischemia/reperfusion induced loss in renal mitochondrial mass by an increase in the expression of PGC1α and its downstream mediators (247). In the present study, though resveratrol partially improved the heart function (S1 Fig), an overall lackluster performance of resveratrol in arresting *Tc*-induced cardiac remodeling and mitochondrial biogenic defects was noted (S2-S5 Figures). This was despite the fact that we have used biologically relevant concentrations of resveratrol as was used in other studies. Our data suggest that delayed treatment in chronic phase when oxidative/inflammatory pathology have already caused tissue damage in the heart was at least partially responsible for resveratrol inefficacy in CCM. The data discussed below with SRT1720 treatment allow us to propose that SIRT1 agonists offered during the clinically asymptomatic phase when host has controlled the acute parasitemia but yet not entered the chronic phase of progressive cardiomyopathy, will be most beneficial in arresting the adverse clinical outcomes in Chagas disease.

We treated mice with SRT1720 (specific and potent SIRT1 agonist) for three weeks during 45-66 days pi. In contrast to untreated/infected mice that developed significant LV systolic dysfunction by ~150 days pi; short-term SRT1720 treatment in the clinically asymptomatic phase was effective in preserving the heart function in chronically infected mice (Fig 1). This is the first study demonstrating that SRT1720 treatment rescued the heart function following a chronic *T. cruzi* infection. The effects of SRT1720 in improving the LV function in chagasic mice were associated with a significant increase in SIRT1 activity and deacetylation of PGC1α (Fig 3), as has also been noted in models of metabolic disease (248, 249). Others have shown that long-term SRT1720 treatment produced benefits in increasing the organ function and lifespan in mice (230). SRT1720 stimulated the mitochondrial biogenesis and effectively reversed the conditions associated with metabolic deficiencies (125, 248, 250). Surprisingly, despite SIRT1 activation and PGC1α deacetylation suggested to be required for mitochondrial biogenesis, SRT1720 treatment did not reverse the mitochondrial biogenic defects in the myocardium of chagasic mice (Fig 4). A recent study showed the deacetylation by SIRT1 decreased PGC1α activity and mitochondria number in myotubes (251). Others have shown that kidney-specific overexpression of SIRT1 was protective against metabolic kidney disease though mitochondrial number was not changed. Further studies will be required to delineate the SIRT1/PGC1α dynamics in maintaining the mitochondrial biogenesis in normal and disease conditions. Yet, our data allows us to surmise that activators of the sirtuin family of proteins may be important in the development of new therapeutic strategies for treating

cardiac dysfunction in Chagas disease.

Multiple sources of ROS including mitochondrial electron transport chain leakage and NADPH oxidases, sometimes in response to cytokines and growth factors, are noted in Chagas disease (reviewed in (252)). In this study, we found that SIRT1 agonists enhanced the antioxidant capacity and reversed the oxidative/nitrosative injuries (Fig 5 & S4 Fig), inflammatory cytokine response (Fig 6, Fig 7 and S5 Fig), and infiltration of inflammatory infiltrate in the myocardium of chronically infected mice (Fig 6). Consistent with these results, SRT1720 has been reported to decrease the levels of 3-nitrotyrosine and iNOS in ischemia perfusion induced renal injury in mice (247). SRT1720 was also shown to ameliorate vascular endothelial dysfunction by enhancing COX2 signaling and reducing oxidative stress and inflammation with aging in mice (253); and increase the levels of catalase, thus reducing ROS level and apoptosis and retaining kidney function in mice (254). SIRT1 can deacetylate the FoxO factors and stimulate the expression of antioxidants (255), and inhibit NFκB signaling that is a major induced of inflammatory responses (256). The role of FoxO in preserving antioxidant/oxidant balance in CCM remains to be investigated. However, others and we have shown the activation of NFκB by *T. cruzi* in a variety of immune and non-immune cells (222, 257). A variable degree of loss in SIRT1 activity associated with steady hyper-activation of NFκB-p65 is observed in many chronic inflammatory diseases (157), including CCM in this study (Fig 7). SRT1720 treatment inhibited the nuclear translocation of p65/Rel A, NFκB transcriptional activity, and

NFκB-dependent inflammatory cytokines' gene expression in cells infected by *T. cruzi* (Fig 7). SIRT1 influenced the chronic inflammation in chagasic disease by directly deacetylating the p65/Rel A (Fig 7). SIRT1 can also inhibit the NFκB target genes by co-localizing with p65 and p300, the latter a histone acetyl transferase with a broad range of substrates. While SIRT1's ability to regulate NFκB activity is shown in macrophages (184, 258), ours is the first observation demonstrating SIRT1 regulation of NFκB in stressed cardiomyocytes. The observation of no increase in *T. cruzi* burden in mice treated with SRT1720 (Fig 6) implies that NF-κB-induced inflammatory responses were more detrimental to the host than to the parasite. Further, our finding that SIRT1 agonist (SRT1720) restricted the ROS and oxidative stress markers (3NT and 4HNE) that otherwise were significantly induced by *T. cruzi* infection (Fig 6) suggest that SIRT1/NFκB axis coordinates the oxidative stress as well as inflammation in chronic CCM and heart failure.

In summary, we have shown that mitochondrial biogenesis is compromised in chronic chagasic mice. A loss of SIRT1 activity contributed to NFκB-p65 activation and chronic cardiac pathology and heart failure in CCM. SRT1720 treatment enhanced the SIRT1/PGC1α activity but failed to improve the mitochondrial biogenesis in CCM. Instead, SRT1720 influenced the SIRT1/NFκB regulation of oxidative, nitrosative, and inflammatory responses, and, consequently, preserved the cardiac function in chagasic mice. We conclude that activators of the sirtuin family of proteins will provide promising new therapeutic strategies for treating cardiac dysfunction in chronic

Chagas disease.

Table 1. Transthoracic echocardiography in *T. cruzi*-infected (±SRT1720 treatment) mice

Parameters	Mode	WT	WT x *T. cruzi*
Heart rate (HR, beats per minute)	B mode	472 ± 51	464 ± 44
End systolic volume (ESV, µl)	B mode	16.56± 3.93	37.16± 2.82***
End diastolic volume (EDV, µl)	B mode	55.22± 7.72	51.42± 6.88
Stroke volume (SV=EDV–ESV, µl)	M mode	47.96± 2.08	29.60± 3.72***
Cardiac output (HR x SV, ml/min)	M mode	17.25± 2.76	8.52± 2.75***
% Ejection fraction (% EF = EDV-ESV x 100 / EDV)	M mode	65.78± 6.31	41.50± 5.60***
LVID, end systole ($LVID_s$, mm)	M mode	1.48± 0.21	3.16 ± 0.21***
% Fractional shortening (% FS = ($LVID_d$ – $LVID_s$) x 100 / $LVID_d$	M mode	34.95± 5.24	22.44± 1.46***
Interventricular septum (IVS_s, mm)	M mode	0.84 ± 0.23	1.21 ± 0.22*
IVS_d, mm	M mode	0.62± 0.14	1.04±0.20***
LV posterior wall ($LVPW_s$, mm)	M mode	1.45±0.30	0.85± 0.14***
LVPWd, mm	M mode	0.92± 0.17	0.67± 0.13*
IVS_s / $LVPW_s$ ratio	M mode	0.59± 0.15	1.4± 0.37***
Area systole (mm^2)	B mode	11.29± 2.67	15.77± 3.29*
Area diastole (mm^2)	B mode	17.67± 2.72	24.07±5.88*
LV mass (mg)	M mode	69.91± 10.44	97.86± 11.54***

C57BL/6 mice were infected with *T. cruzi* (10,000 parasites per mouse).

a Mice were treated with resveratrol (20 mg/L) in drinking water during days 90-111post-infection (pi).

b Mice were treated with SRT1720 (1 mg/mouse, intraperitoneal) during days 45-66 pi. Treatment was given three times a week.

Transthoracic echocardiography was performed in B and M mode at ~150 days post-infection using a Vevo 2100 System.

Data are presented as mean value ± SD. Significance is plotted as *normal vs. infected and #WT.*Tc* vs. WT.*Tc* + treatment, and presented as *,# <0.05, **,## p<0.01, ***,### p<0.001 (n = 6-10 per group per experiment).

Table 2. Oligonucleotides used in this study

Gene Name	Protein Name	Genbank Accession #	Oligo-nucleotide	Oligonucleotide sequence 5'-3'	Amplicon size (bp)
mRNA amplification					
ND1	NADH dehydrogenase subunit 1, mt	NC_001569	ND1 F ND1 R	TCACTATTCGGAGCTTTACGAGC CATATTATGGCTATGGGTCAGGC	173
COIII	Cytochrome oxidase complex subunit III, mt	NC_005089.1	COIII F COIII R	TGCTGACCTCCAACAGGAAT TTCTGAAGCTTGGAGGATGG	198
ATP6	ATP synthase 6, mt	NC_000067.6	ATP6 F ATP6 R	TCACTTGCCCACTTCCTTCC TTAGCTGTAAGCCGGACTGC	119
POLG1	DNA polymerase gamma subunit 1, mt	NC_000073.6	POLG1 F POLG1 R	GAGCCTGCCTTACTTGGAGG GGCTGCACCAGGAATACCA	294
SSBP1	Single-stranded dna binding protein, mt	NC_000072.6	SSBP1 F SSBP1 R	CAACAAATGAGATGTGGCGATCA ACGAGCTTCTTACCAGCTATGA	565
TOP1	Topoisomerase (DNA) I, mt	XM_00539252	TOP1 F TOP1 R	GACCATCTCCACAACGATTCC ATGCCGGTGTTCTCGATCTTT	96
COLI	Collagen I	NC_000077.6	COLI F COLI R	GAGCGGAGAGTACTGGATCG GCTTCTTTTCCTTGGGGTTC	158
COLIII	Collagen III	NC_000067.6	COLIII F COLIII R	GTCCACGAGGTGACA AAGGT GATGCCCACTTGTTCCATCT	535
αSMA	Smooth muscle actin alpha	NC_000080.6	SMA F SMA R	CTGGGCAAATCCAACAACTT TCTTGCCTCCTTTGCCTTTA	869
IFNγ	Interferon-gamma	NC_000076.6	IFNG F IFNG R	CATTGAAAGCCTAGAAAGTCTG CTCATGAATGCATCCTTTTTCG	201
IL1β	Interleukin-1 beta	NC_000068.7	IL1B F IL1B R	GAGCTTCAGGCAGGCAG GGGATCCACACTCTCCAGC	459
IL10	Interleukin 10	NM_010548.2	IL10 F IL10R	GCTCTTACTGACTGGCATGAG CGCAGCTAGGAGCATGTG	103
Arg1	Arginase 1	NM_007482.3	Arg1 F Arg1 R	CAGAAGAATGGAAGAGTCAG CAGATAGCAGGGAGTCACC	249
TNFα	Tumor necrosis factor-alpha	NC_000083.6	TNFA F TNFA R	GTTCTATGGCCCAGACCCTCACA TACCAGGGTTTGAGCTCAGC	836
GAPDH	Glyceraldehyde 3-phosphate	NC_000067.6	GAPDH F GAPDH R	TGGCAAAGTGGAGATTGTTG TTCAGCTCTGGGATGACCTT	402
hIL1β	Interleukin 1 beta	XM_01700398	hIL1B F hIL1B R	ACAGATGAAGTGCTCCTTCCA GTCGGAGATTCGTAGCTGGAT	73
hIL6	Interleukin 6	XM_01151539	hIL6 F hIL6 R	GTAGCCGCCCCACACAGA CATGTCTCCTTTCTCAGGGCTG	101
DNA amplification					
COII	Cytochrome oxidase complex subunit II, mt	NC_012387	COII F COII R	ATTGCCCTCCCCTCTCTACGCA CGTAGCTTCAGTATCATTGGTGCC	402
CYTB	Cytochrome b, mt	NC_010339.1	CYTB F CYTB R	GCAACCTTGACCCGATTCTTCGC TGAACGATTGCTAGGGCCGCG	71
β-Globin	Beta globin	NC_000073.6	β-Glob F β-Glob R	AGCCACAGATCCTATTGCCATGC TGTTGCTTGGTAAACACAGA	239
Tc18S rDNA	*T. cruzi* 18S ribosomal DNA	NC_018331.1	*Tc*18S F *Tc*18S R	TTTT GGGC AACA GCAG GTCT CTGC GCCT ACGA GACA TTCC	200

Unless specified, all oligonucleotides are based on mouse cDNA sequence. Human cDNAs are presented as hIL1β and hIL6.

CHAPTER 3: SRT1720 prevents the polarization of M1 macrophages and inhibits inflammatory responses in chronic Chagas disease

2.1 Introduction

Trypanosoma cruzi (*T. cruzi*) is the etiological agent of Chagas disease that is one of the most frequent causes of heart failure and sudden death in Latin America (259). Approximately 13 million people in Latin America are infected with *T. cruzi*, and 120 million people are at risk of infection. About 30% to 40% of infected individuals eventually develop clinical symptoms of chronic chagasic cardiomyopathy (11). Patients present with different degrees of severity, myocarditis, fibrosis, arrhythmia, myocardial hypertrophy and heart failure (260). Due to the immigration of infected persons to large urban cities and non-endemic countries, the epidemiological profile of the Chagas disease has changed to a globalized problem. Currently only two drugs are available for the treatment of Chagas disease (CD) and they are curative only in early infection phase. There is a need for the development of novel drugs for the treatment of chronic Chagas' disease.

The parasite load in the acute phase may influence the activation of host immune system and the progression of chronic Chagas disease (261). Although the mechanisms that mediate control of parasitemia have not been well defined, it is believed that innate immune cells such as natural killer (NK) cells, dendritic cells, neutrophils, and macrophages play a major role in elimination of parasitism (114). In response to *T. cruzi* infection, macrophages secrete various endogenous mediators, including cytokines, nitric oxide (NO), and reactive oxygen species (ROS) to mediate

pathogen killing in the acute phase (115-117). The role of macrophage activation in chronic Chagas disease have not been elucidated.

Macrophages are immune cells which quiescently survey the various tissue milieu for early signs of infection or damage (170). Macrophages can be found in tissues or circulate in peripheral blood. The plasticity of the inflammatory monocytes allows them to change their phenotype based on the environment cues or alter the immune responses after exposure to a specific stimulus. Classically activated of macrophage (also called M1 macrophage) occurs when the cell receives stimuli such as LPS, IFN-γ and granulocyte-macrophage colony stimulating factor (GM-CSF). Alternatively activated macrophage (also called M2 macrophage) is induced by fungal cells, parasite infections, macrophage colony stimulating factor (M-CSF), IL-4, IL-13, IL-10 and TGF-β. M1 and M2 macrophages have different functions. The M1 macrophages play a central role in host defense against bacterial and viral infections (174, 175). They help to drive antigen specific Th1 and Th17 cell inflammatory responses, produce pro-inflammatory cytokines, toxic reactive oxygen intermediates (ROS) and NO (176-178). In contrast, M2 macrophages lead to the secretion of extracellular matrix (ECM) components, angiogenic and chemotactic factors and high amounts of IL-10. They play a central role in parasite control, wound-healing, fibrosis, tumor progression and immune regulation (178). On the basis of the stimulus from the microenvironment and their distinct gene expression profiles, M2 macrophages can be further divided into subsets, specifically M2a, M2b, M2c and M2d (179, 180).

Sirtuins, initially named as Silent information regulator 2 (Sir2) proteins, are

defined as NAD dependent class III histone deacetylases. SIRT1 is the closest homologue of yeast Sir2 and has been studied most (97). SIRT1 mediates deacetylation and regulates the function of a number of proteins involved in critical physiological processes including oxidative stress, metabolism, cell proliferation, and genomic stability. SIRT1 inhibition has been reported to associate with chronic inflammatory diseases, metabolic dysfunctions, neurodegenerative diseases and cardiovascular dysfunction (104-107). SRT1720 is a potent SIRT1 agonist that binds to the SIRT1 enzyme-peptide substrate complex, and it has been reported to enhance deacetylation of SIRT1 target proteins in both cells and animals (122, 123). SRT1720 treatment has been shown to prevent secretion of TNFα in primary intraperitoneal macrophages (188) and inhibit LPS-stimulated NF-κB inflammatory pathways in RAW macrophages (118). The role of SIRT1720 in macrophage polarization and function in parasite disease is not known.

In this study, our objective was to determine (i) whether macrophage activation/polarization plays a role in chronic Chagas disease and (ii) how SIRT1 agonist contributes to the macrophage phenotype and function. For this, we infected C57BL/6 mice with *T. cruzi*, treated with SRT1720 after the end of acute parasitemia, and monitored macrophages phenotype and function in chronic phase. Our data suggest that splenic macrophages of chronically infected macrophages were primarily of M1 phenotype. SRT1720 prevented the polarization of M1 macrophages and inhibited inflammatory and oxidative responses in chronic Chagas disease. This finding suggest that small molecular activators of SIRT1 could be effective strategy to

prevent chronic inflammatory diseases through regulation of macrophage activation.

3.2 Material and methods

Ethics statement

All animal experiments were performed following NIH guidelines for Care and Use of Experimental Animals, and in accordance with protocols approved by the Institutional Animal Care and Use Committee (IACUC) at the University of Texas Medical Branch, Galveston (protocol number: 0805029).

Mice, parasites, and cell culture

C57BL/6 mice (6 to 8 weeks old) were purchased from Jackson Laboratory (Sacramento, CA). Trypomastigotes of *T. cruzi* (SylvioX10/4 strain, ATCC 50823) were maintained and propagated by continuous *in vitro* passage in C2C12 cells. Mice were infected with *T. cruzi* (10,000 trypomastigotes/mouse, intraperitoneal), and harvested at days 150 post-infection (pi) corresponding to chronic disease phase. To enhance the SIRT1 activity, mice were given SRT1720 (1 mg/100 µl/mouse, intraperitoneally, Selleck Chemicals, Houston, TX) three times per week during day 45-66 pi.

Flow cytometry

Single-cell suspensions of spleen cells were isolated and resuspended in PBS containing 0.5% BSA and 0.02% sodium azide. Isolated splenocytes were washed in

staining buffer and stained with fixable viability dye (eFluor 506) according to the manufacturer's instructions. Nonspecific binding was blocked by incubation with (anti-CD16/CD32; BD Pharmingen) for 15 min at 4°C. Cells were divided into two groups. Group1 were labeled with PerCP/Cy5.5-αF4/80, APC/Cy7- αCD11b, eFluor 450-αLy6G, APC-αCD80 and group 2 were labeled with PerCP/Cy5.5-αF4/80, APC/Cy7- αCD11b, eFluor 450-αLy6G, Alexa Fluor 647- αCD64 and PE-αCD200 antibodies for 30 min at 4°C in the dark. Group 1 were washed twice in PBS and further fixed with 2% paraformaldehyde, re-suspended in 100-μl permeabilization buffer (0.1% saponin/1% FBS in PBS), and then utilized for intracellular staining with fluorescence- conjugated PE-CD206 antibody. Anti-CD16/32 and fluorescence conjugated APC/Cy7- αCD11b, and Alexa Fluor 647-αCD64 antibodies were purchased from BD Pharmingen (San Diego, CA). APC-αCD80, PerCP/Cy5.5-αF4/80, and PE-CD206 antibodies were purchased from BioLegend (San Diego, CA). Fixable viability dye (eFluor 405), eFluor 450-αLy6G and PE-αCD200 antibodies were purchased from eBioscience (San Diego, CA). Fluorescent cells were visualized by using a FACSCalibur Cell Analyzer (BD Biosciences) and analyzed by using FlowJo software (version 7.6.5, Tree-Star, San Carlo, CA).

Isolation of monocytes/macrophages

Single cell suspension of splenocytes was made in isolation buffer (PBS containing 0.5% BSA and 2 mM EDTA), and CD11b+ monocytes/macrophages were positively selected from the total splenocytes using the MACS Microbeads

technology (Miltenyi Biotec Inc., San Diego, CA, #130-049-601) according to the manufacturer's instructions. Briefly, the monocytes/macrophages were magnetically labeled with CD11b microbeads and passed through MACS separation column while placed in the magnetic field. The columns were then washed three times with 5 ml MACS buffer, and the CD11b+ cells were collected. To remove CD11b+ cells from the column, the cells were washed with 5 ml MACS buffer away from the magnetic field. Isolated cells were stained with PerCP/Cy5.5-αF4/80, APC/Cy7- αCD11b and eFluor 450-αLy6G antibodies, and then subjected to flow analysis to confirm the purity of macrophages.

In vitro stimulation of monocytes/macrophages and intracellular cytokines

Isolated monocytes/macrophages ($5x10^5$ cells/1ml RPMI) were distributed in 12-well plates, and incubated in the presence of *T. cruzi* trypomastigotes (cell: parasite ratio, 1:3) for 24 h at 37°C, 5% CO_2. Cell free supernatants were collected for the measurement of cytokine release (IL-6 and TNF-α) using optEIA enzyme-linked immunosorbent assay (ELISA) kits (Pharmingen, San Diego, CA), according to the manufacturer's specifications.

Gene expression analysis

RNA was isolated by chloroform/isopropanol/ethanol method form both non-stimulated and *in vitro* stimulated monocytes/macrophages. After reverse transcription of RNA with poly(dT)18 using an iScript cDNA Synthesis Kit (Bio-Rad), first-strand

cDNA was used as a template in a real time quantitative PCR (qPCR) on an iCycler Thermal Cycler with SYBR-Green Supermix (Bio-Rad). Primer sequences used are as follows: mTNFα forward: 5'- GCTCTTACTGACTGGCATGAG-3', mTNFα reverse: 5'- TACCAGGGTTTGAGCTCAGC-3'; mIL-6 forward: 5'- TTCTCATTTCCACGATTTCCCAG-3', mIL-6 reverse: 5'- TTCCATCCAGTTGCCTTCTTG-3'; mIL-10 forward: 5'- GCTCTTACTGACTGGCATGAG-3', mIL-10 reverse: 5'- CGCAGCTAGGAGCATGTG-3'; mArg1 forward: 5'- CAGAAGAATGGAAGAGTCAG-3', mArg1 reverse: CAGATAGCAGGGAGTCACC-3'. The PCR base line subtracted curve fit mode was applied for threshold cycle (Ct), and mRNA level was calculated using iCycler iQ real-time detection system software (Bio-Rad). The threshold cycle Ct values of target mRNAs were normalized to mean of GAPDH mRNA, and the relative expression level of each target gene calculated from Ct values using the formula: $2^{-\Delta Ct}$, where ΔCt represents the Ct (sample) - Ct (control) (233, 234).

ROS measurement

Supernatants (50 μL/well) from *in vitro* stimulation of monocytes/macrophages were added in triplicate to 96-well flat-bottomed plates and mixed with 50 μL of 100 μmol/L 10-acetyl-3,7-dihydroxyphenoxazine (amplex red, Molecular Probes) and 50 μL of 0.1 U/mL horseradish peroxidase. The H_2O_2-dependent oxidation of amplex red to fluorescent resorufin ($Ex563_{nm}/Em587_{nm}$) was measured by using a SpectraMax M2 microplate reader (Molecular Devices) (262).

Immunohistochemistry

To visualize in situ population, paraffin-embedded 5 µm tissue sections (3 slides/mouse, n= 5/group) were deparaffinized and treated with 10 minutes of microwave oven heating in 0.01m sodium citrate buffer (pH 6.0). Slides were then washed twice in PBS, incubated with 5% normal goat serum to reduce non-specific staining for 30 min and with 3% H2O2 in methanol for 30 min to inactivate endogenous peroxidase. Tissue sections were incubated overnight at 4°C with mouse monoclonal anti-Mac-1 (1:50 dilution; Abcam, Cambridge, MA) antibody. After washing, slides were incubated at room temperature for 30 min each with biotinylated anti-mouse IgG (1:100 dilution) and streptavidin-conjugated alkaline phosphatase, and red color was developed with a Red AP Kit I (Vector Laboratories, Burlingame, CA, SK-5100). Slides were then treated by another round of microwave heating in order to prevent an antibody cross reaction and also improve antibody access to nuclei. Following a second preincubation step as above, sections were labeled with the rabbit anti-iNOS (1:50 dilution, Santa Cruz Biotech, Dallas, TX, sc-651) or rabbit anti-Arginase (1:50 dilution, Santa Cruz Biotech, Dallas, TX, sc-20150) antibodies at 4°C overnight. After washing, sections were labeled with biotinylated anti-rabbit (1:100 dilution) and streptavidin-conjugated horseradish peroxidase (1:100 dilution) and brown color was developed with a DAB Peroxidase (HRP) Substrate Kit (Vector Laboratories, Burlingame, CA, SK-4100). Sections were then counterstained with methyl green (stains nuclei).

Data analysis

Mice were randomly assigned to three groups (no treatment, *T. cruzi* infection, *Tc* infection followed by SRT1720 treatment, n=5 mice per group per experiment). All experiments were conducted with triplicate observations per /sample/time (at least two experiments per group). Data are presented as mean ± standard deviation (SD). All data were analyzed using GraphPad Prism5 software (GraphPad Software, La Jolla, CA). Data were analyzed by student's t test (for comparison of 2 groups) and one-way analysis of variance (ANOVA) with Tukey's post hoc test (comparisons of more than two groups). Significance is presented by **Tc*-infected vs. normal or $^{\#}$*Tc* infected vs. *Tc*/SRT1720-treated) ($^{*,\#}p<0.05$, $^{**,\#\#}p<0.01$, $^{***,\#\#\#}p<0.001$).

3.3 Results

Macrophages can be identified by using flow cytometry. Previous studies have used F4/80 and CD11b to identify monocytes and macrophages in both lymphoid and non-lymphoid tissues. In order to identify macrophages in spleen, we utilized a combination of antibodies against Gr-1, F4/80, and CD11b to characterize the macrophage cell population in mouse spleen. After exclusion of debris, doublets, nonviable cells and gating out $Ly6G^{+}$ neutrophils, a clear population of $F4/80^{+}CD11b^{+}$ cells could be found in mouse spleen cell population. In chagasic (vs. normal) mice, splenic percentage of macrophages was significantly increased.

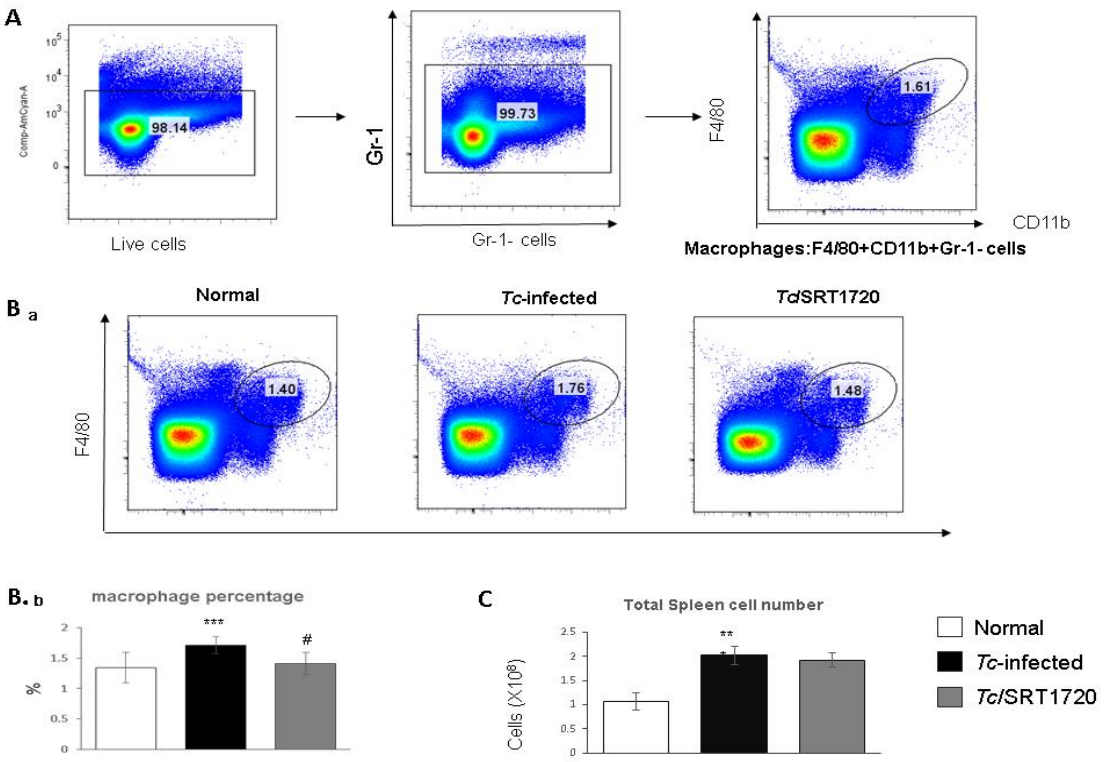

Fig 3.1. *In vivo* splenic cell analysis by flow cytometry. C57BL/6 mice were infected with *Trypanosoma cruzi* (10,000 *Tc*/mouse, ip), and treated with SRT1720 (SIRT1 agonist) during 45-66 days post-infection (pi), as described in materials and methods. The mice were harvested at 150 days pi. **(A)** Total splenocytes were stained with CD11b, F4/80, Gr-1. We define the CD11b+F4/80+Gr-1- cells as macrophages. **(A&B)** Percentage of macrophages in splenocytes from chagasic mice (±SRT1720). **(C)** The total number of splenic cells from chagasic mice (±SRT1720).

Treatment of chagasic mice with SRT1720 decreased the macrophage population to normal levels (Fig 1 A, 1 B. a-b). However, a similar number of splenocytes were observed in all mice, thus, suggesting that SRT1720 did not have any adverse impact on total spleen cell number (Fig 1 C).

To evaluate the phenotype(s) of the macrophages present in the spleen during chronic *T. cruzi* infection and the effect of SRT1720 treatment, we designed a flow cytometry panel to detect surface markers of M1 and M2 phenotypes. The C80 and CD64 expression were used to identify mouse M1 subtype, whereas CD206 and

CD200R were used for the identification of the M2 subtype. The samples were stained concurrently with two different cocktails. The first cocktail contained antibodies against CD11b, F4/80, Ly6G, CD80 and CD206 while the second cocktail contained antibodies against CD11b, F4/80, Ly6G, CD64 and CD200R. After gating out debris, doublets, and nonviable cells, sub-populations of F4/80^{+}CD11b^{+}Gr-1^{-} cells were gated as macrophages. We observed that the frequency of CD64^{+} and CD80^{+} macrophages was significantly increased in chagasic mice, and decreased by 18% in chagasic mice treated with SRT1720 (Fig 2A. a&b, Fig 2B. a&b). The frequency of CD206+ and CD200R+ macrophages was also enhanced significantly in chagasic mice, but no significant effect of SRT1720 was observed on splenic CD206^{+} and CD200R^{+} macrophages in chagasic mice (Fig 2A. c&d, Fig 2B. c&d). These results suggested that 1) *T. cruzi* infection stimulates the activation of both M1 and M2 (M1>M2) macrophages during the chronic phase. 2) SRT1720 decreased the proinflammatory differentiation of macrophages in chagasic cardiomyopathy.

Next, we determined if surface expression of physiological indicators of macrophage phenotype correlated with the proinflammatory versus anti-inflammatory

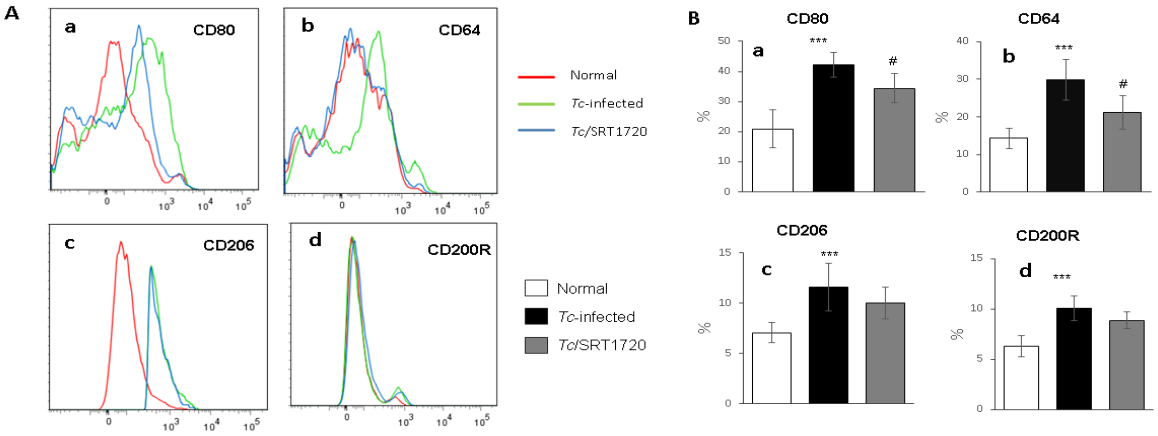

Fig 3.2. SRT1720 inhibited *T. cruzi* induced increasing M1 markers expression in spleen. Mice were infected, SRT1720-treated, and harvested as in Fig 1. Gated macrophages were additionally examined for expression of phenotypic markers by flow cytometry. **(A)** Fluorescence intensity of surface expression of M1markers (a&b, CD80 and CD64) and M2 markers (c&d, CD206 and CD200R) from normal (red), *Tc*-infected (green), and SRT1720 treated/chagasic (blue) mice. **(B)** The mean percentage of cells expressing the M1 markers (a&b, CD80 and CD64) and M2 markers (c&d, CD206 and CD200R) was acquired by flow cytometry analysis.

activation profile. Splenic CD11b$^+$ monocytes/macrophages were isolated by using anti-CD11b antibody-coated micro-beads. Isolated monocytes/macrophages from chagasic mice exhibited up to 15-fold to 30-fold increases in mRNA level for proinflammatory cytokines TNF-α and IL-6 (Fig 3A. a&b), respectively, and around 10-fold increases in immunomodulatory Arg-1 and IL-10 gene expression, compared to that noted in monocytes/macrophages isolated from normal mice (Fig 3B. a&b). These results suggested that a mixed pro-inflammatory and anti-inflammatory cytokine response with a predominance of proinflammatory activation is presented in splenic monocytes/macrophages of chronically infected chagasic mice. In comparison, splenic monocytes/macrophages isolated from SRT1720-treated chagasic mice exhibited no basal level of TNF-α and IL-6 mRNA (similar to normal controls) (Fig 3A. a&b). However, Arg-1 and IL-10 mRNA levels in SRT1720-treated chagasic mice were similar to that noted in untreated/chagasic mice (Fig 3B. a-b). These data suggested that SRT1720 decreased the pro-inflammatory cytokine production but did not alter the anti-inflammatory cytokine's expression in splenic monocytes/macrophages of chagasic mice.

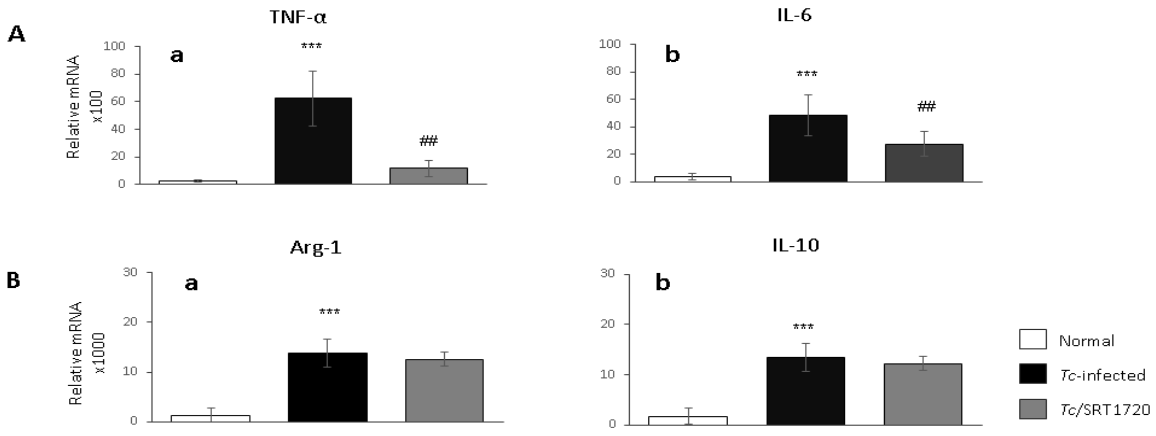

Fig 3.3: *In vivo* macrophage profile in chronic chagasic mice (±SRT1720). Mice were infected, SRT1720-treated, and harvested as in Fig 1. Splenic macrophages were isolated by using MACS CD11b MicroBeads as describe in materials and metods. The total RNA of macrophages was isolated and gene expression of pro-inflammatory cytokines TNF-α and IL-6 **(A.a&b)** and anti-inflamatory cytokines IL-10 and Arg-1 **(B.a&b)** was determined by real-time RT-PCR.

Isolated splenic monocytes/macrophages from WT, chronically-infected and infected/SRT1720-treated mice were incubated for 24 h with *T. cruzi*. Splenic monocytes/macrophages of chagasic mice responded to *in vitro* incubation with *T. cruzi* by a >10-fold increase in TNF-α and IL-6 mRNA levels (Fig 4A. a&b) and >3-fold further stimulation of Arg-1 and IL-10 expression (Fig 4B. a&b). These results indicated that monocytes/macrophages from chagasic mice are capable of responding to stimuli

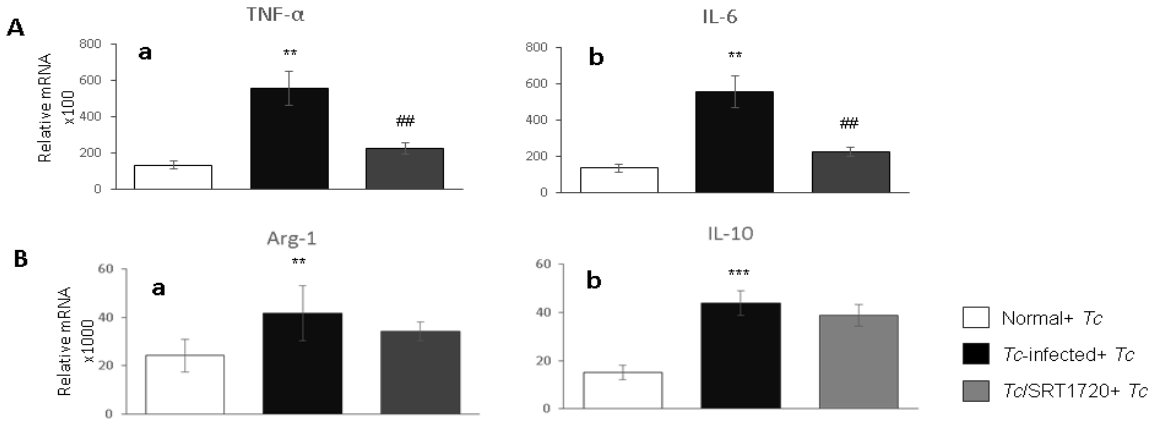

Fig 3.4: *In vitro* functional activation of macrophages from chagasic mice (±SRT1720) in response to *Tc* infection. Mice were infected, SRT1720-treated, and harvested as in Fig 1. Splenic macrophages were isolated as in Fig4. Splenic macrophages were *in vitro* incubated with *Tc* for 24h. The supernatant were collected and the macrophages were stored. The total RNA of macrophages was isolated and gene expression of pro-inflammatory cytokines TNF-a and IL-6 **(A.a&b)** and anti-inflamatory cytokines IL-10 and Arg-1 **(B.a&b)** was determined by real-time RT-PCR.

by further increase in proinflammatory cytokine response. Splenic monocytes/macrophages of normal as well as chagasic mice (±SRT1720) responded to *in vitro* stimulation with *T. cruzi* by mixed cytokine response (TNF-α+IL-6>Arg-1+IL-10) (Fig 4A&4B). The release of cytokines in supernatants of splenic macrophages incubated with *T. cruzi* for 24 h was measured by an ELISA. Our data showed that pro-inflammatory cytokines (TNF-α and IL-6) release was increased by 2-3-fold in macrophages from infected mice *in vitro* infected with *T. cruzi* as compared to that noted with normal controls (Fig 5A&5B). IL-4 and IL-10 were not detectable by ELISA in the supernatants (data not shown). And TNF-α and IL-6 were decreased to the normal level in macrophage from SRT1720 infected mice (Fig 5A&5B). A similar outcome was observed as described above for fluorometric evaluation of H2O2 release in the supernatant (Fig 5C). All these results suggested that SRT1720 did not change the macrophage's ability to respond to stimuli, rather the proinflammatory stimulus was decreased in SRT1720-treated chagasic mice.

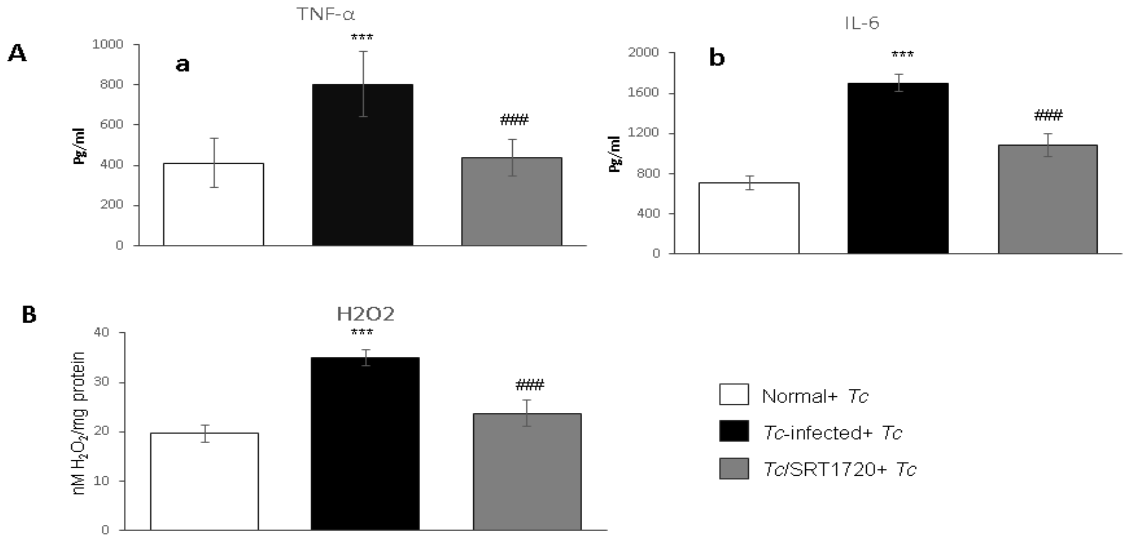

Fig 3.5: *In vitro* cytokine and ROS production from chagasic mice (±SRT1720) in response to *Tc* infection. Mice were infected, SRT1720-treated, and harvested as in Fig 1. Splenic monocytes/macrophages were isolated as in Fig4. Splenic monocytes/macrophages were *in vitro* incubated with *Tc* for 24h. The supernatant was collected. **(A)** The TNF-α **(a)**, IL-6 **(b)** levels in cell-free supernatant were measured by an ELISA. **(B)** ROS level in the supernatant was measured by Amplex Red Assay.

In order to determine the extent of monocyte/macrophage infiltration and phenotypes of the monocytes/macrophages present in the hearts of infected and SRT1720 treated mice during the chronic disease phase, we examined markers of functional populations of M1 and M2 subtypes. The iNOS expression was used for identifying rodent M1 subtype, whereas arginase-1 was used as phenotypic marker for M2 macrophages. We observed the expression of iNOS (brown color) and Arg-1(brown color) on infiltrated Mac-1 positive monocytes/macrophages (red color) in heart tissues by double immunohistochemistry. Immunohistochemistry with anti-mac1 antibody (monocytes/macrophage marker) showed that the monocyte/macrophage infiltration was significantly decreased in the hearts of SRT1720 treated chronically

infected mice compared to non-treated chronically infected mice (Fig. 6, compare panels b and c, panels e and f, panels h and i). Most of the infiltrating monocytes/macrophages in the myocardium of chronically infected mice were iNOS positive. We noted a significant decline in myocardial levels of iNOS in SRT1720 treated chronically infected mice compared with non-treated chronically infected mice (Fig. 6, compare panels d and e). We observed similar numbers of Arg-1 positive cells in the hearts of SRT1720 treated and non-treated chronically infected mice (Fig. 6, compare panels h and i). In chronically infected mice, all of the iNOS and arginase-1-expressing cells appeared to be not overlapping with CD11b+ macrophages, revealing

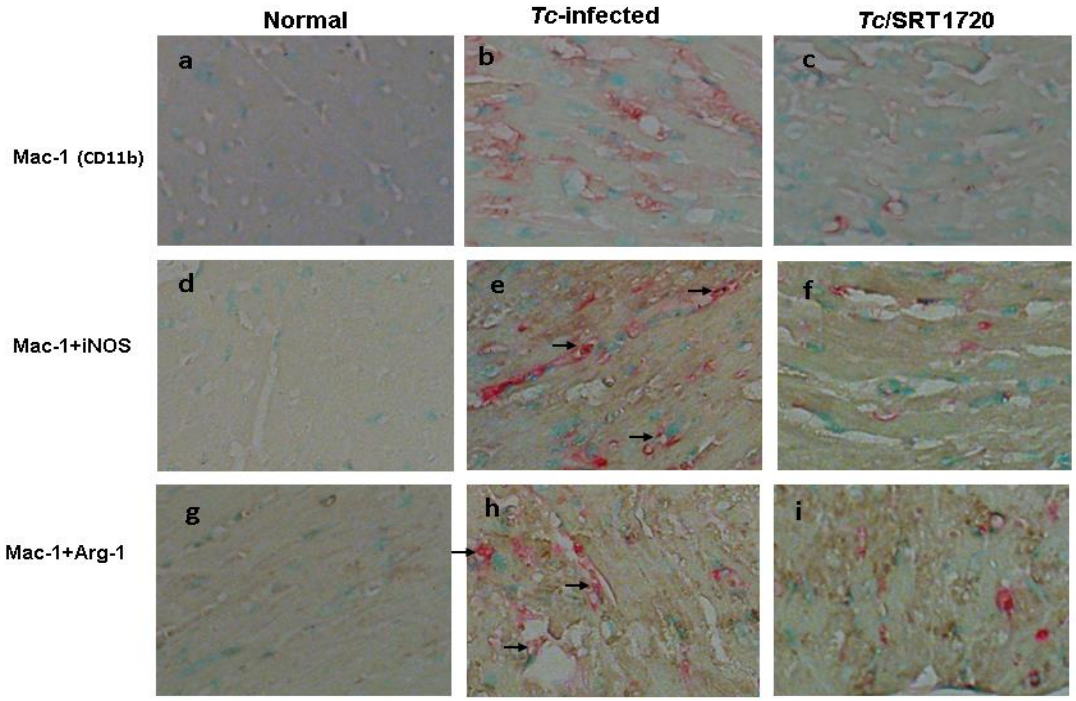

Fig 3.6. *In vivo* monocyte/macrophage infiltration and phenotype in chagasic mice (±SRT1720). Mice were infected, SRT1720-treated, and harvested as in Fig 1. Paraffin-embedded heart tissue sections were subjected to immunostaining with antibodies against CD11b, (Mϕ, pink color), anti-iNOS (M1ϕ) and anti-Arg-1(M2ϕ) (brown color). **(a-c)** Immunostaining with anti-Mac-1 antibody. **(d-f)** Immunostaining with anti-Mac-1/anti-iNOS (arrows indicate the pink/brown staining of iNOS+ monocytes/macrophages). **(g-i)** Immunostaining with anti Mac-1/anti-Arg-1 (arrows indicate the pink/brown staining of Arg-1+ monocytes/macrophages).

that some of iNOS and arginase-1 in the myocardium are produced by other cell types. All together these results suggested that SRT1720 significantly declined proinflammatory monocyte/macrophage infiltration in the myocardium and these results are consistent with the results of flow cytometry as described in Fig. 2.

3.4 Discussion

Chronic chagasic cardiomyopathy (CCM) is presented by increased oxidative/inflammatory stress. SIRT1 has also been reported to inhibit the oxidative stress and inflammation through regulation of the transcription factors and histones (226). We have previously shown that SRT1720 treatment enhanced the SIRT1 activity, controlled the NFκB signaling of oxidative, nitrosative, and proinflammatory cytokines responses and consequently helped preserve the left ventricular function in chronic chagasic mice.

Studies have suggested that macrophages could be used as potential cancer therapeutic targets by manipulating macrophage functional phenotypes (263-265) . This study was designed to test whether SIRT1 agonist SRT1720 has therapeutic effects against chronic Chagas disease through regulating functional polarization of macrophages. We reasoned that macrophage is required for regulating immune response to prevent tissue damage in chronic Chagas disease. We then administrated SRT1720 to *T. cruzi*-infected mice to test our hypothesis. First, we determined that both M1 and M2 were activated in response to *T. cruzi* but the primary cell type is M1

macrophages during the chronic phases. And pro-inflammatory cytokines were significantly increased in monocytes/macrophages isolated from chronic chagasic mice. Second, we found that SRT1720 treatment was able to suppress proinflammatory differentiation of monocytes/macrophages (M1 macrophages) in chagasic cardiomyopathy and reduced proinflammatory cytokine production in spleen. However, SRT1720 treatment did not change the frequency of M2 macrophages and anti-inflammatory cytokine production. We also examined the macrophage's phenotype in heart tissue sections and found that there is a decline in M1 phenotype monocyte/macrophage infiltration in the myocardia which is consistent with our finds in spleen. Our data clearly support the hypothesis that the full capacity of SRT1720 to prevent tissue damage requires suppression of M1 type macrophage infiltration and activation through reducing pro-inflammatory cytokines and ROS production.

During the early phase of infection, *T. cruzi* induces a broad inflammatory response that persists and contributes to the pathogenesis of the disease (266). Macrophages serve as the first responders to *T. cruzi* infection and play a significant role in the direct killing of *T. cruzi* (49). Previous studies have shown that spleen or peritoneal macrophages isolated from acutely *T. cruzi* infected mice release high levels of TNF-α, IL-6, IL-1β, and nitric oxide (NO), thus, suggesting M1 polarization of macrophages in response to first exposure to *T. cruzi* (267, 268). At the same time, macrophages produce regulatory cytokines such as IL-10 and IL-4 to prevent the harmful effects lead to M2 polarization (269). Thus, both M1 and M2 macrophages are

induced during the acute stage of infection. Acute parasitemia is controlled by innate and adaptive immune responses against *T. cruzi*; however, chronic inflammation persists in the host. In this study, we provide first evidence that both M1 and M2 type macrophages are activated in spleen and myocardium during the chronic *T. cruzi* infection but primary M1 macrophages are present. Macrophages exist as a mixed population of M1/M2 in chronic Chagas disease may enable their proper adaptation to the changing environments. We also found that macrophages produced high amount of proinflammatory cytokines TNF-α and IL-6 as well as ROS.

Our observation that SRT1720 treatment did not change the peripheral and tissue parasite burden in chronically infected mice (data not shown) suggest that besides *T. cruzi*, other stimuli present in chronically infected mice that contribute to inflammatory macrophage activation. We showed that macrophages incubated *in vitro* with sera from chronically infected mice, in comparison to mice that were immunized with a subunit vaccine and controlled parasitemia and disease, polarized toward a proinflammatory phenotype with extensive production of TNF-α (270). Likewise, microparticles isolated from sera samples of chagasic patients with clinical disease symptoms (in comparison to seropositive/no disease patients) elicited a proinflammatory profile in human macrophages (266). In another study, we have shown that cardiac lysates of chagasic mice consist of oxidized proteins and incubation of macrophages with cardiac lysates of chagasic (vs. normal) mice elicited inflammatory cytokine and ROS response (44). We postulate that SRT1720 treatment decreased the generation of damage associated molecules (e.g. oxidized cardiac

proteins) and thereby removed the stimuli that contribute to proinflammatory activation of macrophages.

As macrophage infiltration plays an important role in tissue inflammation in chronic Chagas disease and SIRT1 has anti-inflammatory property, we proposed the hypothesis that SRT1720 treatment will inhibit macrophage's migration to the spleen as well as to the heart in chronic Chagas disease. In several rodent models of chronic inflammation, SIRT1 has been reported to regulate macrophage infiltration or migration. In a mouse model of type 1 diabetes, resveratrol prevented the macrophage migration from peripheral lymphoid organs to the pancreas (190). In addition, resveratrol treatment decreased percentage of CD11b+ monocytes/macrophages to the normal level in mesenteric lymph nodes and the lamina propria in a mouse model of colitis (191). In contrast, SIRT1 KO mice displayed increased macrophage infiltration in the synovial tissues as compared to WT mice in inflammatory arthritis (189). Our results are in agreement with previous finds and provide more evidence for the importance of SIRT1 in regulating macrophage activation, especially M1 macrophage infiltration in the spleen and heart in chronic Chagas disease.

In our model, we observed that SRT1720 inhibited M1 macrophage polarization and decreased expression of pro-inflammatory cytokines TNF-α and IL-6 in splenocytes. A large body of literature suggested that SIRT1 regulates macrophage polarization by inhibition of M1 macrophages (118, 188, 193, 194). Indeed, most of the

previous studies using SIRT1 knockout (KO) mice have shown that SIRT1 KO mice display significant increase in macrophage infiltration in target tissues compared with WT mice. Other studies showed that SRT1720 treatment inhibited LPS-stimulated inflammatory pathways, as well as secretion of TNFα in RAW264.7 cells and in primary intraperitoneal macrophages (118). These results are consistent with our *in vivo* and *in vitro* data, which further indicate that decreased differentiation of M1 macrophages and pro-inflammatory cytokine production is associated with SIRT1 activation. Our study is also consistent with previous findings that SRT1720 regulates M1 macrophage differentiation but without major effects on M2 macrophages. We further showed that SRT1720 does not inherently mute the macrophages' capability to respond to infectious agents. This is evidenced by the finding that *in vitro* incubation with *T. cruzi* elicited a similar level of pro-inflammatory response in macrophages of chronically infected / SRT1720-treated mice as was observed in macrophages of infected/untreated mice.

In summary, our data suggest that activation of proinflammatory M1 type macrophages occurs due to tissue damage and contributes to tissue damage presented during chronic Chagas disease. We also characterized that SRT1720 treatment prevented the chronic tissue damage in chagasic mice, and this was reflected by SRT1720 inhibition of the pro-inflammatory cytokine and ROS production in macrophages of chagasic mice. This is the first study that uses SRT1720 as the therapeutic approach to study the macrophage biology in chronic Chagas disease.

CHAPTER 4: CONCLUDING REMARKS

Inflammatory and oxidative stress and mitochondrial dysfunction are considered to be pathological factors in progression of chronic chagasic cardiomyopathy and heart failure. SIRT1 is a nicotinamide adenosine dinucleotide (NAD)-dependent deacetylase that participates in a wide variety of functions in biological systems by deacetylation of various proteins. In this study, we aimed to determine whether enhancing the activity of SIRT1 by SRT1720 treatment would have beneficial effects on cardiac function in Chagas disease. We administered SRT1720 to *T. cruzi*-infected mice after the control of acute parasitemia but before the beginning of chronic disease, and harvested them during the chronic disease phase. The activation of SIRT1 by SRT1720 treatment was confirmed by SIRT1 activity assay and the observation that deacetylation of PGC-1α was increased in SRT1720-treated chagasic mice. We found that the administration of SRT1720 for three weeks ameliorated the left ventricular dysfunction in chronic chagasic mice. SRT1720 did not show any beneficial effects against the mitochondrial biogenic defects in chagasic mice. Instead, SRT1720 administration decreased the chronic oxidative/nitrosative stress and inflammatory responses that otherwise were pronounced in chagasic mice. We also found that SIRT1 prevented the chronic inflammation in chagasic disease by directly deacetylating the p65/Rel A.

We studied the effects of SRT1720 on phenotype and function of M1 and M2 macrophages in chronic chagasic mice. SRT1720 decreased the proinflammatory

differentiation of macrophages in spleen of chronic chagasic mice. SRT1720-treated chagasic mice exhibited a significant decline in proinflammatory cytokines' mRNA level and protein level compared to splenic monocytes/macrophages of chagasic mice. However, anti-inflammatory cytokine's expression in splenic monocytes/macrophages was not altered by SRT1720. SRT1720 did not change the macrophage's ability to respond to stimuli, rather the proinflammatory cytokines were decreased in SRT1720-treated chagasic mice. SRT1720 also prevented M1 phenotype monocyte/macrophage infiltration in the chagasic myocardia.

Macrophage is an attractive therapeutic target, and it is important to understand its phenotypes according to their characteristics such as its origins (yolk sac, fetal liver, bone marrow) (271). Macrophages are derived from circulating peripheral-blood mononuclear cells (PBMcs) (171). These PBMcs differentiate from common myeloid progenitor cells in the bone marrow. These progenitor cells originate from hematopoietic stem cell (HSC) monoblasts, and sequentially give rise to a series of differentiation stages: the common myeloid progenitor (CMP) (172), the granulocyte-macrophage progenitor (GMP) (172), the common macrophage and DC precursor (MDP) (173), and finally the monocyte progenitor (cMoP). Then monocytes migrate from the blood and then get recruited to injury sites. The phenotype and function of macrophages can be regulated by the environment from their progenitors (272). Though macrophages in resident tissue can be replenished after infection or other stimulus, the mechanisms that regulate initiation and differentiation of macrophage

subsets from their progenitors remain unknown in chronic Chagas disease. And SIRT1 has been reported to prevent differentiation of monocytes to macrophages in rheumatoid arthritis (183).

Our future research will pay more attention to the characterization of the proliferative progenitors restricted to monocytes and monocyte-derived macrophages in the bone marrow and spleen. We will first investigate the percentage of different myeloid progenitor cells in the bone marrow and spleen. And we will study whether SIRT1 inhibits the differentiation of monocytes into macrophages and whether the myeloid progenitor cells would be altered by SIRT1. Different monocyte surface-marker markers (MDP cells: CD117+CD115+CD135+Ly6C−CD11b−, cMoP cells: CD117+CD115+CD135−Ly6C+CD11b−, and monocytes: CD117−CD115+CD135−Ly6Chi or Ly6Clo CD11b+) will be used and flow cytometry will be performed to identify these monocytes and SIRT1's impact on these monocyte subsets. We expect that myeloid progenitor cells will be different between normal mice and chronic Chagas disease mice both in bone marrow and spleen. We also anticipate SRT1720 will regulate the percentage of myeloid progenitor cells in chronic Chagas disease. The study will fill the gap of how monocyte develop into macrophage and how SIRT1 modulate phenotype and function of macrophages in chronic Chagas disease model.

The mechanism connecting SIRT1 to tissue inflammation/oxidative stress has long been enigmatic, SIRT1 has been demonstrated to exhibit anti-inflammatory

properties through promotion of deacetylation of p65 subunit of NF-kB. However, it is far unclear whether other signaling cascades that may mediate the effects of SIRT1 on proinflammatory macrophage. Further studies are necessary to show the signaling pathways which might be involved in SIRT1 regulating macrophage phenotype and function in chronic Chagas disease.

Poly(ADP-ribose) polymerase (PARP)-1 is an NAD + -dependent enzyme that participates to DNA repair (122). The PARP family of proteins are involved in a number of cellular processes including: DNA damage, DNA response, cell death and cell cycle. Because both SIRT1 and PARP-1 depends on NAD+ availability, cross talk between them has been reported. Deletion of the PARP-1 resulted in increased SIRT1activity. PARP-1 knockout mice displayed an increased mitochondrial content and energy expenditure, and were beneficial in protection of metabolic disease (126). We propose that in chronic Chagas disease model, SRT1720 would prevent macrophage inflammatory response through inhibition of PARP-1. We plan to isolated monocytes/macrophages from normal, chagasic and SRT1720-treated/ chagasic mice, and will examine PARP1 and SIRT1 expression level by Western blot, test PARP1 and SIRT1 activity, determine NAD+ content by NAD/NADH Assay Kit. And we will also isolate monocytes/macrophages from WT mice and PARP1-/- mice and they will be *in vitro* stimulated with *T. crzi* and/or treated with SRT1720. The previous approaches will again be used and we will also determine cytokine expression by Real-Time RT-PCR and ELISA and examine ROS level by Amplex Red Assay.

In conclusion, our data suggest that activation of SIRT1 control tissue oxidative stress and inflammation and contribute to improvement of cardiac function in chronically infected chagasic mice. SIRT1 also prevented phenotypic and functional proinflammatory M1 macrophages in chronic Chagas disease. This study provided us with an impetus to potential utility of SIRT1 agonist and its manipulation of macrophage subsets as the therapy for Chagas disease patients.

REFERENCES

1. Carod-Artal, F. J., and J. Gascon. 2010. Chagas disease and stroke. *Lancet Neurol 9:533*.
2. Dodd, R. Y., and D. A. Leiby. 2004. Emerging infectious threats to the blood supply. *Annu Rev Med 55:191*.
3. Bern, C., and S. P. Montgomery. 2009. An estimate of the burden of Chagas disease in the United States. *Clin Infect Dis 49:e52*.
4. Meurs, K. M., M. A. Anthony, M. Slater, and M. W. Miller. 1998. Chronic Trypanosoma cruzi infection in dogs: 11 cases (1987-1996). *J Am Vet Med Assoc 213:497*.
5. Bradley, K. K., D. K. Bergman, J. P. Woods, J. M. Crutcher, and L. V. Kirchhoff. 2000. Prevalence of American trypanosomiasis (Chagas disease) among dogs in Oklahoma. *J Am Vet Med Assoc 217:1853*.
6. Beard, C. B., G. Pye, F. J. Steurer, R. Rodriguez, R. Campman, A. T. Peterson, J. Ramsey, R. A. Wirtz, and L. E. Robinson. 2003. Chagas disease in a domestic transmission cycle, southern Texas, USA. *Emerg Infect Dis 9:103*.
7. Yabsley, M. J., and G. P. Noblet. 2002. Seroprevalence of Trypanosoma cruzi in raccoons from South Carolina and Georgia. *J Wildl Dis 38:75*.
8. Leiby, D. A., F. J. Rentas, K. E. Nelson, V. A. Stambolis, P. M. Ness, C. Parnis, H. A. McAllister, Jr., D. H. Yawn, R. J. Stumpf, and L. V. Kirchhoff. 2000. Evidence of Trypanosoma cruzi infection (Chagas' disease) among patients undergoing cardiac surgery. *Circulation 102:2978*.
9. Bern, C. 2011. Antitrypanosomal therapy for chronic Chagas' disease. *N Engl J*

Med 364:2527.

10. Bern, C., D. L. Martin, and R. H. Gilman. 2011. Acute and congenital Chagas disease. *Adv Parasitol 75:19*.

11. 2012. Chagas disease (American trypanosomiasis) - fact sheet (revised in August 2012). *Wkly Epidemiol Rec 87:519*.

12. Rassi, A., Jr., A. Rassi, and J. Marcondes de Rezende. 2012. American trypanosomiasis (Chagas disease). *Infect Dis Clin North Am 26:275*.

13. Rassi, A., Jr., J. C. Dias, J. A. Marin-Neto, and A. Rassi. 2009. Challenges and opportunities for primary, secondary, and tertiary prevention of Chagas' disease. *Heart 95:524*.

14. Pinazo, M. J., E. Canas, J. I. Elizalde, M. Garcia, J. Gascon, F. Gimeno, J. Gomez, F. Guhl, V. Ortiz, J. Posada Ede, S. Puente, J. Rezende, J. Salas, J. Saravia, F. Torrico, D. Torrus, and B. Trevino. 2010. Diagnosis, management and treatment of chronic Chagas' gastrointestinal disease in areas where Trypanosoma cruzi infection is not endemic. *Gastroenterol Hepatol 33:191*.

15. Acquatella, H. 2007. Echocardiography in Chagas heart disease. *Circulation 115:1124*.

16. Parker, E. R., and A. Sethi. 2011. Chagas disease: coming to a place near you. *Dermatol Clin 29:53*.

17. Machado, F. S., W. O. Dutra, L. Esper, K. J. Gollob, M. M. Teixeira, S. M. Factor, L. M. Weiss, F. Nagajyothi, H. B. Tanowitz, and N. J. Garg. 2012. Current understanding of immunity to Trypanosoma cruzi infection and pathogenesis of

Chagas disease. *Semin Immunopathol 34:753*.

18. Coura, J. R., and J. Borges-Pereira. 2010. Chagas disease: 100 years after its discovery. A systemic review. *Acta Trop 115:5*.

19. 2012. Congenital transmission of Chagas disease - Virginia, 2010. *MMWR Morb Mortal Wkly Rep 61:477*.

20. Rodriques Coura, J., and S. L. de Castro. 2002. A critical review on Chagas disease chemotherapy. *Mem Inst Oswaldo Cruz 97:3*.

21. Cancado, J. R. 2002. Long term evaluation of etiological treatment of chagas disease with benznidazole. *Rev Inst Med Trop Sao Paulo 44:29*.

22. 2010. Chagas disease (American trypanosomiasis) fact sheet (revised in June 2010). *Wkly Epidemiol Rec 85:334*.

23. Jackson, Y., E. Alirol, L. Getaz, H. Wolff, C. Combescure, and F. Chappuis. 2010. Tolerance and safety of nifurtimox in patients with chronic chagas disease. *Clin Infect Dis 51:e69*.

24. Bern, C., S. P. Montgomery, B. L. Herwaldt, A. Rassi, Jr., J. A. Marin-Neto, R. O. Dantas, J. H. Maguire, H. Acquatella, C. Morillo, L. V. Kirchhoff, R. H. Gilman, P. A. Reyes, R. Salvatella, and A. C. Moore. 2007. Evaluation and treatment of chagas disease in the United States: a systematic review. *JAMA 298:2171*.

25. Olivera, M. J., Z. M. Cucunuba, C. A. Alvarez, and R. S. Nicholls. 2015. Safety Profile of Nifurtimox and Treatment Interruption for Chronic Chagas Disease in Colombian Adults. *Am J Trop Med Hyg 93:1224*.

26. Miller, D. A., S. Hernandez, L. Rodriguez De Armas, S. J. Eells, M. M. Traina,

L. G. Miller, and S. K. Meymandi. 2015. Tolerance of benznidazole in a United States Chagas Disease clinic. *Clin Infect Dis 60:1237*.

27. Wen, J. J., S. Gupta, Z. Guan, M. Dhiman, D. Condon, C. Lui, and N. J. Garg. Phenyl-alpha-tert-butyl-nitrone and benzonidazole treatment controlled the mitochondrial oxidative stress and evolution of cardiomyopathy in chronic chagasic Rats. *J Am Coll Cardiol 55:2499*.

28. Karamanlidis, G., L. Nascimben, G. S. Couper, P. S. Shekar, F. del Monte, and R. Tian. Defective DNA replication impairs mitochondrial biogenesis in human failing hearts. *Circ Res 106:1541*.

29. Puigserver, P., Z. Wu, C. W. Park, R. Graves, M. Wright, and B. M. Spiegelman. 1998. A cold-inducible coactivator of nuclear receptors linked to adaptive thermogenesis. *Cell 92:829*.

30. Schilling, J., and D. P. Kelly. The PGC-1 cascade as a therapeutic target for heart failure. *J Mol Cell Cardiol 51:578*.

31. Dufour, C. R., B. J. Wilson, J. M. Huss, D. P. Kelly, W. A. Alaynick, M. Downes, R. M. Evans, M. Blanchette, and V. Giguere. 2007. Genome-wide orchestration of cardiac functions by the orphan nuclear receptors ERRalpha and gamma. *Cell Metab 5:345*.

32. Yasukawa, T., A. Reyes, T. J. Cluett, M. Y. Yang, M. Bowmaker, H. T. Jacobs, and I. J. Holt. 2006. Replication of vertebrate mitochondrial DNA entails transient ribonucleotide incorporation throughout the lagging strand. *Embo J 25:5358*.

33. Piper, H. M., T. Noll, and B. Siegmund. 1994. Mitochondrial function in the oxygen depleted and reoxygenated myocardial cell. *Cardiovasc Res 28:1*.

34. Vercesi, A. E., A. J. Kowaltowski, M. T. Grijalba, A. R. Meinicke, and R. F. Castilho. 1997. The role of reactive oxygen species in mitochondrial permeability transition. *Biosci Rep 17:43*.

35. Cardoso, S. M., C. Pereira, and R. Oliveira. 1999. Mitochondrial function is differentially affected upon oxidative stress. *Free Radic Biol Med 26:3*.

36. Wan, X., S. Gupta, M. P. Zago, M. M. Davidson, P. Dousset, A. Amoroso, and N. J. Garg. 2012. Defects of mtDNA replication impaired mitochondrial biogenesis during Trypanosoma cruzi infection in human cardiomyocytes and chagasic patients: the role of Nrf1/2 and antioxidant response. *J Am Heart Assoc 1:e003855*.

37. Vyatkina, G., V. Bhatia, A. Gerstner, J. Papaconstantinou, and N. Garg. 2004. Impaired mitochondrial respiratory chain and bioenergetics during chagasic cardiomyopathy development. *Biochim Biophys Acta 1689:162*.

38. Carrasco Guerra, H. A., E. Palacios-Pru, C. Dagert de Scorza, C. Molina, G. Inglessis, and R. V. Mendoza. 1987. Clinical, histochemical, and ultrastructural correlation in septal endomyocardial biopsies from chronic chagasic patients: detection of early myocardial damage. *Am Heart J 113:716*.

39. Palacios-Pru, E., H. Carrasco, C. Scorza, and R. Espinoza. 1989. Ultrastructural characteristics of different stages of human chagasic myocarditis. *Am J Trop Med Hyg 41:29*.

40. Parada, H., H. A. Carrasco, N. Anez, C. Fuenmayor, and I. Inglessis. 1997. Cardiac involvement is a constant finding in acute Chagas' disease: a clinical, parasitological and histopathological study. *Int J Cardiol 60:49*.

41. Garg, N., V. L. Popov, and J. Papaconstantinou. 2003. Profiling gene transcription reveals a deficiency of mitochondrial oxidative phosphorylation in Trypanosoma cruzi-infected murine hearts: implications in chagasic myocarditis development. *Biochim Biophys Acta 1638:106*.

42. Turrens, J. F. 2003. Mitochondrial formation of reactive oxygen species. *J Physiol 552:335*.

43. Cardoni, R. L., M. I. Antunez, C. Morales, and I. R. Nantes. 1997. Release of reactive oxygen species by phagocytic cells in response to live parasites in mice infected with Trypanosoma cruzi. *Am J Trop Med Hyg 56:329*.

44. Dhiman, M., and N. J. Garg. 2014. P47phox-/- mice are compromised in expansion and activation of CD8+ T cells and susceptible to Trypanosoma cruzi infection. *PLoS Pathog 10:e1004516*.

45. Dhiman, M., and N. J. Garg. 2011. NADPH oxidase inhibition ameliorates Trypanosoma cruzi-induced myocarditis during Chagas disease. *J Pathol 225:583*.

46. Diaz, M. L., A. Solari, and C. I. Gonzalez. 2011. Differential expression of Trypanosoma cruzi I associated with clinical forms of Chagas disease: overexpression of oxidative stress proteins in acute patient isolate. *J Proteomics 74:1673*.

47. Diazgranados, C. A., C. H. Saavedra-Trujillo, M. Mantilla, S. L. Valderrama, C. Alquichire, and C. Franco-Paredes. 2009. Chagasic encephalitis in HIV patients: common presentation of an evolving epidemiological and clinical association. *Lancet Infect Dis 9:324*.

48. Escriba, J. M., E. Ponce, D. Romero Ade, P. A. Vinas, A. Marchiol, G. Bassets, P. P. Palma, M. A. Lima, C. Zuniga, and C. Ponce. 2009. Treatment and seroconversion in a cohort of children suffering from recent chronic Chagas infection in Yoro, Honduras. *Mem Inst Oswaldo Cruz 104:986*.

49. Alvarez, M. N., G. Peluffo, L. Piacenza, and R. Radi. 2011. Intraphagosomal peroxynitrite as a macrophage-derived cytotoxin against internalized Trypanosoma cruzi: consequences for oxidative killing and role of microbial peroxiredoxins in infectivity. *J Biol Chem 286:6627*.

50. Uyemura, S. A., M. C. Jordani, A. C. Polizello, and C. Curti. 1996. Heart FoF1-ATPase changes during the acute phase of Trypanosoma cruzi infection in rats. *Mol Cell Biochem 165:127*.

51. Sawyer, D. B., and W. S. Colucci. 2000. Mitochondrial oxidative stress in heart failure: "oxygen wastage" revisited. *Circ Res 86:119*.

52. Ba, X., S. Gupta, M. Davidson, and N. J. Garg. 2010. Trypanosoma cruzi induces the reactive oxygen species-PARP-1-RelA pathway for up-regulation of cytokine expression in cardiomyocytes. *J Biol Chem 285:11596*.

53. Wen, J. J., S. Gupta, Z. Guan, M. Dhiman, D. Condon, C. Lui, and N. J. Garg. 2010. Phenyl-alpha-tert-butyl-nitrone and benzonidazole treatment controlled

the mitochondrial oxidative stress and evolution of cardiomyopathy in chronic chagasic Rats. *J Am Coll Cardiol 55:2499*.

54. Tsutsui, H. 2001. Oxidative stress in heart failure: the role of mitochondria. *Intern Med 40:1177*.

55. Keith, M., A. Geranmayegan, M. J. Sole, R. Kurian, A. Robinson, A. S. Omran, and K. N. Jeejeebhoy. 1998. Increased oxidative stress in patients with congestive heart failure. *J Am Coll Cardiol 31:1352*.

56. Martindale, J. L., and N. J. Holbrook. 2002. Cellular response to oxidative stress: signaling for suicide and survival. *J Cell Physiol 192:1*.

57. Valenzuela, A. 1991. The biological significance of malondialdehyde determination in the assessment of tissue oxidative stress. *Life Sci 48:301*.

58. Beal, M. F. 2002. Oxidatively modified proteins in aging and disease. *Free Radic Biol Med 32:797*.

59. Chevion, M., E. Berenshtein, and E. R. Stadtman. 2000. Human studies related to protein oxidation: protein carbonyl content as a marker of damage. *Free Radic Res 33 Suppl:S99*.

60. Jerca, L., A. Busuioc, G. Nastasia, and I. Haulica. 1996. [Glutathione, a biochemical indicator for different types of cellular stress. The change in the GSH level in the brain of rats with hypoxia]. *Rev Med Chir Soc Med Nat Iasi 100:143*.

61. Ceballos-Picot, I., V. Witko-Sarsat, M. Merad-Boudia, A. T. Nguyen, M. Thevenin, M. C. Jaudon, J. Zingraff, C. Verger, P. Jungers, and B. Descamps-

Latscha. 1996. Glutathione antioxidant system as a marker of oxidative stress in chronic renal failure. *Free Radic Biol Med 21:845*.

62. Wen, J. J., G. Vyatkina, and N. Garg. 2004. Oxidative damage during chagasic cardiomyopathy development: role of mitochondrial oxidant release and inefficient antioxidant defense. *Free Radic Biol Med 37:1821*.

63. Perez-Fuentes, R., J. F. Guegan, C. Barnabe, A. Lopez-Colombo, H. Salgado-Rosas, E. Torres-Rasgado, B. Briones, M. Romero-Diaz, J. Ramos-Jimenez, and C. Sanchez-Guillen Mdel. 2003. Severity of chronic Chagas disease is associated with cytokine/antioxidant imbalance in chronically infected individuals. *Int J Parasitol 33:293*.

64. de Oliveira, T. B., R. C. Pedrosa, and D. W. Filho. 2007. Oxidative stress in chronic cardiopathy associated with Chagas disease. *Int J Cardiol 116:357*.

65. Wen, J. J., P. C. Yachelini, A. Sembaj, R. E. Manzur, and N. J. Garg. 2006. Increased oxidative stress is correlated with mitochondrial dysfunction in chagasic patients. *Free Radic Biol Med 41:270*.

66. Dhiman, M., X. Wan, V. L. Popov, G. Vargas, and N. J. Garg. 2013. MnSODtg mice control myocardial inflammatory and oxidative stress and remodeling responses elicited in chronic Chagas disease. *J Am Heart Assoc 2:e000302*.

67. Teixeira, M. M., R. T. Gazzinelli, and J. S. Silva. 2002. Chemokines, inflammation and Trypanosoma cruzi infection. *Trends Parasitol 18:262*.

68. Van Overtvelt, L., M. Andrieu, V. Verhasselt, F. Connan, J. Choppin, V. Vercruysse, M. Goldman, A. Hosmalin, and B. Vray. 2002. Trypanosoma cruzi

down-regulates lipopolysaccharide-induced MHC class I on human dendritic cells and impairs antigen presentation to specific CD8(+) T lymphocytes. *Int Immunol 14:1135*.

69. Cuellar, A., S. P. Santander, C. Thomas Mdel, F. Guzman, A. Gomez, M. C. Lopez, and C. J. Puerta. 2008. Monocyte-derived dendritic cells from chagasic patients vs healthy donors secrete differential levels of IL-10 and IL-12 when stimulated with a protein fragment of Trypanosoma cruzi heat-shock protein-70. *Immunol Cell Biol 86:255*.

70. Machado, F. S., K. M. Tyler, F. Brant, L. Esper, M. M. Teixeira, and H. B. Tanowitz. 2012. Pathogenesis of Chagas disease: time to move on. *Front Biosci (Elite Ed) 4:1743*.

71. Coelho, P. S., A. Klein, A. Talvani, S. F. Coutinho, O. Takeuchi, S. Akira, J. S. Silva, H. Canizzaro, R. T. Gazzinelli, and M. M. Teixeira. 2002. Glycosylphosphatidylinositol-anchored mucin-like glycoproteins isolated from Trypanosoma cruzi trypomastigotes induce *in vivo* leukocyte recruitment dependent on MCP-1 production by IFN-gamma-primed-macrophages. *J Leukoc Biol 71:837*.

72. Schmitz, V., E. Svensjo, R. R. Serra, M. M. Teixeira, and J. Scharfstein. 2009. Proteolytic generation of kinins in tissues infected by Trypanosoma cruzi depends on CXC chemokine secretion by macrophages activated via Toll-like 2 receptors. *J Leukoc Biol 85:1005*.

73. Camargo, M. M., I. C. Almeida, M. E. Pereira, M. A. Ferguson, L. R. Travassos,

and R. T. Gazzinelli. 1997. Glycosylphosphatidylinositol-anchored mucin-like glycoproteins isolated from Trypanosoma cruzi trypomastigotes initiate the synthesis of proinflammatory cytokines by macrophages. *J Immunol 158:5890*.

74. Campos, M. A., M. Closel, E. P. Valente, J. E. Cardoso, S. Akira, J. I. Alvarez-Leite, C. Ropert, and R. T. Gazzinelli. 2004. Impaired production of proinflammatory cytokines and host resistance to acute infection with Trypanosoma cruzi in mice lacking functional myeloid differentiation factor 88. *J Immunol 172:1711*.

75. Oliveira, A. C., J. R. Peixoto, L. B. de Arruda, M. A. Campos, R. T. Gazzinelli, D. T. Golenbock, S. Akira, J. O. Previato, L. Mendonca-Previato, A. Nobrega, and M. Bellio. 2004. Expression of functional TLR4 confers proinflammatory responsiveness to Trypanosoma cruzi glycoinositolphospholipids and higher resistance to infection with *T. cruzi*. *J Immunol 173:5688*.

76. Monteiro, A. C., V. Schmitz, A. Morrot, L. B. de Arruda, F. Nagajyothi, A. Granato, J. B. Pesquero, W. Muller-Esterl, H. B. Tanowitz, and J. Scharfstein. 2007. Bradykinin B2 Receptors of dendritic cells, acting as sensors of kinins proteolytically released by Trypanosoma cruzi, are critical for the development of protective type-1 responses. *PLoS Pathog 3:e185*.

77. Kayama, H., and K. Takeda. 2010. The innate immune response to Trypanosoma cruzi infection. *Microbes Infect 12:511*.

78. Bafica, A., H. C. Santiago, R. Goldszmid, C. Ropert, R. T. Gazzinelli, and A. Sher. 2006. Cutting edge: TLR9 and TLR2 signaling together account for

MyD88-dependent control of parasitemia in Trypanosoma cruzi infection. *J Immunol 177:3515*.

79. Reed, S. G. 1988. *In vivo* administration of recombinant IFN-gamma induces macrophage activation, and prevents acute disease, immune suppression, and death in experimental Trypanosoma cruzi infections. *J Immunol 140:4342*.

80. Miller, M. J., R. A. Wrightsman, G. A. Stryker, and J. E. Manning. 1997. Protection of mice against Trypanosoma cruzi by immunization with paraflagellar rod proteins requires T cell, but not B cell, function. *J Immunol 158:5330*.

81. Zacks, M. A., J. J. Wen, G. Vyatkina, V. Bhatia, and N. Garg. 2005. An overview of chagasic cardiomyopathy: pathogenic importance of oxidative stress. *An Acad Bras Cienc 77:695*.

82. Cardillo, F., J. C. Voltarelli, S. G. Reed, and J. S. Silva. 1996. Regulation of Trypanosoma cruzi infection in mice by gamma interferon and interleukin 10: role of NK cells. *Infect Immun 64:128*.

83. Silva, J. S., D. R. Twardzik, and S. G. Reed. 1991. Regulation of Trypanosoma cruzi infections *in vitro* and *in vivo* by transforming growth factor beta (TGF-beta). *J Exp Med 174:539*.

84. Holscher, C., M. Mohrs, W. J. Dai, G. Kohler, B. Ryffel, G. A. Schaub, H. Mossmann, and F. Brombacher. 2000. Tumor necrosis factor alpha-mediated toxic shock in Trypanosoma cruzi-infected interleukin 10-deficient mice. *Infect Immun 68:4075*.

85. Landry, J., A. Sutton, S. T. Tafrov, R. C. Heller, J. Stebbins, L. Pillus, and R. Sternglanz. 2000. The silencing protein SIR2 and its homologs are NAD-dependent protein deacetylases. *Proc Natl Acad Sci U S A 97:5807*.

86. Frye, R. A. 1999. Characterization of five human cDNAs with homology to the yeast SIR2 gene: Sir2-like proteins (sirtuins) metabolize NAD and may have protein ADP-ribosyltransferase activity. *Biochem Biophys Res Commun 260:273*.

87. Michishita, E., J. Y. Park, J. M. Burneskis, J. C. Barrett, and I. Horikawa. 2005. Evolutionarily conserved and nonconserved cellular localizations and functions of human SIRT proteins. *Mol Biol Cell 16:4623*.

88. Liszt, G., E. Ford, M. Kurtev, and L. Guarente. 2005. Mouse Sir2 homolog SIRT6 is a nuclear ADP-ribosyltransferase. *J Biol Chem 280:21313*.

89. Mostoslavsky, R., K. F. Chua, D. B. Lombard, W. W. Pang, M. R. Fischer, L. Gellon, P. Liu, G. Mostoslavsky, S. Franco, M. M. Murphy, K. D. Mills, P. Patel, J. T. Hsu, A. L. Hong, E. Ford, H. L. Cheng, C. Kennedy, N. Nunez, R. Bronson, D. Frendewey, W. Auerbach, D. Valenzuela, M. Karow, M. O. Hottiger, S. Hursting, J. C. Barrett, L. Guarente, R. Mulligan, B. Demple, G. D. Yancopoulos, and F. W. Alt. 2006. Genomic instability and aging-like phenotype in the absence of mammalian SIRT6. *Cell 124:315*.

90. Ford, E., R. Voit, G. Liszt, C. Magin, I. Grummt, and L. Guarente. 2006. Mammalian Sir2 homolog SIRT7 is an activator of RNA polymerase I transcription. *Genes Dev 20:1075*.

91. Michishita, E., R. A. McCord, E. Berber, M. Kioi, H. Padilla-Nash, M. Damian, P. Cheung, R. Kusumoto, T. L. Kawahara, J. C. Barrett, H. Y. Chang, V. A. Bohr, T. Ried, O. Gozani, and K. F. Chua. 2008. SIRT6 is a histone H3 lysine 9 deacetylase that modulates telomeric chromatin. *Nature 452:492*.

92. Zhong, L., A. D'Urso, D. Toiber, C. Sebastian, R. E. Henry, D. D. Vadysirisack, A. Guimaraes, B. Marinelli, J. D. Wikstrom, T. Nir, C. B. Clish, B. Vaitheesvaran, O. Iliopoulos, I. Kurland, Y. Dor, R. Weissleder, O. S. Shirihai, L. W. Ellisen, J. M. Espinosa, and R. Mostoslavsky. 2010. The histone deacetylase Sirt6 regulates glucose homeostasis via Hif1alpha. *Cell 140:280*.

93. Dryden, S. C., F. A. Nahhas, J. E. Nowak, A. S. Goustin, and M. A. Tainsky. 2003. Role for human SIRT2 NAD-dependent deacetylase activity in control of mitotic exit in the cell cycle. *Mol Cell Biol 23:3173*.

94. Li, W., B. Zhang, J. Tang, Q. Cao, Y. Wu, C. Wu, J. Guo, E. A. Ling, and F. Liang. 2007. Sirtuin 2, a mammalian homolog of yeast silent information regulator-2 longevity regulator, is an oligodendroglial protein that decelerates cell differentiation through deacetylating alpha-tubulin. *J Neurosci 27:2606*.

95. Nakamura, Y., M. Ogura, D. Tanaka, and N. Inagaki. 2008. Localization of mouse mitochondrial SIRT proteins: shift of SIRT3 to nucleus by co-expression with SIRT5. *Biochem Biophys Res Commun 366:174*.

96. Ahuja, N., B. Schwer, S. Carobbio, D. Waltregny, B. J. North, V. Castronovo, P. Maechler, and E. Verdin. 2007. Regulation of insulin secretion by SIRT4, a mitochondrial ADP-ribosyltransferase. *J Biol Chem 282:33583*.

97. Frye, R. A. 2000. Phylogenetic classification of prokaryotic and eukaryotic Sir2-like proteins. *Biochem Biophys Res Commun 273:793*.

98. Hou, J., Z. Z. Chong, Y. C. Shang, and K. Maiese. 2010. Early apoptotic vascular signaling is determined by Sirt1 through nuclear shuttling, forkhead trafficking, bad, and mitochondrial caspase activation. *Curr Neurovasc Res 7:95*.

99. Solomon, J. M., R. Pasupuleti, L. Xu, T. McDonagh, R. Curtis, P. S. DiStefano, and L. J. Huber. 2006. Inhibition of SIRT1 catalytic activity increases p53 acetylation but does not alter cell survival following DNA damage. *Mol Cell Biol 26:28*.

100. Yuan, Z., X. Zhang, N. Sengupta, W. S. Lane, and E. Seto. 2007. SIRT1 regulates the function of the Nijmegen breakage syndrome protein. *Mol Cell 27:149*.

101. Yeung, F., J. E. Hoberg, C. S. Ramsey, M. D. Keller, D. R. Jones, R. A. Frye, and M. W. Mayo. 2004. Modulation of NF-kappaB-dependent transcription and cell survival by the SIRT1 deacetylase. *EMBO J 23:2369*.

102. Gao, Z., and J. Ye. 2008. Inhibition of transcriptional activity of c-JUN by SIRT1. *Biochem Biophys Res Commun 376:793*.

103. Yuan, J., K. Minter-Dykhouse, and Z. Lou. 2009. A c-Myc-SIRT1 feedback loop regulates cell growth and transformation. *J Cell Biol 185:203*.

104. Hubbard, B. P., and D. A. Sinclair. 2014. Small molecule SIRT1 activators for the treatment of aging and age-related diseases. *Trends Pharmacol Sci 35:146*.

105. Boutant, M., and C. Canto. 2014. SIRT1 metabolic actions: Integrating recent advances from mouse models. *Mol Metab 3:5*.

106. Chang, H. C., and L. Guarente. 2014. SIRT1 and other sirtuins in metabolism. *Trends Endocrinol Metab 25:138*.

107. Herskovits, A. Z., and L. Guarente. 2014. SIRT1 in neurodevelopment and brain senescence. *Neuron 81:471*.

108. Amat, R., A. Planavila, S. L. Chen, R. Iglesias, M. Giralt, and F. Villarroya. 2009. SIRT1 controls the transcription of the peroxisome proliferator-activated receptor-gamma Co-activator-1alpha (PGC-1alpha) gene in skeletal muscle through the PGC-1alpha autoregulatory loop and interaction with MyoD. *J Biol Chem 284:21872*.

109. Gerhart-Hines, Z., J. T. Rodgers, O. Bare, C. Lerin, S. H. Kim, R. Mostoslavsky, F. W. Alt, Z. Wu, and P. Puigserver. 2007. Metabolic control of muscle mitochondrial function and fatty acid oxidation through SIRT1/PGC-1alpha. *EMBO J 26:1913*.

110. Guo, P., H. Pi, S. Xu, L. Zhang, Y. Li, M. Li, Z. Cao, L. Tian, J. Xie, R. Li, M. He, Y. Lu, C. Liu, W. Duan, Z. Yu, and Z. Zhou. 2014. Melatonin Improves mitochondrial function by promoting MT1/SIRT1/PGC-1 alpha-dependent mitochondrial biogenesis in cadmium-induced hepatotoxicity *in vitro*. *Toxicol Sci 142:182*.

111. Gurd, B. J. 2011. Deacetylation of PGC-1 alpha by SIRT1: importance for skeletal muscle function and exercise-induced mitochondrial biogenesis.

Applied Physiology Nutrition and Metabolism-Physiologie Appliquee Nutrition Et Metabolisme 36:589.

112. Sims, J. L., S. J. Berger, and N. A. Berger. 1981. Effects of nicotinamide on NAD and poly(ADP-ribose) metabolism in DNA-damaged human lymphocytes. *J Supramol Struct Cell Biochem 16:281*.

113. Messner, S., M. Altmeyer, H. Zhao, A. Pozivil, B. Roschitzki, P. Gehrig, D. Rutishauser, D. Huang, A. Caflisch, and M. O. Hottiger. 2010. PARP1 ADP-ribosylates lysine residues of the core histone tails. *Nucleic Acids Res 38:6350*.

114. Andrade, D. V., K. J. Gollob, and W. O. Dutra. 2014. Acute chagas disease: new global challenges for an old neglected disease. *PLoS Negl Trop Dis 8:e3010*.

115. Gomes, J. A., A. M. Molica, T. S. Keesen, M. J. Morato, F. F. de Araujo, R. C. Fares, J. A. Fiuza, A. T. Chaves, V. Pinheiro, C. Nunes Mdo, R. Correa-Oliveira, and M. O. da Costa Rocha. 2014. Inflammatory mediators from monocytes down-regulate cellular proliferation and enhance cytokines production in patients with polar clinical forms of Chagas disease. *Hum Immunol 75:20*.

116. Borges, M. M., J. K. Kloetzel, H. F. Andrade, Jr., C. E. Tadokoro, P. Pinge-Filho, and I. Abrahamsohn. 1998. Prostaglandin and nitric oxide regulate TNF-alpha production during Trypanosoma cruzi infection. *Immunol Lett 63:1*.

117. Abel, L. C., L. R. Ferreira, I. Cunha Navarro, M. A. Baron, J. Kalil, R. T. Gazzinelli, L. V. Rizzo, and E. Cunha-Neto. 2014. Induction of IL-12 production in human peripheral monocytes by Trypanosoma cruzi Is mediated by

glycosylphosphatidylinositol-anchored mucin-like glycoproteins and potentiated by IFN- gamma and CD40-CD40L interactions. *Mediators Inflamm 2014:345659*.

118. Yoshizaki, T., S. Schenk, T. Imamura, J. L. Babendure, N. Sonoda, E. J. Bae, D. Y. Oh, M. Lu, J. C. Milne, C. Westphal, G. Bandyopadhyay, and J. M. Olefsky. 2010. SIRT1 inhibits inflammatory pathways in macrophages and modulates insulin sensitivity. *Am J Physiol Endocrinol Metab 298:E419*.

119. Bereswill, S., M. Munoz, A. Fischer, R. Plickert, L. M. Haag, B. Otto, A. A. Kuhl, C. Loddenkemper, U. B. Gobel, and M. M. Heimesaat. 2010. Anti-inflammatory effects of resveratrol, curcumin and simvastatin in acute small intestinal inflammation. *PLoS One 5:e15099*.

120. Thirunavukkarasu, M., S. V. Penumathsa, S. Koneru, B. Juhasz, L. Zhan, H. Otani, D. Bagchi, D. K. Das, and N. Maulik. 2007. Resveratrol alleviates cardiac dysfunction in streptozotocin-induced diabetes: Role of nitric oxide, thioredoxin, and heme oxygenase. *Free Radic Biol Med 43:720*.

121. Barger, J. L., T. Kayo, T. D. Pugh, T. A. Prolla, and R. Weindruch. 2008. Short-term consumption of a resveratrol-containing nutraceutical mixture mimics gene expression of long-term caloric restriction in mouse heart. *Exp Gerontol 43:859*.

122. Durkacz, B. W., O. Omidiji, D. A. Gray, and S. Shall. 1980. (ADP-ribose)n participates in DNA excision repair. *Nature 283:593*.

123. D'Amours, D., S. Desnoyers, I. D'Silva, and G. G. Poirier. 1999. Poly(ADP-

ribosyl)ation reactions in the regulation of nuclear functions. *Biochem J 342 (Pt 2):249*.

124. Minor, R. K., J. A. Baur, A. P. Gomes, T. M. Ward, A. Csiszar, E. M. Mercken, K. Abdelmohsen, Y. K. Shin, C. Canto, M. Scheibye-Knudsen, M. Krawczyk, P. M. Irusta, A. Martin-Montalvo, B. P. Hubbard, Y. Zhang, E. Lehrmann, A. A. White, N. L. Price, W. R. Swindell, K. J. Pearson, K. G. Becker, V. A. Bohr, M. Gorospe, J. M. Egan, M. I. Talan, J. Auwerx, C. H. Westphal, J. L. Ellis, Z. Ungvari, G. P. Vlasuk, P. J. Elliott, D. A. Sinclair, and R. de Cabo. SRT1720 improves survival and healthspan of obese mice. *Sci Rep 1:70*.

125. Smith, J. J., R. D. Kenney, D. J. Gagne, B. P. Frushour, W. Ladd, H. L. Galonek, K. Israelian, J. Song, G. Razvadauskaite, A. V. Lynch, D. P. Carney, R. J. Johnson, S. Lavu, A. Iffland, P. J. Elliott, P. D. Lambert, K. O. Elliston, M. R. Jirousek, J. C. Milne, and O. Boss. 2009. Small molecule activators of SIRT1 replicate signaling pathways triggered by calorie restriction *in vivo*. *BMC Syst Biol 3:31*.

126. Hassa, P. O., S. S. Haenni, M. Elser, and M. O. Hottiger. 2006. Nuclear ADP-ribosylation reactions in mammalian cells: where are we today and where are we going? *Microbiol Mol Biol Rev 70:789*.

127. Johnson, F., and C. Giulivi. 2005. Superoxide dismutases and their impact upon human health. *Mol Aspects Med 26:340*.

128. Deng, J., G. Wang, Q. Huang, Y. Yan, K. Li, W. Tan, C. Jin, Y. Wang, and J. Liu. 2008. Oxidative stress-induced leaky sarcoplasmic reticulum underlying acute

heart failure in severe burn trauma. *Free Radic Biol Med 44:375*.

129. Kaestner, K. H., W. Knochel, and D. E. Martinez. 2000. Unified nomenclature for the winged helix/forkhead transcription factors. *Genes Dev 14:142*.

130. Zhang, L., and R. L. Tarleton. 1999. Parasite persistence correlates with disease severity and localization in chronic Chagas' disease. *J Infect Dis 180:480*.

131. van der Horst, A., L. G. Tertoolen, L. M. de Vries-Smits, R. A. Frye, R. H. Medema, and B. M. Burgering. 2004. FOXO4 is acetylated upon peroxide stress and deacetylated by the longevity protein hSir2(SIRT1). *J Biol Chem 279:28873*.

132. Sengupta, A., J. D. Molkentin, J. H. Paik, R. A. DePinho, and K. E. Yutzey. 2011. FoxO transcription factors promote cardiomyocyte survival upon induction of oxidative stress. *J Biol Chem 286:7468*.

133. Xiong, S., G. Salazar, N. Patrushev, and R. W. Alexander. 2011. FoxO1 mediates an autofeedback loop regulating SIRT1 expression. *J Biol Chem 286:5289*.

134. Yamamoto, T., and J. Sadoshima. 2011. Protection of the heart against ischemia/reperfusion by silent information regulator 1. *Trends Cardiovasc Med 21:27*.

135. Brunet, A., L. B. Sweeney, J. F. Sturgill, K. F. Chua, P. L. Greer, Y. Lin, H. Tran, S. E. Ross, R. Mostoslavsky, H. Y. Cohen, L. S. Hu, H. L. Cheng, M. P. Jedrychowski, S. P. Gygi, D. A. Sinclair, F. W. Alt, and M. E. Greenberg. 2004.

Stress-dependent regulation of FOXO transcription factors by the SIRT1 deacetylase. *Science 303:2011*.

136. Daitoku, H., M. Hatta, H. Matsuzaki, S. Aratani, T. Ohshima, M. Miyagishi, T. Nakajima, and A. Fukamizu. 2004. Silent information regulator 2 potentiates Foxo1-mediated transcription through its deacetylase activity. *Proc Natl Acad Sci U S A 101:10042*.

137. Monsalve, M., S. Borniquel, I. Valle, and S. Lamas. 2007. Mitochondrial dysfunction in human pathologies. *Front Biosci 12:1131*.

138. Chen, H., Y. Wan, S. Zhou, Y. Lu, Z. Zhang, R. Zhang, F. Chen, D. Hao, X. Zhao, Z. Guo, D. Liu, and C. Liang. 2012. Endothelium-specific SIRT1 overexpression inhibits hyperglycemia-induced upregulation of vascular cell senescence. *Sci China Life Sci 55:467*.

139. Ungvari, Z., N. Labinskyy, P. Mukhopadhyay, J. T. Pinto, Z. Bagi, P. Ballabh, C. Zhang, P. Pacher, and A. Csiszar. 2009. Resveratrol attenuates mitochondrial oxidative stress in coronary arterial endothelial cells. *Am J Physiol Heart Circ Physiol 297:H1876*.

140. Shah, S. A., M. Khan, M. H. Jo, M. G. Jo, F. U. Amin, and M. O. Kim. 2017. Melatonin Stimulates the SIRT1/Nrf2 Signaling Pathway Counteracting Lipopolysaccharide (LPS)-Induced Oxidative Stress to Rescue Postnatal Rat Brain. *CNS Neurosci Ther 23:33*.

141. Ding, Y. W., G. J. Zhao, X. L. Li, G. L. Hong, M. F. Li, Q. M. Qiu, B. Wu, and Z. Q. Lu. 2016. SIRT1 exerts protective effects against paraquat-induced injury in

mouse type II alveolar epithelial cells by deacetylating NRF2 *in vitro*. *Int J Mol Med 37:1049*.

142. Altenhofer, S., P. W. Kleikers, K. A. Radermacher, P. Scheurer, J. J. Rob Hermans, P. Schiffers, H. Ho, K. Wingler, and H. H. Schmidt. 2012. The NOX toolbox: validating the role of NADPH oxidases in physiology and disease. *Cell Mol Life Sci 69:2327*.

143. Bedard, K., and K. H. Krause. 2007. The NOX family of ROS-generating NADPH oxidases: physiology and pathophysiology. *Physiol Rev 87:245*.

144. Wosniak, J., Jr., C. X. Santos, A. J. Kowaltowski, and F. R. Laurindo. 2009. Cross-talk between mitochondria and NADPH oxidase: effects of mild mitochondrial dysfunction on angiotensin II-mediated increase in Nox isoform expression and activity in vascular smooth muscle cells. *Antioxid Redox Signal 11:1265*.

145. Zarzuelo, M. J., R. Lopez-Sepulveda, M. Sanchez, M. Romero, M. Gomez-Guzman, Z. Ungvary, F. Perez-Vizcaino, R. Jimenez, and J. Duarte. 2013. SIRT1 inhibits NADPH oxidase activation and protects endothelial function in the rat aorta: implications for vascular aging. *Biochem Pharmacol 85:1288*.

146. Hung, C. H., S. H. Chan, P. M. Chu, and K. L. Tsai. 2015. Quercetin is a potent anti-atherosclerotic compound by activation of SIRT1 signaling under oxLDL stimulation. *Mol Nutr Food Res 59:1905*.

147. Anrather, J., G. Racchumi, and C. Iadecola. 2006. NF-kappaB regulates phagocytic NADPH oxidase by inducing the expression of gp91phox. *J Biol*

Chem 281:5657.

148. Manea, A., S. A. Manea, A. V. Gafencu, and M. Raicu. 2007. Regulation of NADPH oxidase subunit p22(phox) by NF-kB in human aortic smooth muscle cells. *Arch Physiol Biochem 113:163*.

149. Manea, A., L. I. Tanase, M. Raicu, and M. Simionescu. 2010. Transcriptional regulation of NADPH oxidase isoforms, Nox1 and Nox4, by nuclear factor-kappaB in human aortic smooth muscle cells. *Biochem Biophys Res Commun 396:901*.

150. Xie, Q. W., Y. Kashiwabara, and C. Nathan. 1994. Role of transcription factor NF-kappa B/Rel in induction of nitric oxide synthase. *J Biol Chem 269:4705*.

151. Sakitani, K., M. Nishizawa, K. Inoue, Y. Masu, T. Okumura, and S. Ito. 1998. Synergistic regulation of inducible nitric oxide synthase gene by CCAAT/enhancer-binding protein beta and nuclear factor-kappaB in hepatocytes. *Genes Cells 3:321*.

152. Nakajima, S., and M. Kitamura. 2013. Bidirectional regulation of NF-kappaB by reactive oxygen species: a role of unfolded protein response. *Free Radic Biol Med 65:162*.

153. Ghisays, F., C. S. Brace, S. M. Yackly, H. J. Kwon, K. F. Mills, E. Kashentseva, I. P. Dmitriev, D. T. Curiel, S. I. Imai, and T. Ellenberger. 2015. The N-Terminal Domain of SIRT1 Is a Positive Regulator of Endogenous SIRT1-Dependent Deacetylation and Transcriptional Outputs. *Cell Rep*.

154. Pan, W., H. Yu, S. Huang, and P. Zhu. 2016. Resveratrol Protects against TNF-

alpha-Induced Injury in Human Umbilical Endothelial Cells through Promoting Sirtuin-1-Induced Repression of NF-KB and p38 MAPK. *PLoS One 11:e0147034*.

155. Kauppinen, A., T. Suuronen, J. Ojala, K. Kaarniranta, and A. Salminen. 2013. Antagonistic crosstalk between NF-kappaB and SIRT1 in the regulation of inflammation and metabolic disorders. *Cell Signal 25:1939*.

156. Dalpke, A., and K. Heeg. 2002. Signal integration following Toll-like receptor triggering. *Crit Rev Immunol 22:217*.

157. Liu, T. F., and C. E. McCall. 2013. Deacetylation by SIRT1 Reprograms Inflammation and Cancer. *Genes Cancer 4:135*.

158. Liu, T. F., V. T. Vachharajani, B. K. Yoza, and C. E. McCall. 2012. NAD+-dependent sirtuin 1 and 6 proteins coordinate a switch from glucose to fatty acid oxidation during the acute inflammatory response. *J Biol Chem 287:25758*.

159. Michalek, R. D., V. A. Gerriets, S. R. Jacobs, A. N. Macintyre, N. J. MacIver, E. F. Mason, S. A. Sullivan, A. G. Nichols, and J. C. Rathmell. 2011. Cutting edge: distinct glycolytic and lipid oxidative metabolic programs are essential for effector and regulatory CD4+ T cell subsets. *J Immunol 186:3299*.

160. Krawczyk, C. M., T. Holowka, J. Sun, J. Blagih, E. Amiel, R. J. DeBerardinis, J. R. Cross, E. Jung, C. B. Thompson, R. G. Jones, and E. J. Pearce. 2010. Toll-like receptor-induced changes in glycolytic metabolism regulate dendritic cell activation. *Blood 115:4742*.

161. Schug, T. T., and X. Li. 2010. Surprising sirtuin crosstalk in the heart. *Aging*

(Albany NY) 2:129.

162. Rajendrasozhan, S., S. R. Yang, V. L. Kinnula, and I. Rahman. 2008. SIRT1, an antiinflammatory and antiaging protein, is decreased in lungs of patients with chronic obstructive pulmonary disease. *Am J Respir Crit Care Med 177:861*.

163. Qin, W., T. Yang, L. Ho, Z. Zhao, J. Wang, L. Chen, W. Zhao, M. Thiyagarajan, D. MacGrogan, J. T. Rodgers, P. Puigserver, J. Sadoshima, H. Deng, S. Pedrini, S. Gandy, A. A. Sauve, and G. M. Pasinetti. 2006. Neuronal SIRT1 activation as a novel mechanism underlying the prevention of Alzheimer disease amyloid neuropathology by calorie restriction. *J Biol Chem 281:21745*.

164. Gorenne, I., S. Kumar, K. Gray, N. Figg, H. Yu, J. Mercer, and M. Bennett. 2013. Vascular smooth muscle cell sirtuin 1 protects against DNA damage and inhibits atherosclerosis. *Circulation 127:386*.

165. Massudi, H., R. Grant, N. Braidy, J. Guest, B. Farnsworth, and G. J. Guillemin. 2012. Age-associated changes in oxidative stress and NAD+ metabolism in human tissue. *PLoS One 7:e42357*.

166. Serrano-Marco, L., M. R. Chacon, E. Maymo-Masip, E. Barroso, L. Salvado, M. Wabitsch, L. Garrido-Sanchez, F. J. Tinahones, X. Palomer, J. Vendrell, and M. Vazquez-Carrera. 2012. TNF-alpha inhibits PPARbeta/delta activity and SIRT1 expression through NF-kappaB in human adipocytes. *Biochim Biophys Acta 1821:1177*.

167. Imai, S., and L. Guarente. 2014. NAD+ and sirtuins in aging and disease. *Trends Cell Biol 24:464*.

168. Haigis, M. C., and D. A. Sinclair. 2010. Mammalian sirtuins: biological insights and disease relevance. *Annu Rev Pathol 5:253*.

169. Liu, T. F., B. K. Yoza, M. El Gazzar, V. T. Vachharajani, and C. E. McCall. 2011. NAD+-dependent SIRT1 deacetylase participates in epigenetic reprogramming during endotoxin tolerance. *J Biol Chem 286:9856*.

170. Gordon, S. 2003. Alternative activation of macrophages. *Nat Rev Immunol 3:23*.

171. Gordon, S., and P. R. Taylor. 2005. Monocyte and macrophage heterogeneity. *Nat Rev Immunol 5:953*.

172. Akashi, K., D. Traver, T. Miyamoto, and I. L. Weissman. 2000. A clonogenic common myeloid progenitor that gives rise to all myeloid lineages. *Nature 404:193*.

173. Fogg, D. K., C. Sibon, C. Miled, S. Jung, P. Aucouturier, D. R. Littman, A. Cumano, and F. Geissmann. 2006. A clonogenic bone marrow progenitor specific for macrophages and dendritic cells. *Science 311:83*.

174. Mege, J. L., V. Mehraj, and C. Capo. 2011. Macrophage polarization and bacterial infections. *Curr Opin Infect Dis 24:230*.

175. Mosser, D. M., and J. P. Edwards. 2008. Exploring the full spectrum of macrophage activation. *Nat Rev Immunol 8:958*.

176. Forman, H. J., and M. Torres. 2001. Redox signaling in macrophages. *Mol Aspects Med 22:189*.

177. MacMicking, J., Q. W. Xie, and C. Nathan. 1997. Nitric oxide and macrophage function. *Annu Rev Immunol 15:323*.

178. Arnold, C. E., C. S. Whyte, P. Gordon, R. N. Barker, A. J. Rees, and H. M. Wilson. 2014. A critical role for suppressor of cytokine signalling 3 in promoting M1 macrophage activation and function *in vitro* and *in vivo*. *Immunology 141:96*.

179. Mantovani, A., A. Sica, S. Sozzani, P. Allavena, A. Vecchi, and M. Locati. 2004. The chemokine system in diverse forms of macrophage activation and polarization. *Trends Immunol 25:677*.

180. Roszer, T. 2015. Understanding the Mysterious M2 Macrophage through Activation Markers and Effector Mechanisms. *Mediators Inflamm 2015:816460*.

181. Lech, M., R. Grobmayr, M. Weidenbusch, and H. J. Anders. 2012. Tissues use resident dendritic cells and macrophages to maintain homeostasis and to regain homeostasis upon tissue injury: the immunoregulatory role of changing tissue environments. *Mediators Inflamm 2012:951390*.

182. Duluc, D., Y. Delneste, F. Tan, M. P. Moles, L. Grimaud, J. Lenoir, L. Preisser, I. Anegon, L. Catala, N. Ifrah, P. Descamps, E. Gamelin, H. Gascan, M. Hebbar, and P. Jeannin. 2007. Tumor-associated leukemia inhibitory factor and IL-6 skew monocyte differentiation into tumor-associated macrophage-like cells. *Blood 110:4319*.

183. Park, S. Y., S. W. Lee, H. Y. Kim, S. Y. Lee, W. S. Lee, K. W. Hong, and C. D. Kim. 2016. SIRT1 inhibits differentiation of monocytes to macrophages: amelioration of synovial inflammation in rheumatoid arthritis. *J Mol Med (Berl) 94:921*.

184. Schug, T. T., Q. Xu, H. Gao, A. Peres-da-Silva, D. W. Draper, M. B. Fessler, A.

Purushotham, and X. Li. 2010. Myeloid deletion of SIRT1 induces inflammatory signaling in response to environmental stress. *Mol Cell Biol 30:4712*.

185. Suganami, T., K. Tanimoto-Koyama, J. Nishida, M. Itoh, X. Yuan, S. Mizuarai, H. Kotani, S. Yamaoka, K. Miyake, S. Aoe, Y. Kamei, and Y. Ogawa. 2007. Role of the Toll-like receptor 4/NF-kappaB pathway in saturated fatty acid-induced inflammatory changes in the interaction between adipocytes and macrophages. *Arterioscler Thromb Vasc Biol 27:84*.

186. Ichioka, M., T. Suganami, N. Tsuda, I. Shirakawa, Y. Hirata, N. Satoh-Asahara, Y. Shimoda, M. Tanaka, M. Kim-Saijo, Y. Miyamoto, Y. Kamei, M. Sata, and Y. Ogawa. 2011. Increased expression of macrophage-inducible C-type lectin in adipose tissue of obese mice and humans. *Diabetes 60:819*.

187. Le, K. A., S. Mahurkar, T. L. Alderete, R. E. Hasson, T. C. Adam, J. S. Kim, E. Beale, C. Xie, A. S. Greenberg, H. Allayee, and M. I. Goran. 2011. Subcutaneous adipose tissue macrophage infiltration is associated with hepatic and visceral fat deposition, hyperinsulinemia, and stimulation of NF-kappaB stress pathway. *Diabetes 60:2802*.

188. Ka, S. O., M. Y. Song, E. J. Bae, and B. H. Park. 2015. Myeloid SIRT1 regulates macrophage infiltration and insulin sensitivity in mice fed a high-fat diet. *J Endocrinol 224:109*.

189. Hah, Y. S., Y. H. Cheon, H. S. Lim, H. Y. Cho, B. H. Park, S. O. Ka, Y. R. Lee, D. W. Jeong, H. O. Kim, M. K. Han, and S. I. Lee. 2014. Myeloid deletion of SIRT1 aggravates serum transfer arthritis in mice via nuclear factor-kappaB

activation. *PLoS One 9:e87733*.

190. Lee, S. M., H. Yang, D. M. Tartar, B. Gao, X. Luo, S. Q. Ye, H. Zaghouani, and D. Fang. 2011. Prevention and treatment of diabetes with resveratrol in a non-obese mouse model of type 1 diabetes. *Diabetologia 54:1136*.

191. Singh, U. P., N. P. Singh, B. Singh, L. J. Hofseth, R. L. Price, M. Nagarkatti, and P. S. Nagarkatti. 2010. Resveratrol (trans-3,5,4'-trihydroxystilbene) induces silent mating type information regulation-1 and down-regulates nuclear transcription factor-kappaB activation to abrogate dextran sulfate sodium-induced colitis. *J Pharmacol Exp Ther 332:829*.

192. Sica, A., and A. Mantovani. 2012. Macrophage plasticity and polarization: *in vivo* veritas. *J Clin Invest 122:787*.

193. Lumeng, C. N., J. L. Bodzin, and A. R. Saltiel. 2007. Obesity induces a phenotypic switch in adipose tissue macrophage polarization. *J Clin Invest 117:175*.

194. Yang, Z., X. Wang, Y. He, L. Qi, L. Yu, B. Xue, and H. Shi. 2012. The full capacity of AICAR to reduce obesity-induced inflammation and insulin resistance requires myeloid SIRT1. *PLoS One 7:e49935*.

195. Aderem, A., and D. M. Underhill. 1999. Mechanisms of phagocytosis in macrophages. *Annu Rev Immunol 17:593*.

196. Aronoff, D. M., C. Canetti, and M. Peters-Golden. 2004. Prostaglandin E2 inhibits alveolar macrophage phagocytosis through an E-prostanoid 2 receptor-mediated increase in intracellular cyclic AMP. *J Immunol 173:559*.

197. Serezani, C. H., J. Chung, M. N. Ballinger, B. B. Moore, D. M. Aronoff, and M. Peters-Golden. 2007. Prostaglandin E2 suppresses bacterial killing in alveolar macrophages by inhibiting NADPH oxidase. *Am J Respir Cell Mol Biol 37:562*.

198. Zhang, R., H. Z. Chen, J. J. Liu, Y. Y. Jia, Z. Q. Zhang, R. F. Yang, Y. Zhang, J. Xu, Y. S. Wei, D. P. Liu, and C. C. Liang. 2010. SIRT1 suppresses activator protein-1 transcriptional activity and cyclooxygenase-2 expression in macrophages. *J Biol Chem 285:7097*.

199. Crotty Alexander, L. E., B. J. Marsh, A. M. Timmer, A. E. Lin, K. Zainabadi, A. Czopik, L. Guarente, and V. Nizet. 2013. Myeloid cell sirtuin-1 expression does not alter host immune responses to Gram-negative endotoxemia or Gram-positive bacterial infection. *PLoS One 8:e84481*.

200. Liao, X., J. C. Sluimer, Y. Wang, M. Subramanian, K. Brown, J. S. Pattison, J. Robbins, J. Martinez, and I. Tabas. 2012. Macrophage autophagy plays a protective role in advanced atherosclerosis. *Cell Metab 15:545*.

201. Jang, S. Y., H. T. Kang, and E. S. Hwang. 2012. Nicotinamide-induced mitophagy: event mediated by high NAD+/NADH ratio and SIRT1 protein activation. *J Biol Chem 287:19304*.

202. Lee, I. H., L. Cao, R. Mostoslavsky, D. B. Lombard, J. Liu, N. E. Bruns, M. Tsokos, F. W. Alt, and T. Finkel. 2008. A role for the NAD-dependent deacetylase Sirt1 in the regulation of autophagy. *Proc Natl Acad Sci U S A 105:3374*.

203. Ng, F., and B. L. Tang. 2013. Sirtuins' modulation of autophagy. *J Cell Physiol*

228:2262.

204. Liu, B., B. Zhang, R. Guo, S. Li, and Y. Xu. 2014. Enhancement in efferocytosis of oxidized low-density lipoprotein-induced apoptotic RAW264.7 cells through Sirt1-mediated autophagy. *Int J Mol Med 33:523*.

205. Takeda-Watanabe, A., M. Kitada, K. Kanasaki, and D. Koya. 2012. SIRT1 inactivation induces inflammation through the dysregulation of autophagy in human THP-1 cells. *Biochem Biophys Res Commun 427:191*.

206. Song, Y. M., Y. H. Lee, J. W. Kim, D. S. Ham, E. S. Kang, B. S. Cha, H. C. Lee, and B. W. Lee. 2015. Metformin alleviates hepatosteatosis by restoring SIRT1-mediated autophagy induction via an AMP-activated protein kinase-independent pathway. *Autophagy 11:46*.

207. 2015. Correction: Globular Adiponectin Causes Tolerance to LPS-Induced TNF-alpha Expression via Autophagy Induction in RAW 264.7 Macrophages: Involvement of SIRT1/FoxO3A Axis. *PLoS One 10:e0130370*.

208. Lu, G., R. Zhang, S. Geng, L. Peng, P. Jayaraman, C. Chen, F. Xu, J. Yang, Q. Li, H. Zheng, K. Shen, J. Wang, X. Liu, W. Wang, Z. Zheng, C. F. Qi, C. Si, J. C. He, K. Liu, S. A. Lira, A. G. Sikora, L. Li, and H. Xiong. 2015. Myeloid cell-derived inducible nitric oxide synthase suppresses M1 macrophage polarization. *Nat Commun 6:6676*.

209. Fan, W., H. Morinaga, J. J. Kim, E. Bae, N. J. Spann, S. Heinz, C. K. Glass, and J. M. Olefsky. 2010. FoxO1 regulates Tlr4 inflammatory pathway signalling in macrophages. *EMBO J 29:4223*.

210. Coura, J. R., and J. Borges-Pereira. 2012. Chagas disease. What is known and what should be improved: a systemic review. *Rev Soc Bras Med Trop 45:286*.

211. Nagajyothi, F., F. S. Machado, B. A. Burleigh, L. A. Jelicks, P. E. Scherer, S. Mukherjee, M. P. Lisanti, L. M. Weiss, N. J. Garg, and H. B. Tanowitz. 2012. Mechanisms of Trypanosoma cruzi persistence in Chagas disease. *Cell Microbiol 14:634*.

212. Cantey, P. T., S. L. Stramer, R. L. Townsend, H. Kamel, K. Ofafa, C. W. Todd, M. Currier, S. Hand, W. Varnado, E. Dotson, C. Hall, P. L. Jett, and S. P. Montgomery. 2012. The United States Trypanosoma cruzi Infection Study: evidence for vector-borne transmission of the parasite that causes Chagas disease among United States blood donors. *Transfusion*.

213. Bern, C., S. Kjos, M. J. Yabsley, and S. P. Montgomery. 2011. Trypanosoma cruzi and Chagas' Disease in the United States. *Clin Microbiol Rev 24:655*.

214. Morillo, C. A., J. A. Marin-Neto, A. Avezum, S. Sosa-Estani, A. Rassi, Jr., F. Rosas, E. Villena, R. Quiroz, R. Bonilla, C. Britto, F. Guhl, E. Velazquez, L. Bonilla, B. Meeks, P. Rao-Melacini, J. Pogue, A. Mattos, J. Lazdins, A. Rassi, S. J. Connolly, and S. Yusuf. 2015. Randomized Trial of Benznidazole for Chronic Chagas' Cardiomyopathy. *N Engl J Med 373:1295*.

215. Miller, F. J., F. L. Rosenfeldt, C. Zhang, A. W. Linnane, and P. Nagley. 2003. Precise determination of mitochondrial DNA copy number in human skeletal and cardiac muscle by a PCR-based assay: lack of change of copy number with age. *Nucleic Acids Res 31:e61*.

216. Karamanlidis, G., L. Nascimben, G. S. Couper, P. S. Shekar, F. del Monte, and R. Tian. 2010. Defective DNA replication impairs mitochondrial biogenesis in human failing hearts. *Circ Res 106:1541*.

217. Schilling, J., and D. P. Kelly. 2011. The PGC-1 cascade as a therapeutic target for heart failure. *J Mol Cell Cardiol 51:578*.

218. Wan, X.-X., S. Gupta, M. P. Zago, M. M. Davidson, P. Dousset, A. Amoroso, and N. J. Garg. 2012. Defects of mtDNA replication impaired the mitochondrial biogenesis during Trypanosoma cruzi infection in human cardiomyocytes and chagasic patients: The role of Nrf1/2 and antioxidant response. *J Am Heart Assoc 1:e003855*

219. Machado, F. S., W. O. Dutra, L. Esper, K. J. Gollob, M. M. Teixeira, L. M. Weiss, F. Nagajyothi, H. B. Tanowitz, and N. J. Garg. 2012. Current understanding of immunity to Trypanosoma cruzi infection and pathogenesis of Chagas disease. *Seminars in Immunopathology 34:753*.

220. Tanowitz, H. B., J. J. Wen, F. S. Machado, M. S. Desruisseaux, C. Robello, and N. J. Garg. 2016. *Trypanosoma cruzi and Chagas disease: innate immunity, ROS, and cardiovascular system*. Academic Press / Elsevier Inc, Waltham, MA

221. Gupta, S., V. Bhatia, J.-J. Wen, Y. Wu, M.-H. Huang, and N. J. Garg. 2009. *Trypanosoma cruzi* infection disturbs mitochondrial membrane potential and ROS production rate in cardiomyocytes. *Free Radic Biol Med 47:1414*.

222. Ba, X., S. Gupta, M. Davidson, and N. J. Garg. 2010. *Trypanosoma cruzi* induces ROS-PARP-1-RelA pathway for up regulation of cytokine expression in

cardiomyocytes. *J Biol Chem 285:11596*.

223. Dhiman, M., X.-X. Wan, V. PL, G. Vargas, and N. J. Garg. 2013. MnSOD^{tg} mice control myocardial inflammatory and oxidative stress and remodeling responses elicited in chronic Chagas disease. *J Am Heart Assoc 2:e000302*.

224. Bowie, A., and L. A. O'Neill. 2000. Oxidative stress and nuclear factor-kappaB activation: a reassessment of the evidence in the light of recent discoveries. *Biochem Pharmacol 59:13*.

225. Rodgers, J. T., C. Lerin, W. Haas, S. P. Gygi, B. M. Spiegelman, and P. Puigserver. 2005. Nutrient control of glucose homeostasis through a complex of PGC-1alpha and SIRT1. *Nature 434:113*.

226. Vachharajani, V. T., T. Liu, X. Wang, J. J. Hoth, B. K. Yoza, and C. E. McCall. 2016. Sirtuins Link Inflammation and Metabolism. *J Immunol Res 2016:8167273*.

227. Sundaresan, N. R., V. B. Pillai, and M. P. Gupta. 2011. Emerging roles of SIRT1 deacetylase in regulating cardiomyocyte survival and hypertrophy. *J Mol Cell Cardiol 51:614*.

228. Villalba, J. M., and F. J. Alcain. 2012. Sirtuin activators and inhibitors. *Biofactors 38:349*.

229. Funk, J. A., S. Odejinmi, and R. G. Schnellmann. 2010. SRT1720 induces mitochondrial biogenesis and rescues mitochondrial function after oxidant injury in renal proximal tubule cells. *J Pharmacol Exp Ther 333:593*.

230. Minor, R. K., J. A. Baur, A. P. Gomes, T. M. Ward, A. Csiszar, E. M. Mercken, K.

Abdelmohsen, Y. K. Shin, C. Canto, M. Scheibye-Knudsen, M. Krawczyk, P. M. Irusta, A. Martin-Montalvo, B. P. Hubbard, Y. Zhang, E. Lehrmann, A. A. White, N. L. Price, W. R. Swindell, K. J. Pearson, K. G. Becker, V. A. Bohr, M. Gorospe, J. M. Egan, M. I. Talan, J. Auwerx, C. H. Westphal, J. L. Ellis, Z. Ungvari, G. P. Vlasuk, P. J. Elliott, D. A. Sinclair, and R. de Cabo. 2011. SRT1720 improves survival and healthspan of obese mice. *Sci Rep 1:70*.

231. Bhan, A., A. Sirker, J. Zhang, A. Protti, N. Catibog, W. Driver, R. Botnar, M. J. Monaghan, and A. M. Shah. 2014. High-frequency speckle tracking echocardiography in the assessment of left ventricular function and remodeling after murine myocardial infarction. *Am J Physiol Heart Circ Physiol 306:H1371*.

232. Dhiman, M., and N. J. Garg. 2011. NADPH oxidase inhibition ameliorates Trypanosoma cruzi-induced myocarditis during Chagas disease. *J Pathol 225:583*.

233. Bhatia, V., M. Sinha, B. Luxon, and N. Garg. 2004. Utility of the Trypanosoma cruzi sequence database for identification of potential vaccine candidates by in silico and *in vitro* screening. *Infect Immun 72:6245*.

234. Garg, N., A. Gerstner, V. Bhatia, J. DeFord, and J. Papaconstantinou. 2004. Gene expression analysis in mitochondria from chagasic mice: alterations in specific metabolic pathways. *Biochem J 381:743*.

235. Dhiman, M., Y. A. Coronado, C. K. Vallejo, J. R. Petersen, A. Ejilemele, S. Nunez, M. P. Zago, H. M. Spratt, and N. J. Garg. 2013. Innate immune responses and antioxidant/oxidant imbalance are major determinants of human

chagas disease. *Plos NTD 7:e2364*.

236. Wen, J.-J., P. C. Yachelini, A. Sembaj, R. E. Manzur, and N. J. Garg. 2006. Increased oxidative stress is correlated with mitochondrial dysfunction in chagasic patients. *Free Rad Biol Med 41:270*.

237. Wen, J. J., M. Dhiman, E. B. Whorton, and N. J. Garg. 2008. Tissue-specific oxidative imbalance and mitochondrial dysfunction during Trypanosoma cruzi infection in mice. *Microbes Infect 10:1201*.

238. Wen, J.-J., and N. J. Garg. 2010. Mitochondrial complex III defects contribute to inefficient respiration and ATP synthesis in the myocardium of Trypanosoma cruzi-infected mice. *Antioxid Redox Signal 12:27*.

239. Rong, J. X., Y. Qiu, M. K. Hansen, L. Zhu, V. Zhang, M. Xie, Y. Okamoto, M. D. Mattie, H. Higashiyama, S. Asano, J. C. Strum, and T. E. Ryan. 2007. Adipose mitochondrial biogenesis is suppressed in db/db and high-fat diet-fed mice and improved by rosiglitazone. *Diabetes 56:1751*.

240. Semple, R. K., V. C. Crowley, C. P. Sewter, M. Laudes, C. Christodoulides, R. V. Considine, A. Vidal-Puig, and S. O'Rahilly. 2004. Expression of the thermogenic nuclear hormone receptor coactivator PGC-1alpha is reduced in the adipose tissue of morbidly obese subjects. *Int J Obes Relat Metab Disord 28:176*.

241. Richardson, D. K., S. Kashyap, M. Bajaj, K. Cusi, S. J. Mandarino, J. Finlayson, R. A. DeFronzo, C. P. Jenkinson, and L. J. Mandarino. 2005. Lipid infusion decreases the expression of nuclear encoded mitochondrial genes and

increases the expression of extracellular matrix genes in human skeletal muscle. *J Biol Chem 280:10290*.

242. Patti, M. E., A. J. Butte, S. Crunkhorn, K. Cusi, R. Berria, S. Kashyap, Y. Miyazaki, I. Kohane, M. Costello, R. Saccone, E. J. Landaker, A. B. Goldfine, E. Mun, R. DeFronzo, J. Finlayson, C. R. Kahn, and L. J. Mandarino. 2003. Coordinated reduction of genes of oxidative metabolism in humans with insulin resistance and diabetes: Potential role of PGC1 and NRF1. *Proc Natl Acad Sci U S A 100:8466*.

243. Lagouge, M., C. Argmann, Z. Gerhart-Hines, H. Meziane, C. Lerin, F. Daussin, N. Messadeq, J. Milne, P. Lambert, P. Elliott, B. Geny, M. Laakso, P. Puigserver, and J. Auwerx. 2006. Resveratrol improves mitochondrial function and protects against metabolic disease by activating SIRT1 and PGC-1alpha. *Cell 127:1109*.

244. Um, J. H., S. J. Park, H. Kang, S. Yang, M. Foretz, M. W. McBurney, M. K. Kim, B. Viollet, and J. H. Chung. 2010. AMP-activated protein kinase-deficient mice are resistant to the metabolic effects of resveratrol. *Diabetes 59:554*.

245. Chan, A. Y., V. W. Dolinsky, C. L. Soltys, B. Viollet, S. Baksh, P. E. Light, and J. R. Dyck. 2008. Resveratrol inhibits cardiac hypertrophy via AMP-activated protein kinase and Akt. *J Biol Chem 283:24194*.

246. Thandapilly, S. J., P. Wojciechowski, J. Behbahani, X. L. Louis, L. Yu, D. Juric, M. A. Kopilas, H. D. Anderson, and T. Netticadan. 2010. Resveratrol prevents the development of pathological cardiac hypertrophy and contractile dysfunction in the SHR without lowering blood pressure. *Am J Hypertens*

23:192.

247. Khader, A., W. L. Yang, M. Kuncewitch, A. Jacob, J. M. Prince, J. R. Asirvatham, J. Nicastro, G. F. Coppa, and P. Wang. 2014. Sirtuin 1 activation stimulates mitochondrial biogenesis and attenuates renal injury after ischemia-reperfusion. *Transplantation 98:148*.

248. Feige, J. N., M. Lagouge, C. Canto, A. Strehle, S. M. Houten, J. C. Milne, P. D. Lambert, C. Mataki, P. J. Elliott, and J. Auwerx. 2008. Specific SIRT1 activation mimics low energy levels and protects against diet-induced metabolic disorders by enhancing fat oxidation. *Cell Metab 8:347*.

249. Baur, J. A. Biochemical effects of SIRT1 activators. *Biochim Biophys Acta 1804:1626*.

250. Milne, J. C., P. D. Lambert, S. Schenk, D. P. Carney, J. J. Smith, D. J. Gagne, L. Jin, O. Boss, R. B. Perni, C. B. Vu, J. E. Bemis, R. Xie, J. S. Disch, P. Y. Ng, J. J. Nunes, A. V. Lynch, H. Yang, H. Galonek, K. Israelian, W. Choy, A. Iffland, S. Lavu, O. Medvedik, D. A. Sinclair, J. M. Olefsky, M. R. Jirousek, P. J. Elliott, and C. H. Westphal. 2007. Small molecule activators of SIRT1 as therapeutics for the treatment of type 2 diabetes. *Nature 450:712*.

251. Higashida, K., S. H. Kim, S. R. Jung, M. Asaka, J. O. Holloszy, and D. H. Han. 2013. Effects of resveratrol and SIRT1 on PGC-1alpha activity and mitochondrial biogenesis: a reevaluation. *PLoS Biol 11:e1001603*.

252. Gupta, S., J. J. Wen, and N. J. Garg. 2009. Oxidative Stress in Chagas Disease. *Interdiscip Perspect Infect Dis 2009:190354*.

253. Gano, L. B., A. J. Donato, H. M. Pasha, C. M. Hearon, Jr., A. L. Sindler, and D. R. Seals. 2014. The SIRT1 activator SRT1720 reverses vascular endothelial dysfunction, excessive superoxide production, and inflammation with aging in mice. *Am J Physiol Heart Circ Physiol 307:H1754*.

254. Hasegawa, K., S. Wakino, K. Yoshioka, S. Tatematsu, Y. Hara, H. Minakuchi, K. Sueyasu, N. Washida, H. Tokuyama, M. Tzukerman, K. Skorecki, K. Hayashi, and H. Itoh. Kidney-specific overexpression of Sirt1 protects against acute kidney injury by retaining peroxisome function. *J Biol Chem 285:13045*.

255. Sin, T. K., B. Y. Yung, and P. M. Siu. 2015. Modulation of SIRT1-Foxo1 signaling axis by resveratrol: implications in skeletal muscle aging and insulin resistance. *Cell Physiol Biochem 35:541*.

256. Bagul, P. K., N. Deepthi, R. Sultana, and S. K. Banerjee. 2015. Resveratrol ameliorates cardiac oxidative stress in diabetes through deacetylation of NFkB-p65 and histone 3. *J Nutr Biochem 26:1298*.

257. Hall, B. S., W. Tam, R. Sen, and M. E. Pereira. 2000. Cell-specific activation of nuclear factor-kappaB by the parasite Trypanosoma cruzi promotes resistance to intracellular infection. *Mol Biol Cell 11:153*.

258. Yang, Z., B. B. Kahn, H. Shi, and B. Z. Xue. 2010. Macrophage alpha1 AMP-activated protein kinase (alpha1AMPK) antagonizes fatty acid-induced inflammation through SIRT1. *J Biol Chem 285:19051*.

259. Carod-Artal, F. J., and J. Gascon. Chagas disease and stroke. *Lancet Neurol 9:533*.

260. Higuchi Mde, L., L. A. Benvenuti, M. Martins Reis, and M. Metzger. 2003. Pathophysiology of the heart in Chagas' disease: current status and new developments. *Cardiovasc Res 60:96*.

261. Marinho, C. R., M. R. D'Imperio Lima, M. G. Grisotto, and J. M. Alvarez. 1999. Influence of acute-phase parasite load on pathology, parasitism, and activation of the immune system at the late chronic phase of Chagas' disease. *Infect Immun 67:308*.

262. Wen, J. J., and N. J. Garg. 2008. Mitochondrial generation of reactive oxygen species is enhanced at the Q(o) site of the complex III in the myocardium of Trypanosoma cruzi-infected mice: beneficial effects of an antioxidant. *J Bioenerg Biomembr 40:587*.

263. Watkins, S. K., N. K. Egilmez, J. Suttles, and R. D. Stout. 2007. IL-12 rapidly alters the functional profile of tumor-associated and tumor-infiltrating macrophages *in vitro* and *in vivo*. *J Immunol 178:1357*.

264. Gratchev, A., J. Kzhyshkowska, K. Kothe, I. Muller-Molinet, S. Kannookadan, J. Utikal, and S. Goerdt. 2006. Mphi1 and Mphi2 can be re-polarized by Th2 or Th1 cytokines, respectively, and respond to exogenous danger signals. *Immunobiology 211:473*.

265. Sag, D., D. Carling, R. D. Stout, and J. Suttles. 2008. Adenosine 5'-monophosphate-activated protein kinase promotes macrophage polarization to an anti-inflammatory functional phenotype. *J Immunol 181:8633*.

266. Chowdhury, I. H., S. J. Koo, S. Gupta, L. Y. Liang, B. Bahar, L. Silla, J. Nunez-

Burgos, N. Barrientos, M. P. Zago, and N. J. Garg. 2017. Gene Expression Profiling and Functional Characterization of Macrophages in Response to Circulatory Microparticles Produced during Trypanosoma cruzi Infection and Chagas Disease. *J Innate Immun 9:203*.

267. Hideko Tatakihara, V. L., R. Cecchini, C. L. Borges, A. D. Malvezi, V. K. Graca-de Souza, S. F. Yamada-Ogatta, L. V. Rizzo, and P. Pinge-Filho. 2008. Effects of cyclooxygenase inhibitors on parasite burden, anemia and oxidative stress in murine Trypanosoma cruzi infection. *FEMS Immunol Med Microbiol 52:47*.

268. Penas, F., G. A. Mirkin, M. Vera, A. Cevey, C. D. Gonzalez, M. I. Gomez, M. E. Sales, and N. B. Goren. 2015. Treatment *in vitro* with PPARalpha and PPARgamma ligands drives M1-to-M2 polarization of macrophages from *T. cruzi*-infected mice. *Biochim Biophys Acta 1852:893*.

269. Sathler-Avelar, R., D. M. Vitelli-Avelar, A. Teixeira-Carvalho, and O. A. Martins-Filho. 2009. Innate immunity and regulatory T-cells in human Chagas disease: what must be understood? *Mem Inst Oswaldo Cruz 104 Suppl 1:246*.

270. Gupta, S., T. S. Silva, J. E. Osizugbo, L. Tucker, H. M. Spratt, and N. J. Garg. 2014. Serum-mediated activation of macrophages reflects *Tc*Vac2 vaccine efficacy against Chagas disease. *Infect Immun 82:1382*.

271. Wynn, T. A., A. Chawla, and J. W. Pollard. 2013. Macrophage biology in development, homeostasis and disease. *Nature 496:445*.

272. Liu, G., and H. Yang. 2013. Modulation of macrophage activation and programming in immunity. *J Cell Physiol 228:502*.

VITA

Xianxiu Wan was born in Guangze, Fujian Province in China in 1983. In 2001, she was admitted to the China Agricultural University majored at Veterinary Medicine. She received a Master of Science degree in preventive veterinary medicine with parasitology focus from the same University in 2009. She joined Dr. Garg's lab since 2011 and she mainly focused on studying the pathogenesis of Chronic Chagas disease which is characterized by heart failure. She worked as a research associate for some time and then she was enrolled in GSBS as a Ph.D student in the department of Microbiology and Immunology at UTMB in 2012. During her Ph. D study, she received McLaughlin pre-doctoral fellowship in 2014 and awarded American Heart Association (AHA) pre-doctoral fellowship in 2015. And recently she was awarded Jeane B. Kempner Postdoctoral Fellowship for 2017-2018. She has also granted 7 other awards from American Association of Immunologists (AAI), Gordon Research Conference and from the GSBS in UTMB. She published 2 first author papers and 4 co-author papers during 2012-2017.

Xianxiu Wan married Zuliang Jie, currently a Postdoctoral Fellow at MD Anderson Cancer Center, in December, 2009 in Guangze, Fujian, China.

This dissertation is typed by Xianxiu Wan.

EDUCATION

Degree	Institution	Field of Study	Years
B.S.	China Agricultural University	Veterinary Medicine	2001-2006
M.S.	China Agricultural University	Preventive Veterinary Medicine	2006-2009

PUBLICATIONS

Peer-reviewed publications:

1 **Wan X**, Wen JJ, Koo SJ, Liang LY, Garg NJ (2016) SIRT1-PGC1alpha-NFkappaB Pathway of Oxidative and Inflammatory Stress during *Trypanosoma cruzi* Infection: Benefits of SIRT1-Targeted Therapy in Improving Heart Function in Chagas Disease. PLoS Pathog 12: e1005954.

2 Koo SJ, Chowdhury IH, Szczesny B, **Wan X,** Garg NJ (2016) Macrophages Promote Oxidative Metabolism To Drive Nitric Oxide Generation in Response to *Trypanosoma cruzi*. Infect Immun 84: 3527-3541.

3 Wen JJ, **Wan X,** Thacker J, Garg NJ (2016) Chemotherapeutic efficacy of phosphodiesterase inhibitors in chagasic cardiomyopathy. JACC Basic Transl Sci 1: 235-250.

4 Dhiman M, **Wan X,** Popov VL, Vargas G, Garg NJ (2013). MnSODtg mice control myocardial inflammatory and oxidative stress and remodeling responses elicited in chronic Chagas disease. J Am Heart Assoc. 2(5): p. e000302.

5 **Wan X,** Gupta S, Zago MP, Davidson MM, Dousset P, Amoroso A, Garg NJ (2012). Defects of mtDNA replication impaired mitochondrial biogenesis during *Trypanosoma cruzi* infection in human cardiomyocytes and Chagasic patients: The role of Nrf1/2 and antioxidant response. J Am Heart Assoc.; 1(6):e003855.

6 Gupta S, **Wan X,** Zago MP, Martinez Sellers VC, Silva TS, Assiah D, Dhiman M, Nuñez S, Petersen JR, Vázquez-Chagoyán JC, Estrada-Franco JG, Garg NJ (2012). Antigenicity and diagnostic potential of vaccine candidates in

human chagas disease. PLoS Negl Trop Dis. 7(1):e2018.

Manuscript submitted or in preparation

1 **Wan X,** Garg NJ. SRT1720 prevents the polarization and function of M1 macrophage in chronic chagasic mouse. *In preparation*.

2 **Wan X,** Garg NJ. Review. Role of SIRT1 in macrophage. *In preparation*

Abstracts presented at professional meetings

1 **Wan X,** Wen J, Koo SJ, Garg NJ (2016). SRT1720 prevents the polarization and function of M1 macrophage in chronic chagasic mouse. Poster presented in Tropical Infectious Diseases Gordon Research Conference, Galveston, Tx, USA.

2 **Wan X,** Wen J, Koo SJ, Yi L, Garg NJ (2016). SRT1720 inhibition of M1 macrophages and chronic inflammation in Chagas disease. Poster presented in The Annual Meeting of The American Association of Immunologists, Seattle, WA, USA.

3 **Wan X,** Wen J, Koo S, Garg N (2015) Enhancing SIRT1 activity improves heart function through activating mitochondrial biogenesis and inhibiting inflammatory pathways in Chagas disease. Poster presented in American Heart Association's BCVS 2015 Scientific Sessions. New Orleans, LA, USA.

4 **Wan X,** Wen J, Koo S, Garg N (2015). Enhancing the SIRT1 activity would improve mitochondrial function through activating mitochondrial

biogenesis in chronic chagasic mice. Poster presented in McLaughlin Colloquium, UTMB, Galveston, Tx, USA.

5 **Wan X** and Garg N (2014). Enhancing the PGC-1 α activity would improve mitochondrial function through activating mitochondrial biogenesis in chronic chagasic mice. Poster presented in McLaughlin Colloquium, UTMB, Galveston, Tx, USA.

6 **Wan X** and Garg N (2013). Defects of mtDNA replication impaired mitochondrial biogenesis during *Trypanosoma cruzi* infection in human cardiomyoctes and Chagasis patients: the Role of Nrf1/2 and antioxidant response. Poster presented in Gordon Research Conferences, Galveston, Tx, USA.